

AD-A283 324



ESL-TR-92-32

EVALUATION OF OXIDATION PROCESSES FOR TREATING AQUEOUS CHEMICAL MIXTURES

T. MILL, C.C. DAVID YAO, HER-KING SONG, S. SMEDLEY

SRI INTERNATIONAL
333 RAVENSWOOD AVENUE
MENLO PARK CA 94025

APRIL 1994

FINAL REPORT

JUNE 1990 - JUNE 1992

DTIC
ELECTE
AUG 12 1994
S B D

APPROVED FOR PUBLIC RELEASE:
DISTRIBUTION UNLIMITED



ENVIRONICS DIVISION
Air Force Civil Engineering Support Agency
Civil Engineering Laboratory
Tyndall Air Force Base, Florida 32403



94 8 11 007

NOTICE

PLEASE DO NOT REQUEST COPIES OF THIS REPORT FROM HQ AFCESA/RA (AIR FORCE CIVIL ENGINEERING SUPPORT AGENCY). ADDITIONAL COPIES MAY BE PURCHASED FROM:

**NATIONAL TECHNICAL INFORMATION SERVICE
5285 PORT ROYAL ROAD
SPRINGFIELD, VIRGINIA 22161**

FEDERAL GOVERNMENT AGENCIES AND THEIR CONTRACTORS REGISTERED WITH DEFENSE TECHNICAL INFORMATION CENTER SHOULD DIRECT REQUESTS FOR COPIES OF THIS REPORT TO:

**DEFENSE TECHNICAL INFORMATION CENTER
CAMERON STATION
ALEXANDRIA, VIRGINIA 22314**

REPORT DOCUMENTATION PAGE

Form Approved
OMB No. 0704-0188

Public reporting burden for this collection of information is estimated to average 1 hour per response, including the time for reviewing instructions, searching existing data sources, gathering and maintaining the data needed, and completing and reviewing the collection of information. Send comments regarding this burden estimate or any other aspect of the collection of information, including suggestions for reducing this burden, to Washington Headquarters Services, Directorate for Information Operations and Resources, 1215 Jefferson Davis Highway, Suite 1204, Arlington, VA 22202-4302, and to the Office of Management and Budget, Paperwork Reduction Project 0704-0188, Washington, DC 20503.

1. AGENCY USE ONLY (Leave blank)	2. REPORT DATE	3. REPORT TYPE AND DATES COVERED
	April 1994	Final Report (6/90-6/92)
4. TITLE AND SUBTITLE		5. FUNDING NUMBERS
Evaluation of Oxidation Processes for Treating Aqueous Chemical Mixtures		F08635-90-0061
6. AUTHOR(S)		
Theodore Mill, C.C. David Yao, Her-King Song, Stuart Smedley		
7. PERFORMING ORGANIZATION NAME(S) AND ADDRESS(ES)		8. PERFORMING ORGANIZATION REPORT NUMBER
SRI International 333 Ravenswood Avenue Menlo Park, CA 94025		SRI Project PYU 1204
9. SPONSORING/MONITORING AGENCY NAME(S) AND ADDRESS(ES)		10. SPONSORING/MONITORING AGENCY REPORT NUMBER
Department of the Air Force Headquarters, Air Force Civil Engineering & Support Agency HQ AFCESA/RAVW 130 Barnes Drive Tyndall AFB, FL 32402-5319		ESL-TR-92-32
11. SUPPLEMENTARY NOTES		
12a. DISTRIBUTION/AVAILABILITY STATEMENT		12b. DISTRIBUTION CODE
Approved for public release; distribution unlimited		
13. ABSTRACT (Maximum 200 words)		
<p>The pathways of radical generation and consumption in several advanced oxidation processes (AOPs) involving ozone, peroxide, titanium dioxide, and UV light have been evaluated. HO^\bullet is the principal oxidant in the AOPs at pH 7 and 2 as shown by measuring the relative reactivity ratio between butyrate and propionate ions. Several kinetic models have been developed to describe these oxidation processes in pure water and in a variety of natural waters. Both models and experiments show the importance of HCO_3^- and humic acid in controlling the steady state of HO^\bullet. Good agreement between data from experiments and kinetic models shows that the models predict the changes in concentration of hydrogen peroxide, ozone and butyrate ion reasonably well. The models can be used to optimize the efficiency of AOPs.</p> <p>A preliminary study of the electrooxidation of organics in water was conducted using PbO_2/Pt electrode. Rates of oxidation were relatively slow and the relative reactivity ratio for propionate and butyrate ions was close to one indicating a diffusion controlled process in which the organic was oxidized directly on the electrode.</p>		
14. SUBJECT TERMS		15. NUMBER OF PAGES
AOPs, kinetic models, optimization, efficiency, electrooxidation HO^\bullet radical, oxidation, ozone, hydrogen peroxide, butyrate		9
		16. PRICE CODE
17. SECURITY CLASSIFICATION OF REPORT	18. SECURITY CLASSIFICATION OF THIS PAGE	19. SECURITY CLASSIFICATION OF ABSTRACT
Unclassified	Unclassified	Unclassified
		20. LIMITATION OF ABSTRACT

EXECUTIVE SUMMARY

A. OBJECTIVE

The objectives of this study were (1) to evaluate existing and new advanced oxidation processes (AOPs) to quantify and characterize their underlying oxidation chemistries and compare their relative efficiencies for oxidation in order to select and optimize the most efficient processes for Air Force needs (2) to evaluate direct electrochemical oxidation of organics and (3) to develop improved catalysts for oxidizing organics with hydroxyl radical ($\text{HO}\cdot$) in waste streams.

B. BACKGROUND

This project responds to the need of the Air Force to evaluate existing methods for the oxidative treatment of hazardous waste containing fuels, solvents, propellants, and explosives, and, if possible to develop new oxidative methods for treating hazardous waste. Effective and efficient treatment of chemical waste streams and contaminated groundwater is important for Air Force operations, where significant volumes of dilute aqueous waste can be generated. For toxic dilute chemicals, where conventional disposal methods often are impractical or too costly, the use of aqueous chemical oxidation is often an attractive alternative for reducing concentrations of organics to acceptable limits, either for water reuse or for further biological treatment.

Many published reports have provided conflicting results concerning the chemistry of the ozone/UV system since the 1950s. Taube (1) reported that hydrogen peroxide is the main product in aqueous ozone photolysis. Prengle (2) has continued to assume that the photolysis of aqueous ozone yields $\text{HO}\cdot$. To understand the chemistry, Staehelin and Hoigné (3) modeled the reactions of aqueous ozone in pure water and in the presence of solutes. Peyton and Glaze (4-6) provided additional data to support earlier findings that hydrogen peroxide is the major or sole product of the aqueous ozone photolysis. They derived a model based on the work of Staehelin and Hoigné (3) with addition of the photolysis step. Peyton and Glaze (5) extended their model to include the effect of the presence of an organic solute. Peyton (7) concluded that photolysis of aqueous ozone yields hydrogen peroxide directly, which participates in secondary reactions to produce $\text{HO}\cdot$, the principal oxidant in the ozone/UV system. Namba and Nakayama (8) also demonstrated that hydroxyl radical was the active species in the ozone/peroxide system.

The above conclusions raise several questions: (1) Is HO radical the principal oxidant in all AOPs? (2) Is an ozone/UV system intrinsically more expensive to operate than an ozone/H₂O₂/UV system or an H₂O₂/UV system, even though the treatment time is shorter? (3) Is an ozone/H₂O₂/UV systems intrinsically more expensive than an ozone/H₂O₂ system even though the treatment time is about the same? (3) If some of the systems are intrinsically more expensive than others, why they are still on the market?

C. SCOPE

SRI has conducted detailed experimental and modeling studies with several AOPs (1) to characterize the underlying chemistry of each process and (2) to develop kinetic models to accurately predict how experimental parameters will affect the rates and efficiencies of oxidation of organics in dilute solution.

Experimental studies used mixtures of 6 μ m each of butyrate (B) and propionate (P) ions to distinguish among several different kinds of oxidant. Experiments were conducted at pH 2.2 and 6-8 with H₂O₂ or O₃ and UV light or H₂O₂ and O₃ at pH 9 without UV light. The rates of loss of B and P were measured in each system with added HCO₃⁻ ion and humic acid, from which we concluded that all systems generate and mainly use HO• radical to oxidize organics.

Computer kinetic models were developed to describe the complex chemistry of each AOP in enough detail to accurately account for effects of added HCO₃⁻ and humic acid. Results from models were compared with experiments and then modified where necessary to bring the results into better agreement.

Optimized models were used to estimate the efficiency of each AOP in oxidizing 10 ppm B to 0.1 ppm in a fixed time with 100-200 mM H₂O₂ or O₃. From this information, we estimated the cost of treating 1000 gal of water containing 10 ppm organic.

Electrochemical oxidation of organics in water was examined briefly with two approaches: (1) direct oxidation (of an organic) at the electrode and (2) indirect oxidation via formation of H₂O₂ followed by conversion of H₂O₂ to HO• radical. Direct oxidation on a doped Pb electrode led to slow oxidation of P and B, but indirect oxidation experiments were not completed because of problems in converting H₂O₂ to HO• radical. Catalyst development was limited to a few experiments with Fe³⁺ on a fluoropolymer.

D. METHODOLOGY

Because of the many possible reactions in each AOP, simple kinetic evaluations generally will not distinguish among possible oxidation pathways nor the effects of external variables such as pH, humic acid or HCO_3^- concentration on the reaction rates and efficiencies. Kinetic models, which can simulate kinetic features of AOPs, are useful for optimization and for predicting the efficiencies of AOPs.

E. TEST DESCRIPTION

This report summarizes experiments and modeling conducted with several different advanced oxidation processes (AOPs) in which UV light with hydrogen peroxide or ozone or titanium dioxide have been used to oxidize low concentrations of butyrate (B) and propionate (P) ions in water at 25°C. The loss of oxidant (O_3 or H_2O_2) and B or P were followed with time to develop kinetic data.

Computer kinetic models were used to estimate the loss rates in these complex systems and would accurately account for effects of added HCO_3^- and humic acid.

F. RESULTS

This study has shown that HO^\bullet is the major oxidant in all the AOPs we examined. Therefore, choice of an AOP for a specific treatment is based on the most cost efficiency in generating HO^\bullet . The most efficient system for generating HO^\bullet is the $\text{H}_2\text{O}_2/\text{UV}$ system. However, this AOP is too slow to use with high flow systems where short residence times require high rates of HO^\bullet generation. Faster rates could be obtained, but only at much higher cost.

Ozone AOPs use 250 nm UV light very efficiently, but only 5% of the photolyzed ozone forms HO^\bullet . Thus only above pH 7 where HO_2^- is available is the ozone AOP an efficient source of HO^\bullet . This also means that above pH 7, the ozone/UV system has no advantage over the $\text{O}_3/\text{H}_2\text{O}_2/\text{Dark}$ system for generating HO^\bullet and oxidizing organics. The efficiency for generating HO^\bullet in the $\text{O}_3/\text{H}_2\text{O}_2/\text{Dark}$ system is unaffected by adding more H_2O_2 to speed up the reaction, thus this AOP can both rapidly and efficiently make and use HO^\bullet for oxidations. Physical mixing of H_2O_2 with ozone is the chief limitation on the amount of H_2O_2 that can be added to speed up this reaction.

Attachment for

THIS REPORT	<input checked="" type="checkbox"/>
DATA SHEET	<input type="checkbox"/>
COMPUTER	<input type="checkbox"/>
APPENDIX	<input type="checkbox"/>

Page 1 of 1

A-1

Kinetic models to describe the time dependence of the AOP reactions were developed for peroxide and ozone AOPs and shown to be reliable predictors of the rates and concentrations of the oxidants and organics in the systems.

G. CONCLUSIONS

The models provide a valuable tool for optimizing conditions and for selecting and efficiently using a specific AOP with a specific hazardous waste stream. However, the models did not include any direct reaction of ozone with organics or subsequent oxidations of initial oxidation products.

H. RECOMMENDATIONS

The model provides reliable predictions of the rates and concentrations of the oxidants and initial organics in the systems. The models can be used to select the most cost effect process, to suggest the range of competitive ability of each AOP among the several processes, and to indicate where special attention is needed in designing the reactor.

Current limitations on use of these kinetic models include varying effects of humic acids on rates of oxidation of organics, possible complications associated with oxidations of halogenated compounds and the detailed oxidation of initial oxidation products.

Electrochemical oxidation of organics in water are needed in two different areas: (1) efficient electrochemical generation of H_2O_2 and O_3 and (2) improved catalysts for converting H_2O_2 to HO .

PREFACE

This report was prepared by SRI International, 333 Ravenswood Avenue, Menlo Park, California 94025-3493 under contract F08635-90-C-0061 for the Department of the Air Force, HQ AFCESA/RAVV, Tyndall Air Force Base, Florida.

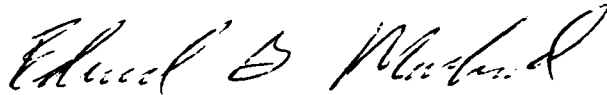
This report summarizes work done between 5 June 1990 and 4 June 1992. Captain Edward Marchand was the Air Force Project Officer.

The authors express their appreciation to Dr. Werner Haag, formerly of SRI International, for his contributions.

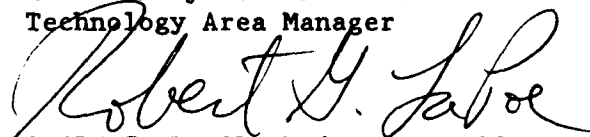
Mention of trademarks or trade names of material and equipment does not constitute endorsement or recommendation for use by the Air Force, nor can the report be used for advertising the product.

This report has been reviewed by the Public Affairs (PA) office and is releasable to the National Technical Information Service (NTIS). At NTIS, it will be available to the general public, including foreign nationals.

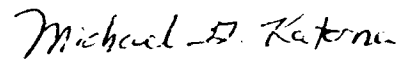
This technical report has been reviewed and is approved for publication.



EDWARD G. MARCHAND, Capt, USAF, BSC
Chemical/Physical Treatment
Technology Area Manager



ROBERT G. LAPOE, Maj, USAF, BSC
Chief, Site Remediation
R&D Division



MICHAEL G. KATONA, PhD, USAF
Chief Scientist



NEIL J. LAMB, Col, USAF
Deputy Director,
Envirronics Directorate

TABLE OF CONTENTS

Section	Title	Page
I	INTRODUCTION	1
	A. OBJECTIVE	1
	B. BACKGROUND.....	1
	1. Previous Studies.....	1
	2. Kinetics of Aqueous Ozone Photolysis	2
	3. Simple Kinetic Relations in Advanced Oxidation Processes (AOPs).....	6
	C. SCOPE/APPROACH.....	7
II	EVALUATION OF EXISTING AQUEOUS OXIDATION PROCESSES...	8
	A. CHARACTERIZATION OF OXIDANTS IN AOPs	8
	1. H_2O_2/UV System.....	9
	2. Ozone Systems.....	9
	3. TiO_2/UV Systems.....	11
	4. Reactivity Ratios for B and P in AOPs.....	12
	B. COMPARISON OF EXPERIMENTS WITH THE MODEL.....	12
	1. H_2O_2/UV System.....	15
	2. Ozone Systems.....	23
	3. TiO_2/UV System.....	38
	4. Humic Acid Effects on AOPs	38
	C. OXIDATION RATES AND RELATIVE CHEMICAL EFFICIENCIES	43
III	SELECTION AND OPTIMIZATION OF AOPs	50
	A. FACTORS IN SELECTION OF AOPs.....	50
	B. UV LAMPS	50
	C. DEFINITION OF CHEMICAL EFFICIENCY AND OPERATION .. COST EFFICIENCY	51
	D. AN EXAMPLE IN SELECTION AND OPTIMIZATION OF AOPs ..	51
	1. Literature Information	52
	2. Model Results	57

TABLE OF CONTENTS (CONCLUDED)

Section	Title	Page
IV	ELECTROCHEMICAL OXIDATION	63
	A. BACKGROUND.....	63
	B. CONSTRUCTION OF THE REACTION CELLS.....	64
	C. RESULTS AND DISCUSSIONS.....	64
V	FeO _x OR Fe ³⁺ CATALYSTS.....	68
VI	CONCLUSIONS.....	70
VII	EXPERIMENTAL METHODS AND CALCULATIONS	71
	A. STOCK SOLUTIONS.....	71
	B. UV LIGHT SOURCE	72
	C. REACTION SYSTEMS	72
	D. OZONE MONITORING METHODS: UV AND INDIGO	72
	E. MEASUREMENT OF H ₂ O ₂	77
	F. MEASUREMENT OF ORGANIC SUBSTRATES	77
	G. INSTRUMENTS.....	77
	H. COMPUTER SYSTEM AND PROGRAMS.....	78
	REFERENCES.....	79

LIST OF FIGURES

Figure	Title	Page
1	Reactions of Aqueous Ozone in "Pure Water".....	3
2	Oxidation of Organics with Ozone	4
3	Ozone/UV System.....	5
4	Reactivity Ratio Plot for Oxidation of Propionate and Butyrate Ions by H_2O_2 in the Presence and Absence of HA and HCO_3^-	10
5	Reactivity Ratio Plots for Propionate and Butyrate Ions in Different Oxidation Systems at pH 7.0	13
6	Reactivity Ratio Plot for Propionic and Butyric Acids in H_2O_2/UV and O_3/UV Systems at pH 2.2.....	14
7	Comparison of Peroxide Loss in the Experiments and Model with Bicarbonate at pH 8	19
8	Comparison of Peroxide Loss in the Experiment and Model with 5 ppm Humic Acid at pH 8.....	20
9	Calculated Hydrogen Peroxide Loss in the Absence of Butyrate and Propionate Ions under Various Conditions.....	21
10	Calculated Peroxide Increases in the Light and in the Absence of BH and PH for Different Percentage of Direct Generation of HO Radical from 100 μM Ozone at pH 2.2.....	28
11	Measured and Calculated Losses of Ozone and the Increases of Hydrogen Peroxide in the O_3/UV System in the Presence of 6 μM BH and PH at pH 2.2	29
12	Measured and Calculated Ozone Losses and Peroxide Increases in a $O_3/H_2O_2/UV$ System in the Presence of 6 μM BH and PH at pH 7.0.....	30
13	Measured Ozone Loss in the Absence of Peroxide in a $O_3/H_2O_2/Dark$ System at Different pHs	31
14	Calculated Ozone Loss in the Absence of Peroxide in a $O_3H_2O_2/Dark$ Model at Different pHs.....	32
15	Measured Ozone Loss in the Presence of 10 μM Peroxide in a $O_3/H_2O_2/Dark$ System at Different pHs	34

LIST OF FIGURES (CONCLUDED)

Figure	Title	Page
16	Calculated Ozone Loss in the Presence of 10 μM Peroxide in a $\text{O}_3/\text{H}_2\text{O}_2/\text{Dark}$ Model at Different pHs	35
17	Measured and Calculated Losses of B in a O_3/Dark System in the Presence of 6 μM B and P and in the Absence of Peroxide at pH 7.0	36
18	Measured and Calculated Losses of Ozone in a O_3/Dark System in the Presence of 6 μM B and P and in the Absence of Peroxide at pH 7.0	37
19	Measured Losses of Butyrate in a TiO_2 System at pH 7.2.....	39
20	PCBA Loss as a Function of Ozone Addition	41
21	Measured B/BH Losses in the Presence and Absence of 5 ppm HA in a O_3/UV System at pH 2.2 and 7.0.....	42
22	Measured Ozone Losses in the Presence and Absence of HA in a O_3/UV System in the Presence of B/BH and P/PH at pH 2.2 and 7.0	44
23	Loss of Butyrate versus the Loss of Oxidants in the Different Conditions in a O_3/UV System.....	45
24	UV Spectra for Ozone and Peroxide	46
25	Comparison of Measured Loss Rates of Oxidants in Different AOPs in the Absence of BH and PH.....	47
26	Comparison of Calculated Butyrate Loss Rates in the $\text{O}_3/\text{H}_2\text{O}_2$ Systems with 1 mM O_3 and 0.1 mM Butyrate at pH 9.0.....	59
27	Efficiency Comparisons of the $\text{O}_3/\text{H}_2\text{O}_2/\text{Dark}$ System with Different Concentrations of H_2O_2	60
28	Fluidized Bed Cell for Electrochemical Oxidation.....	65
29	Fixed Bed Cell for Electrochemical Oxidation	66
30	Oxidation of Acetophenone with Fe-Exchange Nafion	69
31	Spectrum of Filter Solution for UV Light Source	73
32	Peroxide/UV Reaction System.....	74
33	Ozone/UV Reaction System.....	75
34	TiO_2/UV and $\text{TiO}_2/\text{UV/Sonication}$ Systems	76

LIST OF TABLES

Table	Title	Page
1	REACTIONS AND RATE CONSTANTS USED TO MODEL PHOTOOXIDATIONS WITH H ₂ O ₂ /UV MODEL	16
2	OXIDATION RATES FOR H ₂ O ₂ IN THE PRESENCE AND ABSENCE OF BUTYRATE AND PROPIONATE: EXPERIMENTS VERSUS MODEL	22
3	OXIDATION RATES FOR BUTYRATE ION: EXPERIMENTS VERSUS MODEL	22
4	REACTIONS AND RATE CONSTANTS USED IN THE O ₃ /DARK AND O ₃ /UV MODELS.....	24
5	ZERO ORDER RATES OF OXIDATION OF BUTYRATE IN AOPs.....	48
6	EFFICIENCIES OF AOPs.....	49
7	ESTIMATED COST FOR TREATING CONTAMINANTS IN GROUNDWATER TO REDUCE THEM BELOW DRINKING WATER LIMITS	53
8	TREATMENT COSTS FOR TOC INDUSTRIAL/MUNICIPAL WASTEWATER	54
9	EFFICIENCY AND COST FOR GENERATING PHOTONS	57
10	REACTIONS OF OZONE WITH IMPORTANT SPECIES IN AOPs.....	58
11	ESTIMATED COST FOR TREATING ALIPHATIC ORGANIC COMPOUNDS IN A pH 9 SOLUTION TO REDUCE CONCENTRATION FROM 10 PPM TO 0.1 PPM	61
12	SUMMARY OF ELECTROCHEMICAL OXIDATION RATES FOR PROPIONATE AND BUTYRATE.....	67

SECTION I

INTRODUCTION

A. OBJECTIVE

This project responds to the need of the Air Force to evaluate existing methods for the oxidative treatment of hazardous waste containing fuels, solvents, propellants, and explosives, and, if possible to develop new oxidative methods for treating hazardous waste. Effective and efficient treatment of chemical waste streams and contaminated groundwater is important for Air Force operations, where significant volumes of dilute aqueous waste can be generated. For toxic dilute chemicals, where conventional disposal methods often are impractical or too costly, the use of aqueous chemical oxidation is often an attractive alternative for reducing concentrations of organics to acceptable limits, either for water reuse or for further biological treatment.

Recent interest has focused on oxidation methods that can operate below 100°C with high efficiency and minimal contamination by added chemical catalysts. Several systems oxidize chemicals efficiently in water at lower temperatures using air or oxygen, and promoted or catalyzed by ozone, peroxide, electron beams, or TiO_2 . In some cases, these promoters are used in combination with ultraviolet (UV) light or metal ions. All these systems generate reactive oxidants such as hydroxyl ($HO\cdot$) radical to transform organic compounds into nontoxic products such as acetate or carbonate.

The objectives of this study were (1) to evaluate existing and new aqueous oxidation processes to quantify and characterize their underlying oxidation chemistries and compare their relative efficiencies for oxidation to select and optimize the most efficient processes for Air Force needs (2) to evaluate direct electrochemical oxidation of organics and (3) to develop improved catalysts for oxidizing organics with $HO\cdot$ radical (HO) in waste streams.

B. BACKGROUND

1. Previous Studies

Many published reports have provided conflicting results concerning the chemistry of the ozone/UV system since the 1950s. Taube (1) reported that hydrogen peroxide is the main product

in aqueous ozone photolysis. Prengle (2) has continued to assume that the photolysis of aqueous ozone yields HO[•]. To understand the chemistry, Staehelin and Hoigné (3) modeled the reactions of aqueous ozone in pure water (Figure 1) and in the presence of solutes (Figure 2). Peyton and Glaze (4-6) provided additional data to support earlier findings that hydrogen peroxide is the major or sole product of the aqueous ozone photolysis. They derived a model based on the work of Staehelin and Hoigné (3) with addition of the photolysis step. Peyton and Glaze (5) extended their model to include the effect of the presence of an organic solute (Figure 3). Peyton (7) concluded that photolysis of aqueous ozone yields hydrogen peroxide directly, which participates in secondary reactions to produce HO[•], the principal oxidant in the O₃/hv/UV system. Namba and Nakayama (8) also demonstrated that hydroxyl radical was the active species in the ozone/peroxide system.

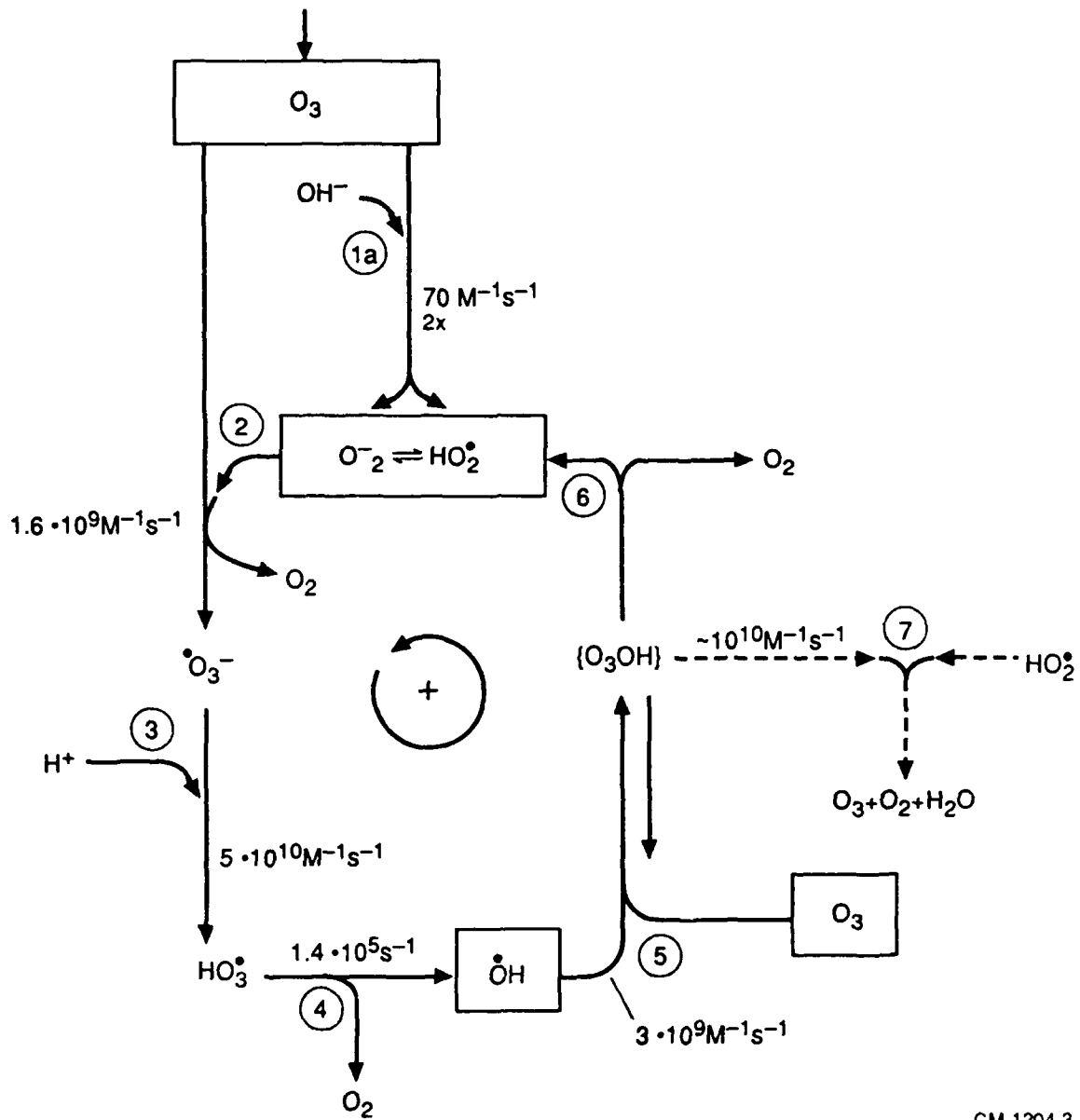
The above conclusions raise several questions: (1) Is an ozone/UV system intrinsically more expensive to operate than an ozone/H₂O₂/UV system or an H₂O₂/UV system, even though the treatment time is shorter? (2) Is an ozone/H₂O₂/UV system intrinsically more expensive than an ozone/H₂O₂ system although the treatment time is about the same? (3) If some of the systems are intrinsically more expensive than others, why are they still on the market?

After reviewing applications of oxidation systems, Peyton (7) commented that "at the present state of knowledge it is better to consider treatment options within the framework of the given treatment goals on a case-by-case basis." Glaze et al. (9) compared the ozone/UV and the peroxide/UV systems for destruction of PCE and TCE. They concluded that, in the absence of substrate photolysis, "the use of UV to generate hydrogen peroxide makes little sense." Peyton (7) commented that "this generalization may prove true in a number of cases but it is probably an oversimplification of the trade-offs between the ozone/UV and ozone/peroxide reactions."

2. Kinetics of Aqueous Ozone Photolysis

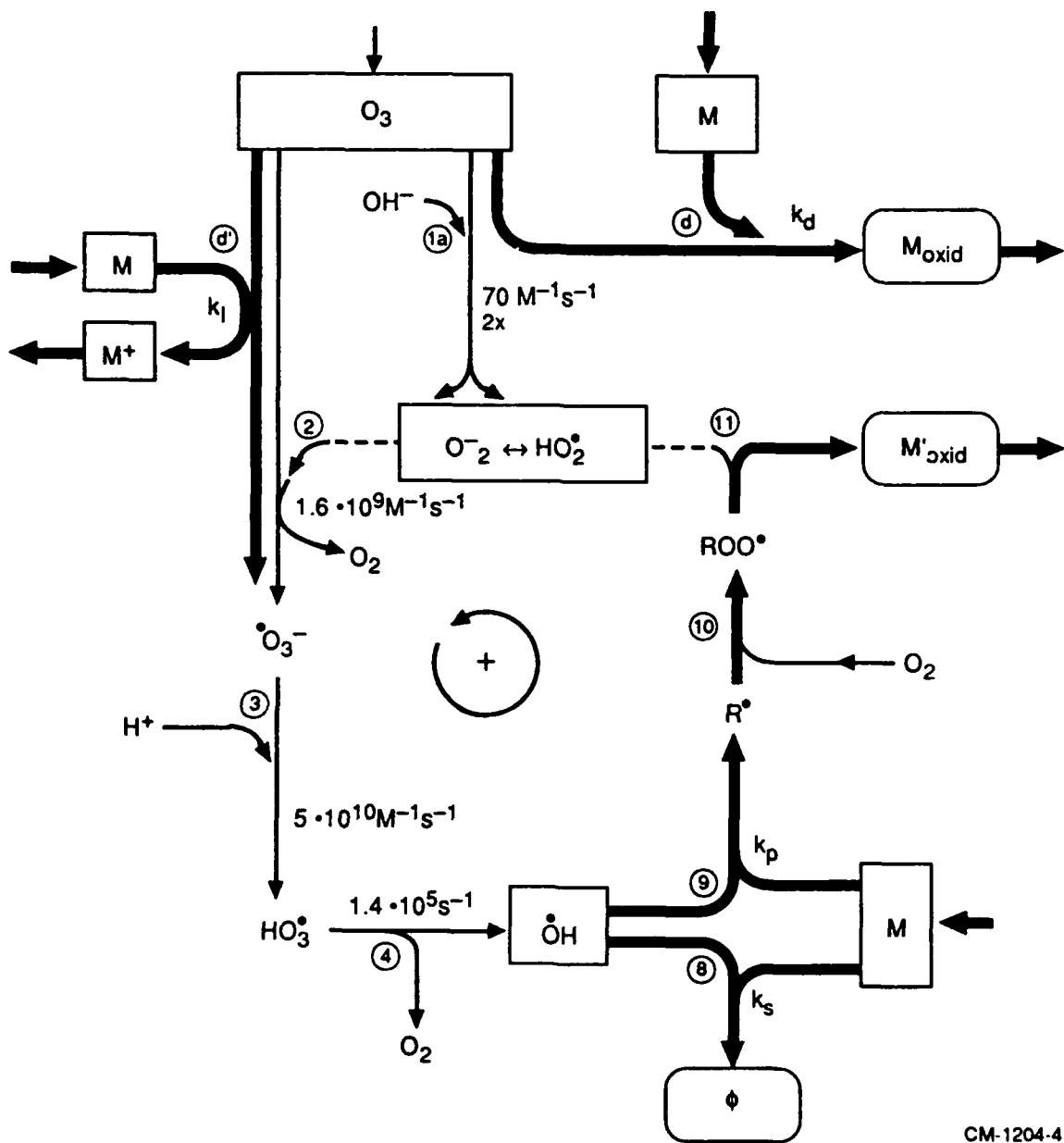
Zepp and Cline (10) have described the relations governing direct photolysis (R_p) in solution. For any solution, the photolysis rate can be expressed as

$$-\frac{d[C]}{dt} = I_d(1 - 10^{-(\epsilon [C]l)})\Phi_a/j \quad (1)$$



CM-1204-3

Figure 1. Reactions of Aqueous Ozone in "Pure Water".
Ref. 3 Reprinted by permission.



CM-1204-4

Figure 2. Oxidation of Organics with Ozone.
Ref. 3 Reprinted by permission.

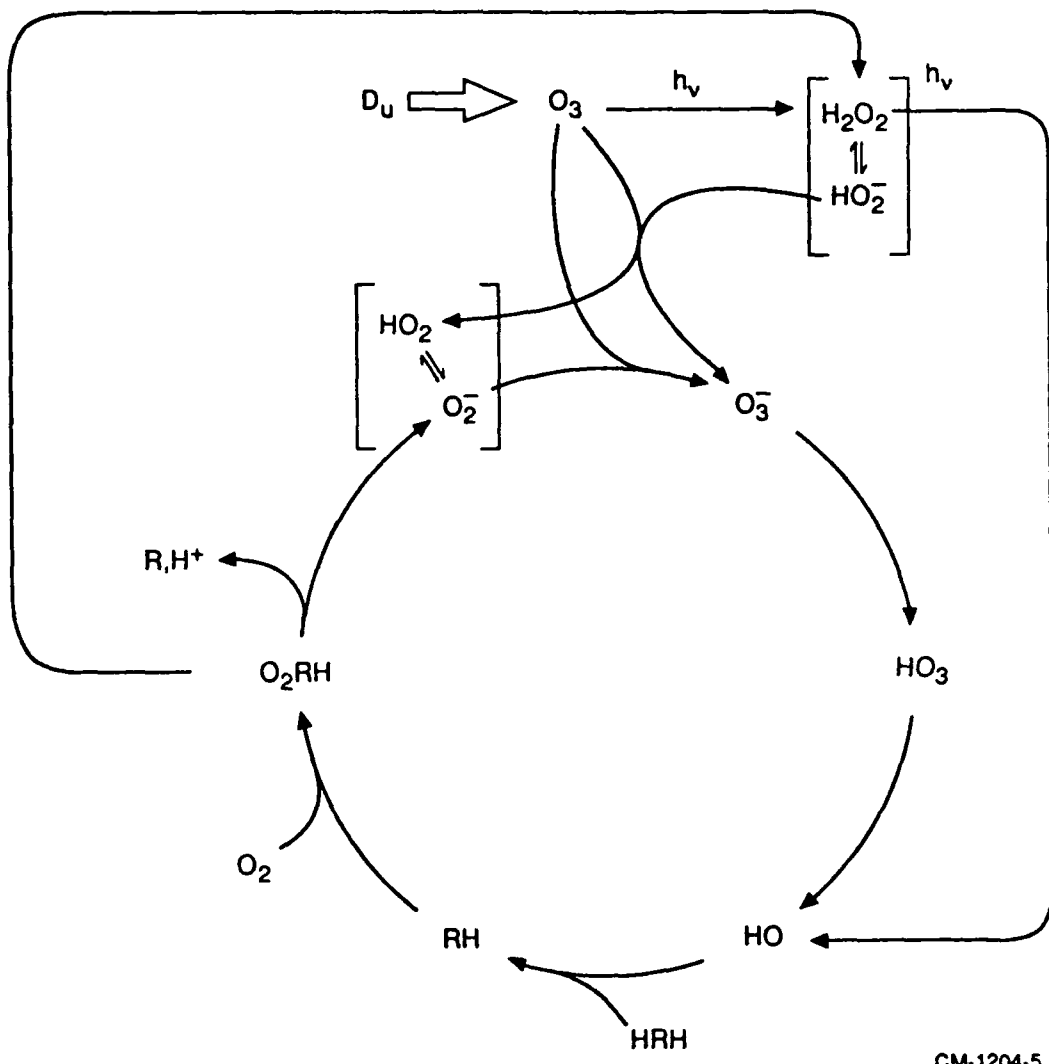


Figure 3. Ozone/UV System.
Ref. 5. Reprinted by permission.

where $[C]$ is the concentration of the chemical, I_d is the intensity of the light, ϵ is the molar absorptivity, l is the pathlength, Φ_a is the quantum yield of photolysis, and j is a conversion factor. When $\epsilon [C]l \geq 1$, Equation (1) simplifies to Equation (2) which is independent of C

$$-\frac{d[C]}{dt} = I_d \Phi_a / j \quad (2)$$

The loss of C is zero order. When $\epsilon [C]l \geq 0.05$, equation (1) changes to equation (3)

$$-\frac{d[C]}{dt} = 2.3 I_d \epsilon [C]l \Phi_a / j \quad (3)$$

and the loss of C is first order.

If we assume that the Φ_a of ozone is ~ 1 , the optical pathlength is 4 cm, and ϵ is about $2850 \text{ M}^{-1} \text{ cm}^{-1}$ at 254 nm, the loss of ozone is zero order when the ozone concentration is $100 \mu\text{M}$ but becomes first order with the last $5 \mu\text{M}$ ozone. Over this range of concentration, the loss of ozone is between zero and first order.

3. Simple Kinetic Relations in Advanced Oxidation Processes (AOPs)

Previous workers have shown that free radicals, and notably $\text{HO}\cdot$, must play a major role in oxidation of most kinds of organic compounds in AOP systems because peroxide and ozone are themselves relatively unreactive and are useful oxidants for only a few classes of organic compounds. In their simplest form, kinetic expressions for oxidation take the form

$$\text{Rate} = \sum k_{\text{ox}} [\text{Ox}]_{\text{ss}} [\text{Org}] \quad (4)$$

where k_{ox} is the specific second order rate constant for oxidant Ox reacting with an organic Org at some specific molecular site. The kinetic steady state concentration $[\text{Ox}]_{\text{ss}}$ of the oxidant Ox results from the competition between the rate of formation of Ox ($R_f \text{Ox}$, where R_f is the formation rate of the oxidant) and the sum of the rates of all of the reactions that consume Ox ($\sum R_d \text{Ox}$, R_d is the rate of loss of the oxidant).

$$[\text{Ox}]_{\text{ss}} = R_f \text{Ox} / \sum R_d \text{Ox} \quad (5)$$

For example, HO[•] will react with humic acid (HA) and bicarbonate/carbonate ion found in most natural waters in proportion to their concentrations, and these constituents can control [HO[•]]_{ss} and thus the rate of oxidation of the organic. In the absence of an organic HA, bicarbonate ion scavenges 24, 75, and 98 percent of HO[•] in 100 μ M, 1 mM, and 15 mM bicarbonate solutions, respectively. In the absence of any organic and in the presence of 25 μ M HA, 96 percent of generated HO[•] is scavenged by HA.

C. SCOPE AND APPROACH

SRI has conducted detailed experimental and modeling studies with several advanced oxidation processes (AOPs) (1) to characterize the underlying chemistry of each process and (2) to develop kinetic models to accurately predict how experimental parameters will affect the rates and efficiencies of oxidation of organics in dilute solution.

Experimental studies used mixtures of 6 μ M each of butyrate (B) and propionate (P) ions at pH 2.2 and pH 6-8 with H₂O₂ or O₃ and UV or just H₂O₂ and O₃ at pH 9. The rates of loss of B and P were measured in each system with added HCO₃⁻ ion and humic acid, from which we concluded that all systems generate and mainly use HO[•] radical to oxidize organics.

Kinetic models were constructed using standard software to describe the complex chemistry of each AOP in enough detail to accurately account for effects of added HCO₃⁻ and humic acid. The peroxide/UV model has 45 reactions while the ozone models have 80-90 reactions. Results from models were compared with experiments and then modified where necessary to bring the results into better agreement.

Finally, optimized models were used to estimate the efficiency of each AOP in oxidizing 10 ppm B to 0.1 ppm in a fixed time with 100-200 mM H₂O₂ or O₃. From this information, we estimated the cost of treating 1000 gal of water containing 10 ppm of an aliphatic organic.

Electrochemical oxidation of organics in water was examined briefly with two approaches: (1) direct oxidation (of an organic) at the electrode and (2) indirect oxidation via formation of H₂O₂ followed by conversion of H₂O₂ to HO[•] radical. Direct oxidation on a doped Pb electrode led to slow oxidation of P and B, but indirect oxidation experiments were not completed because of problems in converting H₂O₂ to HO[•] radical.

SECTION II

EVALUATION OF EXISTING AQUEOUS OXIDATION PROCESSES

The evaluation of the aqueous oxidation processes includes characterization of the AOPs, quantification of underlying oxidation chemistries, comparison of rates and relative chemical efficiencies among the AOPs, and selection and optimization of AOPs.

A. CHARACTERIZATION OF OXIDANTS IN AOPS

One way to characterize the major oxidant(s) in any oxidation is to measure the reactivity ratio of the oxidant toward different organics (A and B) (Scheme 1). For a specific oxidant, the loss rate ratio for A and B should be the same as the ratio of the rate constants (k_A/k_B) (11). It is unlikely that two different oxidants will have the same reactivity ratio toward the selected chemicals.



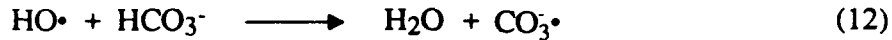
$$k_A/k_B = \ln ([A_0]/[A_t])/\ln ([B_0]/[B_t])$$

Scheme 1

Butyrate (B) and propionate (P) ions were chosen as kinetic probes for AOP experiments because they are analytically detectable at 6- μ M concentrations, they have no UV spectra above 210 nm, they produce no halogen atoms on oxidation, and they have well-known reactivities toward HO \cdot which gives a reactivity ratio of 2.4 for the anions ($k_B = 2.0 \times 10^9$ and $k_P = 8.2 \times 10^8$; (12) Moreover B and P have negligible reactivity toward ozone and secondary radicals such as HO $_2\cdot$ and RO $_2\cdot$ (13).

1. H₂O₂/UV System

The H₂O₂/UV system generates HO• by photolyzing the peroxide HO-OH bond with UV light near or below 300 nm (Scheme 2). The light of a low pressure mercury lamp (mainly 254 nm light) was filtered to remove light below 250 nm in our experimental system. All experiments were conducted with 100 μM peroxide in a batch reactor. Experiments were conducted with 6 μM each of B and P at pH 7 with H₂O₂/UV, where losses of B and P gave a reactivity ratio for B and P of 2.2, nearly the same as the calculated ratio of 2.4 (Figure 4). Since the H₂O₂/UV system is a well known primary producer of HO•, this experiment also checks the independent measurements of k_{ox} for the B and P system (12).

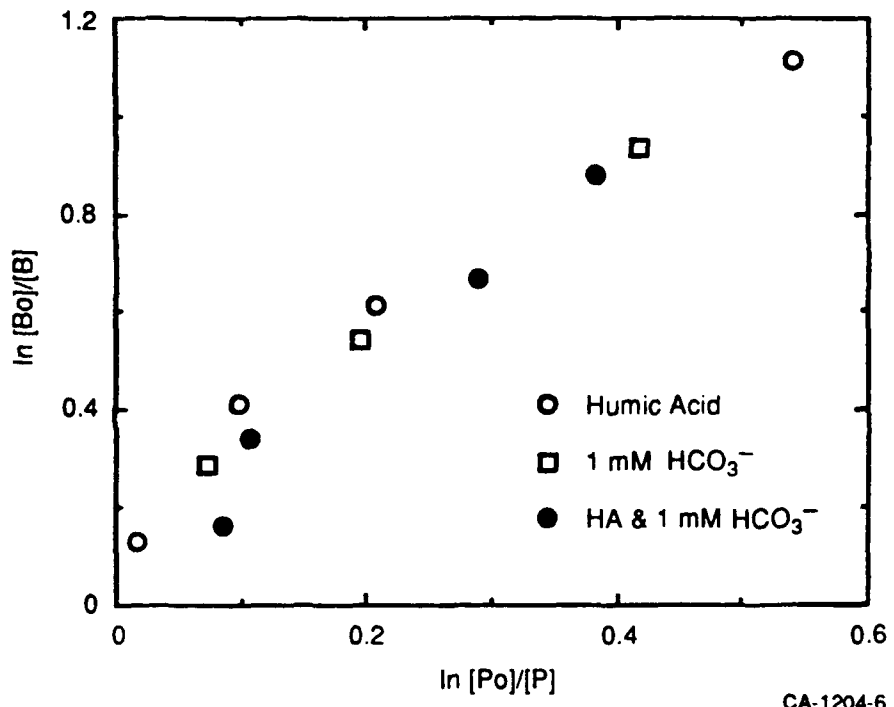


Scheme 2

Secondary oxidants such as HO₂• or RO₂• are unreactive with B or P and do not contribute to the relative reactivity ratio (14). We estimate that for •CO₃⁻ to play a significant role in the oxidation, R_(•CO₃⁻) must be >10% of R_(HO[•]). However, the reactivity ratio of CO₃⁻/HO[•] toward acetate ion is < 1 x 10⁻⁵ and it is unlikely that the •CO₃⁻ steady-state concentration is 10⁴ times that of HO[•] (12,13). The similarities in relative reactivities of B and P in the presence and absence of HCO₃⁻ and humic acid indicate that HO[•] is the dominant oxidant despite the presence of •CO₃⁻ as an additional oxidant.

2. Ozone Systems

Photolysis of ozone produces O(¹D) oxygen atoms, which either inserts in water to form H₂O₂ or form HO[•], which can rapidly decompose ozone or oxidize B and P. H₂O₂ also reacts



CA-1204-6

Figure 4. Reactivity Ratio Plot for Oxidation of Propionate and Butyrate Ions by H_2O_2 in the Presence and Absence of HA HCO_3^- .

rapidly with ozone at pH > 7 to form HO[•]. A simplified O₃/H₂O₂/UV model is presented in Scheme 3.



Scheme 3

3. TiO₂/UV System

The oxidation of organic chemicals on illuminated TiO₂ is well documented, according to the equations in Scheme 4 (15,16).

UV photons promote electrons from the TiO₂ valence band to the conduction band, creating electron/hole pairs. The hole and electron can either recombine or diffuse to the surface where holes and electrons react with surface-adsorbed species, producing HO[•] radical and superoxide ions. HO[•], either bound at the surface or in solution, is believed to be responsible for the oxidation of organic molecules.



Scheme 4

4. Reactivity Ratios for B and P in AOPs

Figures 5 shows results from reactivity ratio measurements with B and P at pH 7.0 in six AOP systems. The reactivity ratio for B and P was found to be 2.2 in all AOPs, close to the calculated ratio based on literature values of k_{HO^\bullet} for B and P (12). The constancy of the reactivity ratio in these systems points to HO^\bullet as the dominant oxidant in all AOPs.

To confirm this conclusion, we also performed experiments with B and P at pH 2.2. The reactivity ratio for butyric and propionic acids (BH and PH) in the $\text{H}_2\text{O}_2/\text{UV}$ and O_3/UV systems are shown in Figure 6. Ratios in Figure 6 are close to 3.5, the same as the ratio of reactivities of BH and PH towards HO^\bullet measured independently at pH 2.2 (Buxton et al., 1988). Again, we find that HO^\bullet is the principal oxidant in AOPs.

B. COMPARISON OF EXPERIMENTS WITH THE MODEL

We believe that the most reliable way to approach identification and quantification of the underlying oxidation chemistries among the AOPs is to develop kinetic models which incorporate all possible important elementary processes together with their rate constants, use existing computer software to solve the differential equations and estimate concentrations of all species as a function of time. The output is then compared with the experiments. The model is a valuable tool for identifying neglected or unneeded reactions, as well as indicating conditions for each AOP needed to achieve optimum efficiency.

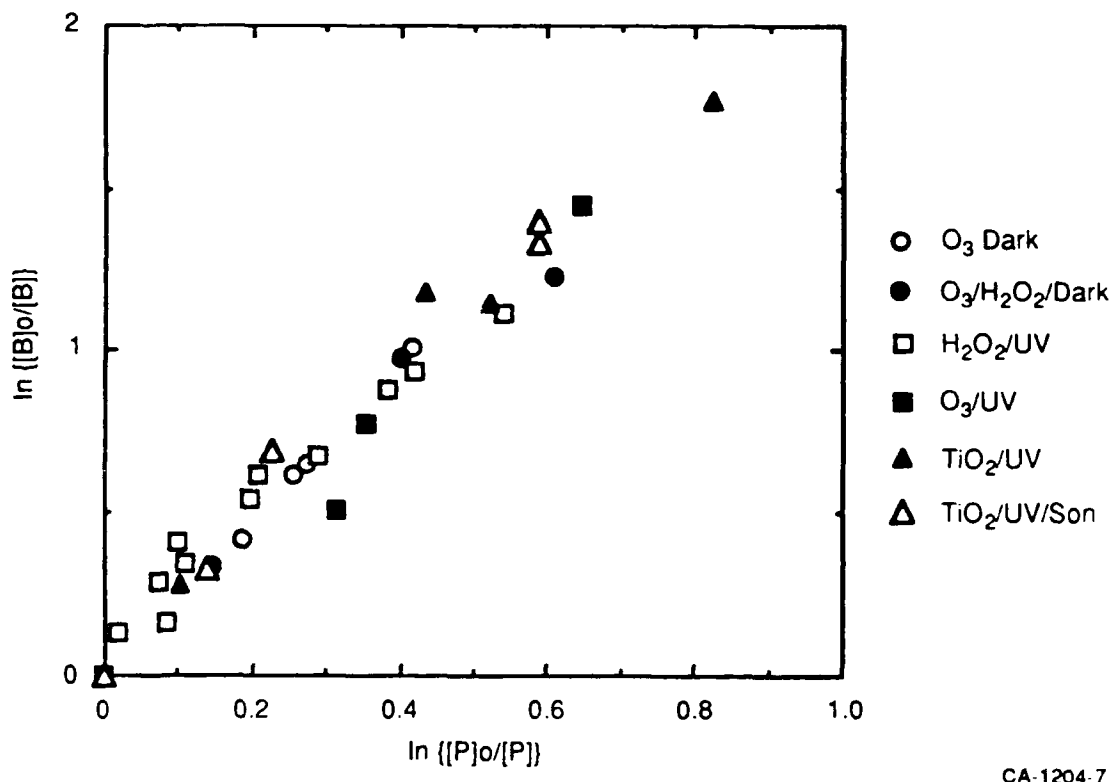


Figure 5. Reactivity Ratio Plot for Propionate and Butyrate Ions in Different Oxidation Systems at pH 7.0.

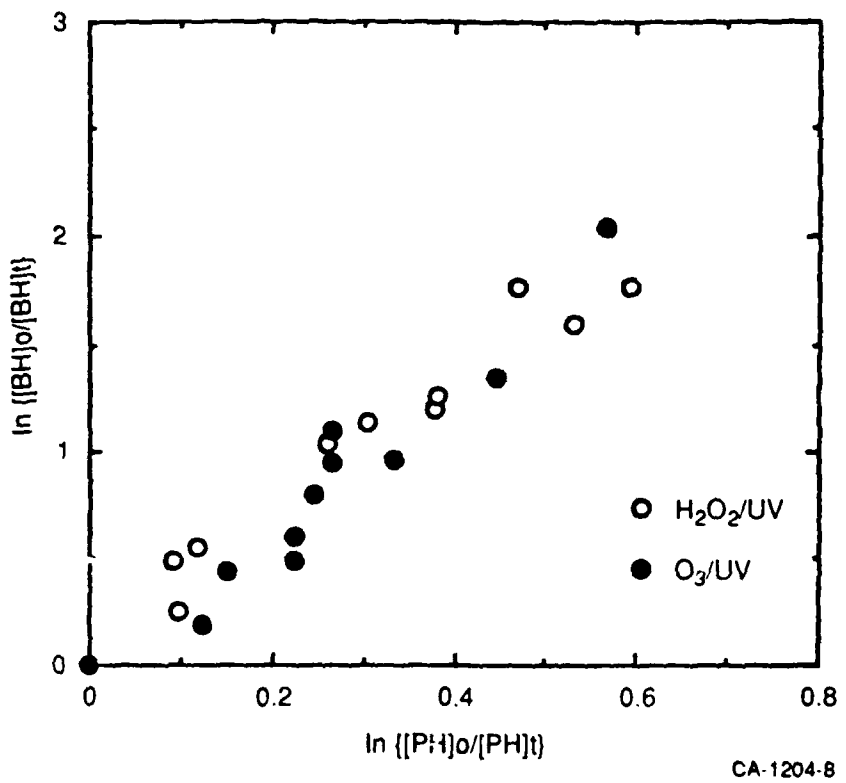


Figure 6. Reactivity Ratio Plot for Propionic and Butyric Acids in $\text{H}_2\text{O}_2/\text{UV}$ and O_3/UV Systems at pH 2.2.

A $\text{H}_2\text{O}_2/\text{UV}$ kinetic model with 45 reactions and an O_3/UV model with 84 reactions were developed to evaluate the role of HO^\bullet in the AOPs (17). Both models were developed with AcuChem software (18). Each model includes four sections: initiation, oxidation, termination steps, and protonation/deprotonation steps for radicals and ionic species. Rate constants are in units of M s^{-1} for zero-order reactions, s^{-1} for unimolecular reactions, and $\text{M}^{-1} \text{s}^{-1}$ for bimolecular reactions. Most of the rate constants are literature values, some are estimated values according to our experimental results, and some are assigned values, based on our best estimates.

1. $\text{H}_2\text{O}_2/\text{UV}$ System

a. $\text{H}_2\text{O}_2/\text{UV}$ Model

In the $\text{H}_2\text{O}_2/\text{UV}$ model (Table 1), chain reactions are initiated by photolysis of peroxide by reaction (R1), carried by the four radical intermediates HO^\bullet , HO_2^\bullet , $\cdot\text{O}_2^-$, and $\cdot\text{CO}_3^-$ (R2, R3, R7, and R8) and terminated through interactions of these radicals (R11-R22). Note that bicarbonate and carbonate* ions scavenge HO^\bullet and generate the secondary carbonate ion radical, $\cdot\text{CO}_3^-$ (R7 -R8); $\cdot\text{CO}_3^-$ terminates with $\cdot\text{O}_2^-$, $\cdot\text{CO}_3^-$, and HO^\bullet (R20-R22). Proton addition and removal steps are included to account for pH effects by adjusting the ratio of forward and reverse reactions equal to 10^{-pK_a} for each species (R23-R38).

R39-R41 and R45-R47 yield no net changes in the concentrations of the oxidized products denoted as A^\bullet , $\cdot\text{B}(\text{O})\text{O}^-$, $\cdot\text{P}(\text{O})\text{O}^-$, $\cdot\text{OOA}$, $\cdot\text{OOB}(\text{O})\text{O}^-$, and $\cdot\text{OOP}(\text{O})\text{O}^-$, respectively, since oxidation of B or P produces products such as alcohol and carbonyl that are about as reactive as the parent compounds toward HO^\bullet (12); Hoigné and Bader (19) also mentioned that extensive oxidation of humic acid with HO^\bullet does not change its HO^\bullet scavenging ability. Reactions of $\cdot\text{O}^-$ are unimportant at pH values below 10 and are not included in the model. Similarly, we found that inclusion of self-reactions of RO_2^\bullet had no effect on the rates of loss of reactants and were ignored, although, under some circumstances, these reactions might play a role.

b. $\text{H}_2\text{O}_2/\text{UV}$ Experiments

To evaluate the role of HO^\bullet in the $\text{H}_2\text{O}_2/\text{UV}$ system, we conducted experiments in the absence and presence of 6 μM B and P each and with different concentrations of HCO_3^- and HA.

* Bicarbonate (HCO_3^-) and carbonate (CO_3^{2-}) ions are included in the model because atmospheric carbon dioxide dissolves in water to generate a carbonate equilibrium system. About 100 μM (C_1) of carbon dioxide ($C_1 = [\text{H}_2\text{CO}_3]^\bullet + [\text{HCO}_3^-] + [\text{CO}_3^{2-}]$; $[\text{H}_2\text{CO}_3]^\bullet = [\text{CO}_2]_{\text{aq}} = K_{\text{HPCO}_2}$) is found in Milli Q water when atmospheric CO_2 is at constant partial pressure ($\text{pCO}_2 = 10^{-3.5}$ atm) above Milli Q water open to the air (20).

TABLE 1. REACTIONS AND RATE CONSTANTS USED TO MODEL PHOTOOXIDATIONS WITH $\text{H}_2\text{O}_2/\text{UV}$ MODEL.

Reaction No.	Reaction Partners	Products	Rate Constant ^a (s^{-1} or $\text{M}^{-1} \text{s}^{-1}$)	Reference
1	$\text{H}_2\text{O}_2 + h\nu$	$= \text{HO}^\bullet + \text{HO}^\bullet$	0.13E-03	b
2	$\text{HO}^\bullet + \text{H}_2\text{O}_2$	$= \text{H}_2\text{O} + \text{HO}_2^\bullet$	0.27E+08	c
3	$\text{HO}^\bullet + \text{HO}_2^-$	$= \text{O}_2^\bullet^- + \text{H}_2\text{O}$	0.75E+10	c
4	$\text{HO}^\bullet + \text{B(O)O}^-$	$= \bullet\text{B(O)O}^- + \text{H}_2\text{O}$	0.20E+10	c
5	$\text{HO}^\bullet + \text{P(O)O}^-$	$= \bullet\text{P(O)O}^- + \text{H}_2\text{O}$	0.82E+09	c
6	$\text{HO}^\bullet + \text{HA}$	$= \text{A}^\bullet + \text{H}_2\text{O}$	0.30E+10	e
7	$\text{HO}^\bullet + \text{HCO}_3^-$	$= \text{H}_2\text{O} + \text{CO}_3^\bullet^-$	0.85E+07	c
8	$\text{HO}^\bullet + \text{CO}_3^{2-}$	$= \text{HO}^\bullet + \text{CO}_3^\bullet^-$	0.39E+09	c
9	$\text{HO}^\bullet + \text{B(O)OH}$	$= \bullet\text{B(O)O}^- + \text{H}_2\text{O}$	0.22E+10	c
10	$\text{HO}^\bullet + \text{P(O)OH}$	$= \bullet\text{P(O)O}^- + \text{H}_2\text{O}$	0.62E+09	c
11	$\text{CO}_3^\bullet^- + \text{P(O)O}^-$	$= \bullet\text{P(O)O}^- + \text{HCO}_3^-$	0.10E+04	f
12	$\text{CO}_3^\bullet^- + \text{B(O)O}^-$	$= \bullet\text{B(O)O}^- + \text{HCO}_3^-$	0.10E+04	f
13	$\text{CO}_3^\bullet^- + \text{H}_2\text{O}_2$	$= \text{HCO}_3^- + \text{HO}_2^\bullet$	0.43E+06	d
14	$\text{CO}_3^\bullet^- + \text{HO}_2^\bullet$	$= \text{O}_2^\bullet + \text{HCO}_3^-$	0.30E+08	d
15	$\text{HO}_2^\bullet + \text{O}_2^\bullet^-$	$= \text{O}_2 + \text{H}_2\text{O}_2$	0.97E+08	c
16	$\text{HO}^\bullet + \text{HO}^\bullet$	$= \text{H}_2\text{O}_2$	0.11E+11	c
17	$\text{HO}^\bullet + \text{HO}_2^\bullet$	$= \text{H}_2\text{O} + \text{O}_2$	0.66E+10	c
18	$\text{HO}^\bullet + \text{O}_2^\bullet^-$	$= \text{HO}^\bullet + \text{O}_2$	0.70E+10	c
19	$\text{HO}_2^\bullet + \text{HO}_2^\bullet$	$= \text{H}_2\text{O}_2 + \text{O}_2$	0.87E+06	g
20	$\text{CO}_3^\bullet^- + \text{O}_2^\bullet^-$	$= \text{CO}_3^{2-} + \text{O}_2$	0.45E+09	d
21	$\text{HO}^\bullet + \text{CO}_3^\bullet^-$	$= \text{zz}$	0.50E+11	f, i
22	$\text{CO}_3^\bullet^- + \text{CO}_3^\bullet^-$	$= \text{xx}$	0.14E+08	d, i
23	HO_2^\bullet	$= \text{O}_2^\bullet^- + \text{H}^+$	0.32E+06	g
24	$\text{O}_2^\bullet^- + \text{H}^+$	$= \text{HO}_2^\bullet$	0.20E+11	g
25	$\text{CO}_3^\bullet^- + \text{H}^+$	$= \text{HCO}_3^\bullet$	0.50E+11	d
26	HCO_3^\bullet	$= \text{H}^+ + \text{CO}_3^\bullet^-$	0.63E+03	d
27	$\text{HCO}_3^- + \text{H}^+$	$= \text{H}_2\text{CO}_3$	0.47E+11	c
28	H_2CO_3	$= \text{H}^+ + \text{HCO}_3^-$	0.21E+05	c
29	$\text{CO}_3^{2-} + \text{H}^+$	$= \text{HCO}_3^-$	0.47E+11	c
30	HCO_3^-	$= \text{H}^+ + \text{CO}_3^{2-}$	0.22E+01	c

TABLE 1. REACTIONS AND RATE CONSTANTS USED TO MODEL
PHOTOXIDATIONS WITH $\text{H}_2\text{O}_2/\text{UV}$ MODEL
(concluded)

Reaction No.	Reaction Partners	Products	Rate Constant ^a (s^{-1} or $\text{M}^{-1} \text{s}^{-1}$)	Reference
31	$\text{H}^+ + \text{HO}^-$	$= \text{H}_2\text{O}$	0.14E+12	h
32	H_2O	$= \text{H}^+ + \text{HO}^-$	0.25E-04	h
33	$\text{H}^+ + \text{HO}_2^-$	$= \text{H}_2\text{O}_2$	0.50E+11	c
34	H_2O_2	$= \text{H}^+ + \text{HO}_2^-$	0.10E+00	c
35	$\text{B}(\text{O})\text{O}^- + \text{H}^+$	$= \text{B}(\text{O})\text{OH}$	0.50E+11	h
36	$\text{B}(\text{O})\text{OH}$	$= \text{B}(\text{O})\text{O}^- + \text{H}$	0.80E+06	h
37	$\text{P}(\text{O})\text{O}^- + \text{H}^+$	$= \text{P}(\text{O})\text{OH}$	0.50E+11	h
38	$\text{P}(\text{O})\text{OH}$	$= \text{P}(\text{O})\text{O}^- + \text{H}^+$	0.80E+06	h
39	$\text{HO}^\cdot + \text{A}^\cdot$	$= \text{A}^\cdot + \text{H}_2\text{O}$	0.30E+10	f
40	$\cdot\text{B}(\text{O})\text{O}^- + \text{O}_2$	$= \cdot\text{OO B}(\text{O})\text{O}^-$	0.10E+10	f
41	$\cdot\text{P}(\text{O})\text{O}^- + \text{O}_2$	$= \cdot\text{OO P}(\text{O})\text{O}^-$	0.10E+10	f
42	$\cdot\text{A}^\cdot + \text{O}_2$	$= \cdot\text{OOA}$	0.10E+10	f
43	$\text{HO}^\cdot + \cdot\text{OO B}(\text{O})\text{O}^-$	$= \cdot\text{OO B}(\text{O})\text{O}^-$	0.20E+10	f
44	$\text{HO}^\cdot + \cdot\text{OO P}(\text{O})\text{O}^-$	$= \cdot\text{OO P}(\text{O})\text{O}^-$	0.82E+09	f
45	$\text{HO}^\cdot + \cdot\text{OOA}$	$= \cdot\text{OOA}$	0.30E+10	f

aRead 0.1300E-03 as 1.3×10^{-4} .

bEstimated value from experiments.

cBuxton et al., 1988 (Reference 12).

dNeta et al., 1988 (Reference 13).

eThis work.

fAssigned value.

gBielski et al., 1985 (Reference 14).

hAnalytical chemistry.

iz and xx are unknown products.

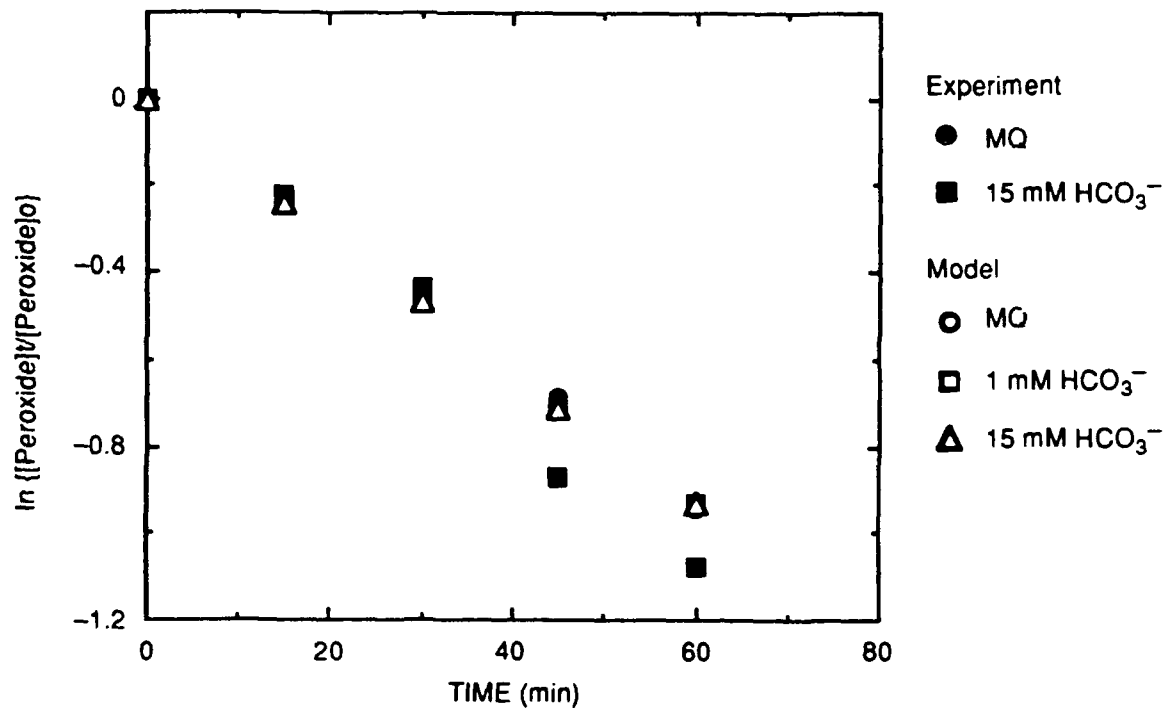
The scavenging rate for HO[•] in this concentration range of HCO₃⁻ and HA should be as large as possible while the concentrations of B and P should be as low as possible, in order not to affect [HO]_{ss} in the system.

Figure 7 shows that the measured and calculated peroxide losses in Milli-Q water alone (0.10 mM HCO₃⁻) or with different amount of bicarbonate ion up to 15 mM are in excellent agreement. Our interpretation of the lack of effect of bicarbonate ion in both model and experiments is that, although high concentrations of HCO₃⁻ scavenge nearly all HO[•] and prevent its attack on H₂O₂, •CO₃⁻ radicals themselves oxidize H₂O₂ efficiently, resulting in the same net loss of H₂O₂, and even 15 mM HCO₃⁻ has no significant effect on the loss rate of H₂O₂.

In the presence of 5 ppm HA, the experimental slope is about 25 percent lower than the slope calculated by the model (Figure 8). This result is consistent humic acid solutions absorbing about 20 percent of the light at 254 nm in this experiment and thus slowing photolysis. Furthermore, we believe that the rate found in the presence of humic acid is the rate of primary photolysis of H₂O₂, because 5 ppm humic acid scavenges all HO[•] and very efficiently suppresses any chain decomposition of H₂O₂. The rate of H₂O₂ consumption in Milli-Q water (Figure 9) is about twice as fast as with humic acid present because, under these conditions, R1 - R3 and R15 control the process and yield a net loss of 2 H₂O₂ per primary photolytic event. Any regeneration of H₂O₂ with HA present would be observed as a reduction in the rate constant for H₂O₂ loss. Thus, the agreement of the slopes for the presence of HA yields the significant conclusion that HO[•] attack on HA does not yield daughter radicals that regenerate H₂O₂ to any great extent. This conclusion will be important in modeling other radical oxidation systems. However, the effect of HA on ozone oxidations is more complicated (see IIB2).

Tables 2 and 3 give the measured and calculated results for the H₂O₂/UV system. Table 2 shows the hydrogen peroxide consumption rates in the presence and absence of B and P. Table 3 summarizes oxidation rates for B. In most cases, replicate experiments for loss of peroxide or B are in good agreement with each other. Only in the case of 1 mM HCO₃⁻ is the difference between experiment and model greater than a factor of two; all other experimental rates for loss of B and peroxide agree well with the predicted results.

In contrast to the lack of effect on oxidation of H₂O₂, HCO₃⁻ inhibits the oxidation of B as expected if •CO₃⁻ radical is very much less reactive than HO[•] in oxidizing CH bonds. Humic acid also inhibits loss of B in good agreement between experiment and model.



CA-1204-9

Figure 7. Comparison of Peroxide Loss in the Experiments and Model with Bicarbonate at pH 8.

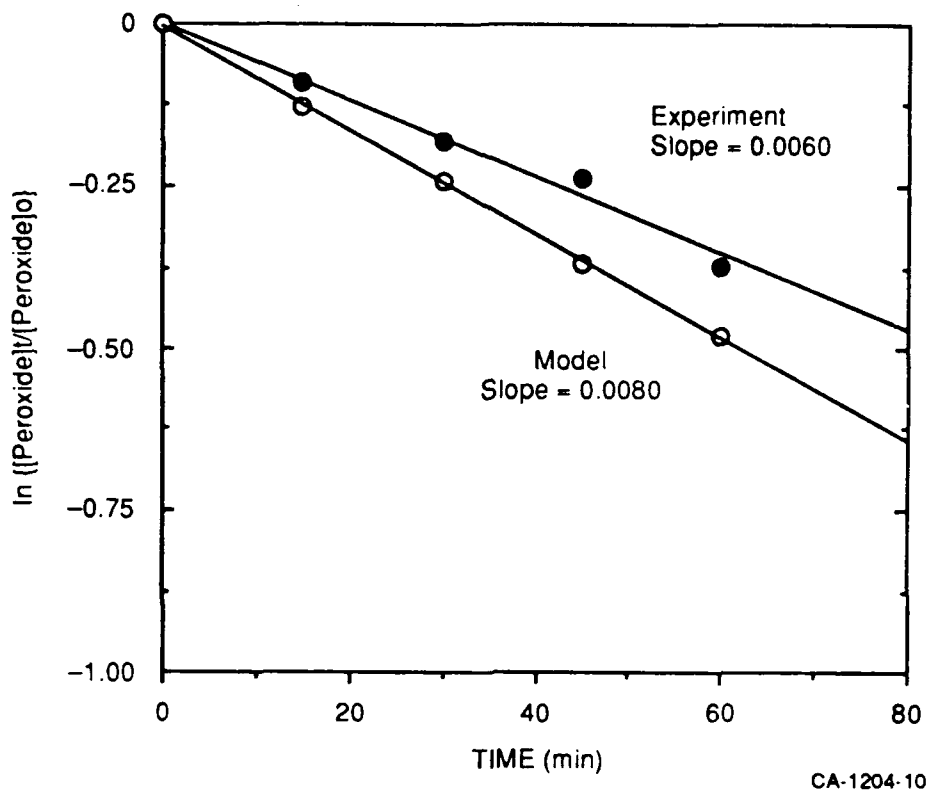


Figure 8. Comparison of Peroxide Loss in the Experiment and Model with 5 ppm Humic Acid at pH 8.

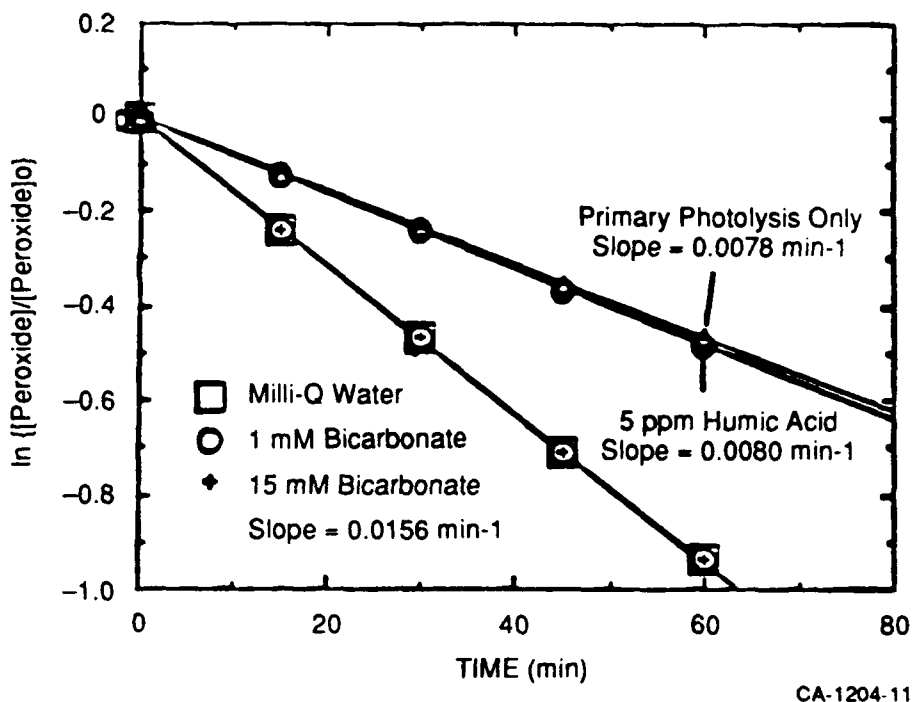


Figure 9. Calculated Hydrogen Peroxide Loss in the Absence of Butyrate and Propionate Ions under Various Conditions.

TABLE 2. OXIDATION RATES FOR H_2O_2 IN THE PRESENCE AND ABSENCE OF BUTYRATE AND PROPIONATE: EXPERIMENTS VERSUS MODEL.

Humic Acid (μM) ^b	HCO_3^- (mM)	$k[\text{H}_2\text{O}_2]_0 \times 10^9 (\text{M s}^{-1})^a$			
		Absence of B & P		Presence of B & P	
Exp	Model	Exp 1	Exp 2	Model	
0	0	26.2	26.0	18.1	19.5
0	1	--	26.0	27.8	30.1
0	15	31.1	26.0	15.1(?)	29.3
					32.9
25	0	12.5	13.5 ^c	12.5	9.5
25	1	--	--	13.5	--

^aPeroxide initial concentration is 100 μM .

^bAssuming the average molecular weight of humic acid is 200 g/mole.

^cThis value is corrected by photoscreening effect.

TABLE 3. OXIDATION RATES FOR BUTYRATE ION: EXPERIMENTS VERSUS MODEL^a

Humic Acid (μM) ^b	HCO_3^- (mM)	$k[\text{Bo}] \times 10^9 (\text{M s}^{-1})$		
		Presence of B & P		Model
Exp 1	Exp 2			
0	0	--	7.6	12.1
0	1	2.2	2.8	8.6
0	15	0.1(?)	0.5, 0.5	1.0
25	0	2.1	3.2	2.1 ^c
25	1	1.7	--	2.3 ^c

^aThe concentrations of H_2O_2 and butyrate ion are 100 μM and 6 μM respectively.

^bAssuming the average molecular weight of humic acid is 200 g.mole.

^cThis value is corrected for photoscreening effect.

2. Ozone Systems

Two kinds of ozone systems were studied: ozone in the dark and ozone in the light. Ozone decomposes in the dark by a chain reaction initiated by HO^- and propagated by $\cdot\text{O}_2^-$. The major products are oxygen and H_2O_2 (6). Peroxide (via HO_2^-) continues the chain (see Figure 3). Thus any kinetic model that is developed to describe ozone decomposition must include the $\text{O}_3/\text{H}_2\text{O}_2$ system as well.

a. Ozone Model

We developed a dual O_3/Dark and O_3/UV kinetic model with 84 reactions that can be applied to both the dark and light systems. The model includes both UV and HO^- initiation as well as the $\text{H}_2\text{O}_2/\text{HO}^\bullet$ system and chain reactions of ozone. Reactions in the model are listed in Table 4. The chain process is initiated in the dark by reaction of ozone with hydroxide ion, peroxide anion, peroxide, and water (R6-R9). Hydroxyl radicals, superoxide CO_2^\bullet and ozonide CO_3^\bullet carry the chain reactions (R10 - R21). Superoxide is the product of R6, R16, and R22. Ozonide comes from R7 and R11 and is the precursor of HO^\bullet . HO^\bullet reacts with ozone and ozonide and generates superoxide (R10 and R22). Carbonate and bicarbonate ions scavenge HO^\bullet (R17-R19) and shorten the chain reactions. R24 - R36 are radical termination reactions involving the inorganic species. R37 - R62 are the equilibrium proton reactions with rate constants adjusted to give proton transfers to anions of $5 \times 10^{10} \text{ M}^{-1} \text{ s}^{-1}$ and the back reactions set to give the value of K_a according to the $\text{pK}_{\text{a}s}$ of the species of interest.

R63 - R65 are the oxidizing reactions for AH, B/BH and P/PH by HO^\bullet . R70-R71 are the representative ways to produce the second generation products. Note that R68-70 and R76-R83 yield no net change in the concentrations of the oxidized products denoted as A^\bullet , $\cdot\text{B}(\text{O})\text{O}^-$, $\cdot\text{P}(\text{O})\text{O}^-$, $\cdot\text{OOA}$, $\cdot\text{OOB}(\text{O})\text{O}^-$, and $\cdot\text{OOP}(\text{O})\text{O}^-$, respectively, to reflect that these products have reactivities similar to the parent compounds toward the free radical species. R79-R83 represent contributions to ozone consumption from direct oxidation of the oxidation products.

b. Ozone Experiments

The ozone system includes three types of initiation species: HO^- , HO_2^- , and UV light. Each initiation step will generate HO^\bullet with its propagation reactions. To evaluate their relative importance, we first performed experiments to understand the role of light in the generation of HO^\bullet in this section. Second, we studied the roles of HO_2^- and HO^\bullet in the ozone

TABLE 4. REACTIONS AND RATE CONSTANTS USED IN THE O₃/DARK AND O₃/UV MODELS.

Reaction No.	Reaction Partners	Products	Rate Constant ^a s ⁻¹ or M ⁻¹ s ⁻¹	Reference
1		= $h\nu$	0.20E-06	f
2	O ₃ + $h\nu$	= O + O ₂	0.10E+10	f
3	O + H ₂ O	= HO [•] + HO [•]	0.11E+08	f
4	O + H ₂ O	= H ₂ O ₂	0.22E+09	f
5	H ₂ O ₂ + $h\nu$	= HO [•] + HO [•]	0.10E-05	b
6	O ₃ + HO [•]	= HO ₂ [•] + O ₂ [•]	0.70E+02	d
7	O ₃ + HO ₂ [•]	= HO ₂ [•] + O ₃ [•]	0.55E+07	d
8	O ₃ + H ₂ O ₂	= H ₂ O + 2O ₂	0.65E-02	d
9	O ₃ + H ₂ O	= ee	0.10E-07	d, l
10	O ₃ + HO [•]	= HO ₂ [•] + O ₂	0.11E+09	c
11	O ₃ + O ₂ [•]	= O ₃ [•] + O ₂	0.16E+10	d
12	O ₃ + CO ₃ ²⁻	= dd	0.10E+06	d, l
13	HO ₃ [•]	= HO [•] + O ₂	0.14E+06	i
14	O [•] + H ₂ O	= HO [•] + HO [•]	0.17E+07	c
15	HO [•] + H ₂ O ₂	= H ₂ O + HO ₂ [•]	0.27E+08	c
16	HO [•] + HO ₂ [•]	= O ₂ [•] + H ₂ O	0.75E+10	c
17	HO [•] + CO ₃ ²⁻	= HO [•] + CO ₃ [•]	0.39E+09	c
18	HO [•] + HCO ₃ ⁻	= CO ₃ [•] + H ₂ O	0.85E+07	c
19	HO [•] + H ₂ CO ₃	= HCO ₃ [•] + H ₂ O	0.10E+07	c
20	CO ₃ [•] + H ₂ O ₂	= HO ₂ [•] + HCO ₃ ⁻	0.43E+06	d
21	CO ₃ [•] + HO ₂ [•]	= O ₂ [•] + HCO ₃ ⁻	0.30E+08	d
22	O ₃ [•] + HO [•]	= O ₂ [•] + HO ₂ [•]	0.60E+10	j
23	O ₃ [•] + HO [•]	= O ₃ + HO [•]	0.25E+10	j
24	HO ₂ [•] + O ₂ [•]	= O ₂ + H ₂ O ₂	0.97E+08	g
25	HO [•] + HO [•]	= H ₂ O ₂	0.11E+11	c
26	HO [•] + O [•]	= HO ₂ [•]	0.20E+11	c
27	HO ₂ [•] + HO [•]	= H ₂ O + O ₂	0.66E+10	c
28	HO [•] + O ₂ [•]	= HO [•] + O ₂	0.80E+10	c
29	HO [•] + HO ₃ [•]	= H ₂ O ₂ + O ₂	0.50E+10	i

TABLE 4. REACTIONS AND RATE CONSTANTS USED IN THE O₃/DARK AND O₃/UV MODELS.

(Continued)

Reaction No.	Reaction Partners	Products	Rate Constant ^a s ⁻¹ or M ⁻¹ s ⁻¹	Reference
30	HO ₃ • + HO ₃ •	= H ₂ O ₂ + O ₂	0.50E+10	i
31	HO ₃ • + O ₂ •	= HO• + O ₂	0.10E+11	i
32	HO ₂ • + HO ₂ •	= H ₂ O ₂ + O ₂	0.87E+07	c
33	CO ₃ • + CO ₃ •	= bb	0.14E+08	d, i
34	CO ₃ • + HO•	= aa	0.50E+10	f, n
35	CO ₃ • + O ₂ •	= CO ₃ ⁻² + O ₂	0.65E+09	d
36	CO ₃ • + O ₃ •	= O ₃ + CO ₃ ⁻²	0.60E+08	d
37	O• + H ⁺	= HO•	0.50E+11	c
38	HO•	= O• + H ⁺	0.63E-01	c
39	HO ₂ •	= O ₂ • + H ⁺	0.32E+05	m
40	O ₂ • + H ⁺	= HO ₂ •	0.20E+10	m
41	HCO ₃ ⁻ + H ⁺	= H ₂ CO ₃	0.47E+11	c
42	H ₂ CO ₃	= H ⁺ + HCO ₃ ⁻	0.21E+05	c
43	CO ₃ ⁻² + H ⁺	= HCO ₃ ⁻	0.47E+11	c
44	HCO ₃ ⁻	= H ⁺ + CO ₃ ⁻²	0.22E+01	c
45	CO ₃ • + H ⁺	= HCO ₃ •	0.50E+11	d
46	HCO ₃ •	= H ⁺ + CO ₃ •	0.63E+03	d
47	HO ₃ •	= O ₃ • + H ⁺	0.33E+03	K
48	O ₃ • + H ⁺	= HO ₃ •	0.52E+11	K
49	H ⁺ + HO•	= H ₂ O	0.14E+12	h
50	H ₂ O	= H ⁺ + HO•	0.25E+04	h
51	H ⁺ + HO ₂ •	= H ₂ O ₂	0.50E+11	c
52	H ₂ O ₂	= H ⁺ + HO ₂ •	0.10E+00	c
53	H ₃ PO ₄	= H ⁺ + H ₂ PO ₄ ⁻	0.32E+09	d
54	H ⁺ + H ₂ PO ₄	= H ₃ PO ₄	0.50E+11	d
55	H ₂ PO ₄ ⁻	= H ⁺ + HPO ₄ ⁻²	0.32E+04	d
56	HPO ₄ ⁻² + H ⁺	= H ₂ PO ₄ ⁻	0.50E+11	d
57	HPO ₄ ⁻²	= H ⁺ + PO ₄ ⁻³	0.22E-02	d
58	PO ₄ ⁻³ + H ⁺	= HPO ₄ ⁻²	0.50E+12	d

TABLE 4. REACTIONS AND RATE CONSTANTS USED IN THE O₃/DARK AND O₃/UV MODELS.

Reaction No.	Reaction Partners	Products	(concluded) Rate Constanta s ⁻¹ or M ⁻¹ s ⁻¹	Reference
59	B(O)O ⁻ + H ⁺	= B(O)OH	0.50E+11	h
60	B(O)OH	= B(O)O ⁻ + H ⁺	0.80E+06	h
61	P(O)O ⁻ + H ⁺	= P(O)OH	0.5E+11	h
62	P(O)OH	= P(O)O ⁻ + H ⁺	0.80E+06	h
63	HO [•] + B(O)O ⁻	= •B(O)O ⁻ + H ₂ O	0.20E+10	c
64	HO [•] + P(O)O ⁻	= •P(O)O ⁻ + H ₂ O	0.82E+09	c
65	HO [•] + HA	= A [•] + H ₂ O	0.30E+10	e
66	HO [•] + B(O)OH	= •B(O)O ⁻ + H ₂ O	0.22E+10	c
67	HO [•] + P(O)OH	= •P(O)O ⁻ + H ₂ O	0.62E+09	c
68	HO [•] + A [•]	= A [•] + H ₂ O	0.30E+10	f, m
69	HO [•] + •B(O)O ⁻	= •B(O)O ⁻ + H ₂ O	0.20E+10	f, m
70	HO [•] + •P(O)O ⁻	= •P(O)O ⁻ + H ₂ O	0.82E+09	f, m
71	CO ₃ ²⁻ + P(O)O ⁻	= •P(O)O ⁻ + H ₂ O	0.10E+04	f, m
72	CO ₃ ²⁻ + B(O)O ⁻	= •B(O)O ⁻ + H ₂ O	0.10E+04	f, m
73	O ₂ + •P(O)O ⁻	= •OOP(O)O ⁻	0.10E+10	g, f
74	O ₂ + •B(O)O ⁻	= •OOB(O)O ⁻	0.10E+10	g, f
75	O ₂ + •A	- •OOA	0.10E+10	f, g
76	HO [•] + •OOA	= •OOA	0.30E+10	f, m
77	HO [•] + •OOP(O)O ⁻	= •OOP(O)O ⁻	0.82E+09	m, f
78	HO [•] + •OOB(O)O ⁻	= •OOB(O)O ⁻	0.20E+10	f, m
79	O ₃ + •OOB(O)O ⁻	= •OOB(O)O ⁻ + HO [•]	0.10E+02	f
80	O ₃ + •OOP(O)O ⁻	= •OOP(O)O ⁻ + HO [•]	0.10E+02	f
81	O ₃ + •OOA	= HO(O)O ⁻	0.10E+02	f
82	O ₃ + HP(O)O ⁻	= •OOP(O)O ⁻	0.50E+01	f
83	O ₃ + HB(O)O ⁻	= HB(O)O ⁻	0.50E+01	f
84	O ₃ + AH	= AH	0.50E+01	f

^aRead 0.1300E-03 as 1.3 x 10⁻⁴. ^bEstimated value from experiments. ^cBuxton et al., 1988.

^dNeta et al., 1988 (Reference 13). ^eThis work. ^fAssigned value. ^gBielski et al., 1985, pka = 4.8.

^hAnalytical chemistry. ⁱHoigné et al., 1984 (Reference 40). ^jTomiyasu et al., 1985 (Reference 41).

^kHoigné et al., 1984a,b (Reference 42). ^laa, bb, dd, ee are unknown products. ^mHoigné et al., 1979 (Reference 19).

chain reactions. Third we compared the relative rates, of these three initiation steps, oxidation rates, and relative efficiencies as described in Section C.

(1) The Role of Light. In the O_3/UV system, ozone is photolyzed to O atom which reacts with water in two ways: one is to generate hydrogen peroxide directly (R4) and one is to generate $HO\cdot$ (R3). To evaluate their relative importance we photolyzed ozone at pH 2.2, where H_2O_2 is stable in the presence of ozone because the ozone- $HO_2\cdot$ chain reaction is unimportant and measured the peroxide formed (Figure 10). To confirm the importance of the ozone- $HO\cdot$ chain reactions, we also photolyzed ozone with H_2O_2 at pH 2.2 in the presence of 6 μM B and P to scavenge any $HO\cdot$. To evaluate the ozone model, the results from models under the same conditions were compared with those from the experiments in both cases.

Figure 10 shows results of monitoring H_2O_2 production on photolysis of 100 μM O_3 . We found a maximum of 20 percent H_2O_2 forms when all O_3 is photolyzed. By modeling the system with different values of R_3/R_4 corresponding to 0.0, 0.01, 0.03, 0.05 and 0.1 we found good agreement with experiment with a value of 0.05 (5 percent). This result is included in the model with 6 μM BH and PH at pH 2.2 as shown in Figure 11 and indicates that the ozone model can reasonably predict the changes of peroxide and ozone at pH 2.2. Peroxide increased from 20 percent to 90 percent, based on ozone lost, because of scavenging of 80 percent of $HO\cdot$ by 6 μM PH and BH, thus cutting the $HO\cdot/O_3$ chain leading to oxygen (R10, R11, R13).

To further evaluate the ozone model, we compared calculated and measured ozone and peroxide changes at pH 7 where peroxide is not stable. The results, shown in Figure 12, also are in good agreement.

Based on the calculated losses of B, ozone, the increase of peroxide, and the measured relative reactivity of B and P, we concluded that $HO\cdot$ is the principal oxidant in the O_3/UV system and $[HO\cdot]_{ss}$ can be simulated properly in the model.

(2) The Roles of $HO_2\cdot$ and $HO\cdot$. To understand the roles of $HO_2\cdot$ and $HO\cdot$ in the ozone chain reactions, we performed experiments with and without hydrogen peroxide. In the absence of hydrogen peroxide, the $O_3/HO\cdot$ system (which includes the $H_2O_2/HO\cdot$ system and ozone chain reactions) indicates the roles of the $HO\cdot$ and chain reactions at different pHs. In the presence of hydrogen peroxide, the system includes $HO_2\cdot$ for consumption of ozone at high pH.

Figures 13 and 14 present the measured and calculated losses of ozone in the dark at pHs 2.7, 7.0, and 9.1 where the measured half-lives are 3.0 hours, 1.1 hours, and 79 seconds, respectively. The calculated half-lives at these same pHs are 1203 hours, 0.7 hours and

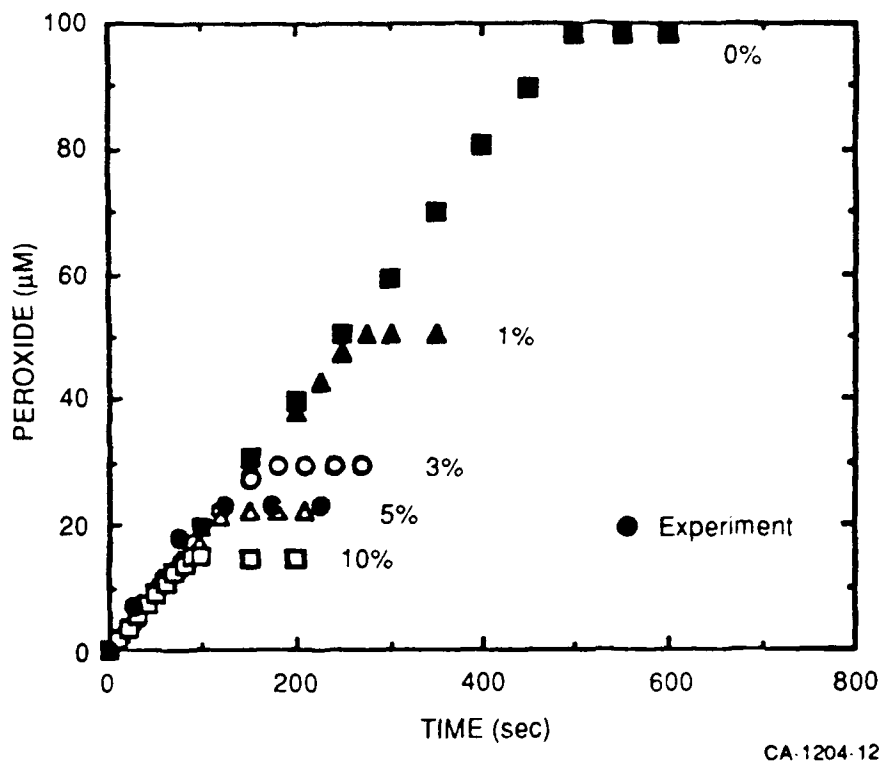
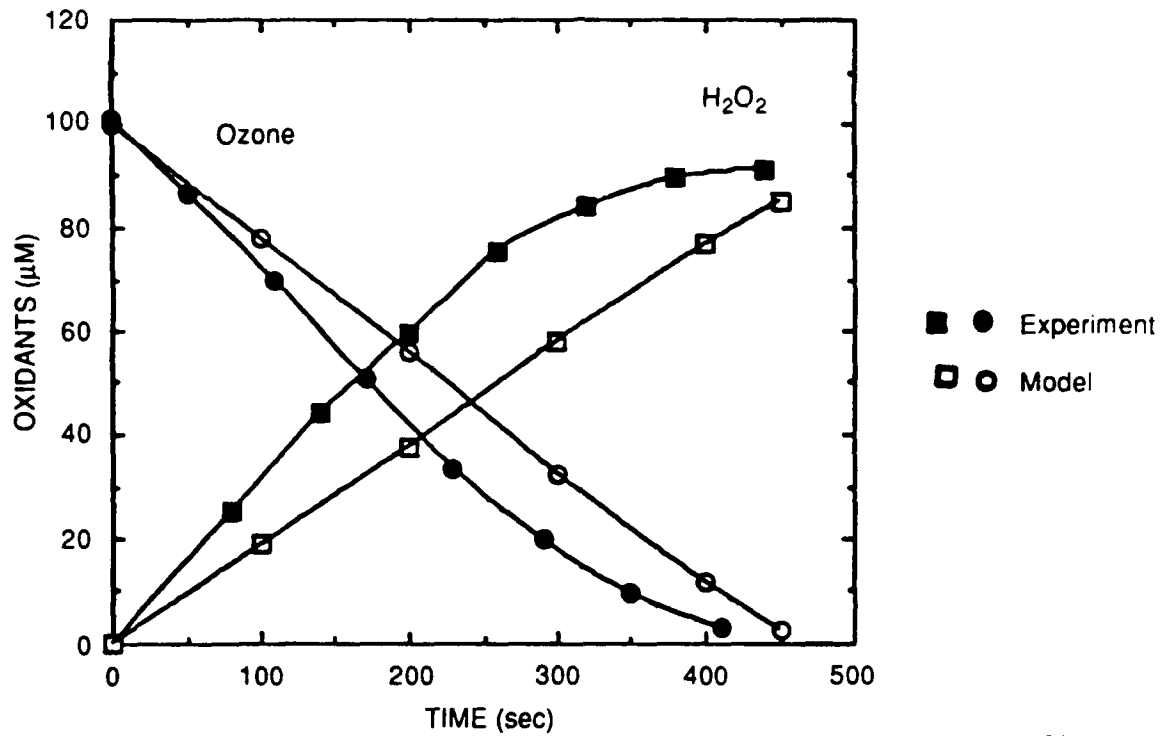
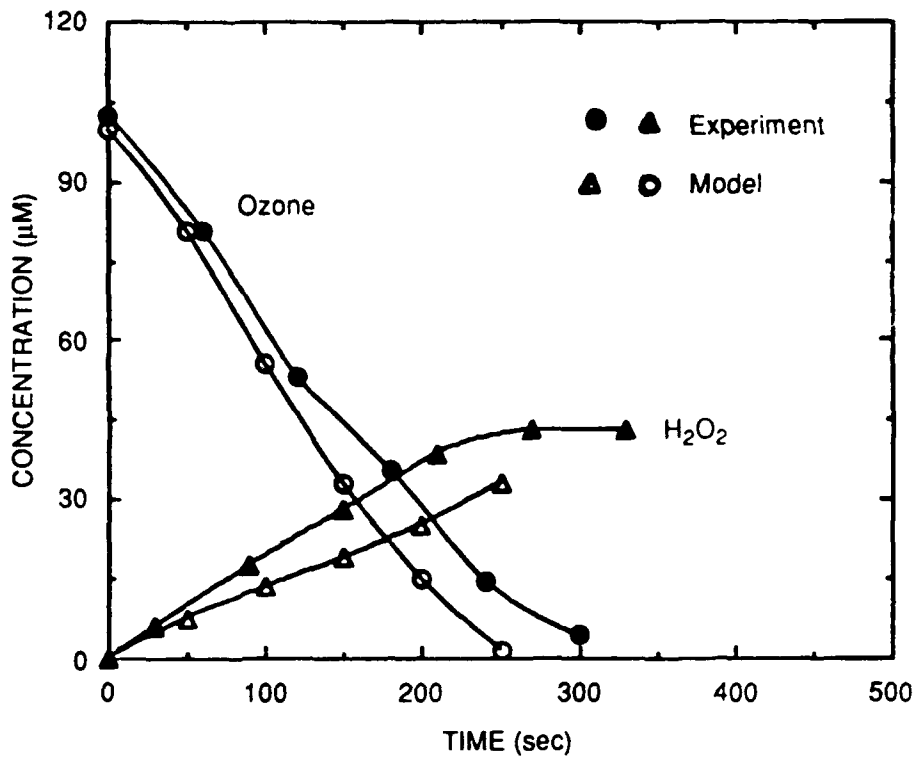


Figure 10. Calculated Peroxide Increases in the Light and in the Absence of BH and PH for Different Percentage of Direct Generation of HO Radical from $100 \mu\text{M}$ Ozone at pH 2.2.



CA-1204-13

Figure 11. Measured and Calculated Losses of Ozone and the Increases of Hydrogen Peroxide in the O₃/UV System in the Presence of 6 μM BH and PH at pH 2.2.



CA-1204-14

Figure 12. Measured and Calculated Ozone Losses and Peroxide Increases in a O₃/H₂O₂/UV System in the Presence of 6 μM BH and PH at pH 7.0.

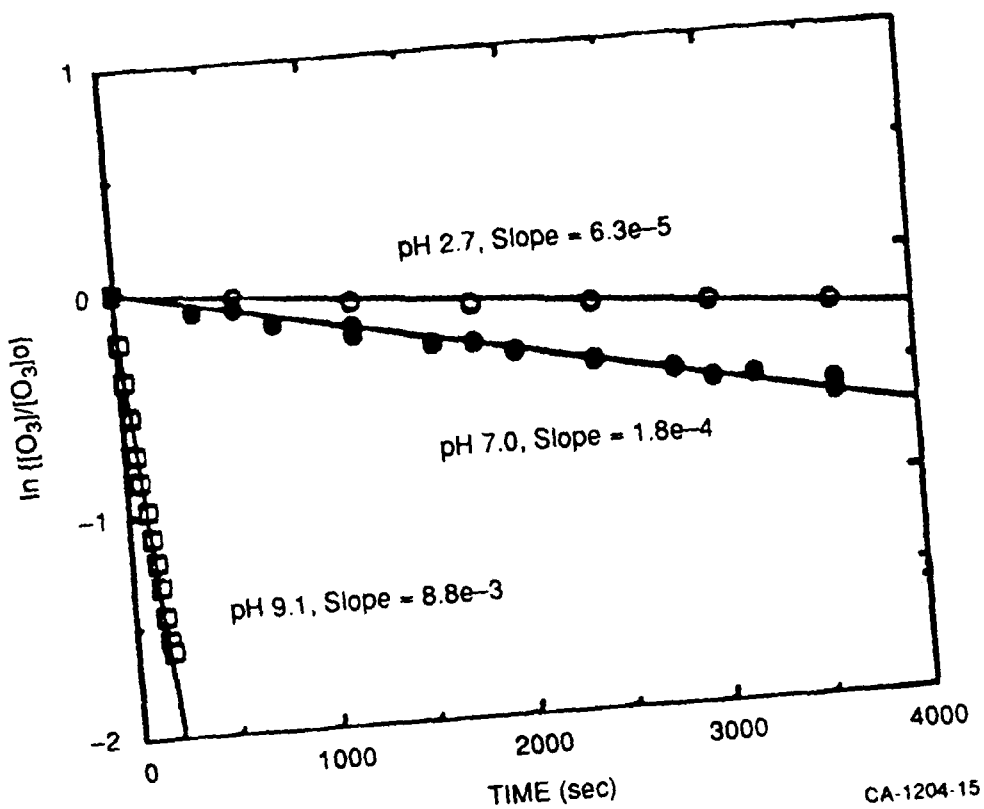
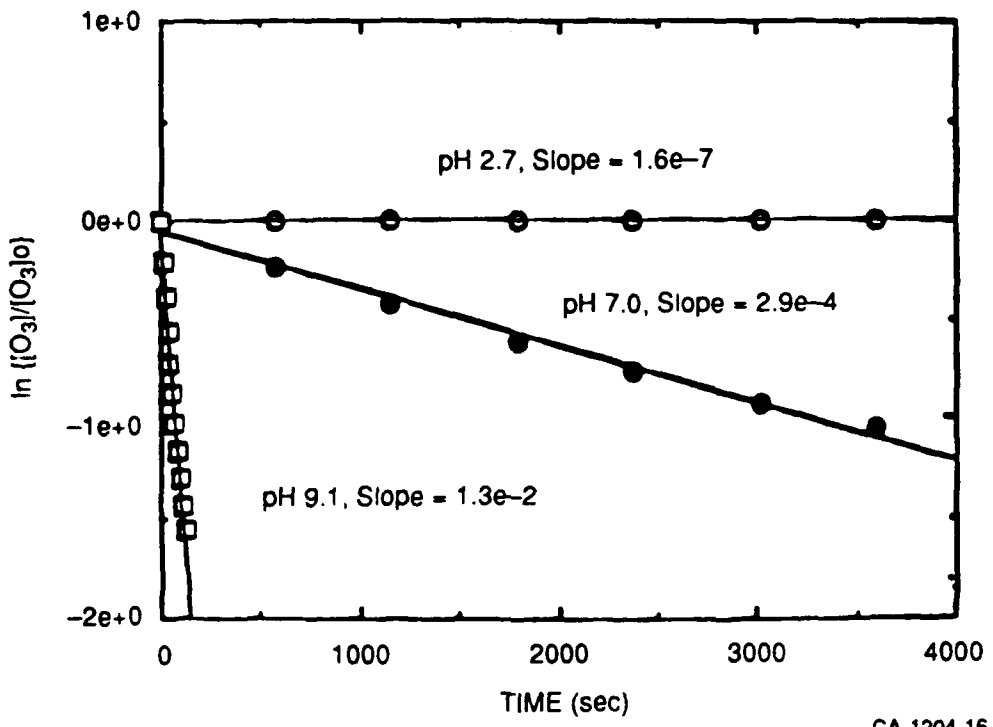


Figure 13. Measured Ozone Loss in the Absence of Peroxide in a $O_3/H_2O_2/\text{Dark}$ System
at Different pHs.



CA-1204-16

Figure 14. Calculated Ozone Loss in the Absence of Peroxide in a O_3/H_2O_2 /Dark Model at Different pHs.

53 seconds, respectively. The ozone half-lives from the model agree with those from the experiments within a factor two at pH 7 and 9.1 but not at pH 2.7, where the observed rate is nearly 400 times faster, indicating the influence of unknown catalysts.

In the absence of B, P and HA, natural bicarbonate ion (100 μM) competes with ozone to scavenge ~8 percent and ~80 percent of HO^\bullet when the ozone concentration is 100 μM and 10 μM , respectively. Therefore, bicarbonate plays an important role in shortening the chain length of the HO^\bullet chain reactions.

When the pH changes from 7.0 to 9.1, the consumption rate of ozone increases about 50 times while hydroxide ion concentration ($[\text{HO}^-]$) increases 100 times, both in experiments and in the model illustrating the dominant, but not sole, role of HO^\bullet in destroying ozone at higher pH. However, ozone half-lives at pH 2.7 to 7.0 are in the range of hours, but the changes are not consistent between the experiments and the model. The consumption rate of ozone increases only 3 times in experiments at pH 2.7 and 7.0 but about 2000 times in the model, while $[\text{HO}^-]$ increases 2.0×10^4 times. These differences are due to unexplained catalysis of the pH 2.7 reactions which makes the rate similar to the pH 7 rate. At pH 7 HO^\bullet is much more important as an initiator.

The effect of added peroxide on ozone loss rates is shown in Figures 15 and 16. The measured losses of ozone have half-lives of 2.6 hours and 29 seconds at pH 2.7 and 6.9, respectively (Figure 15), in fair to good agreement with model values of 7.7 hours and 39 seconds (Figure 16). Again, the larger discrepancy at pH 2.7 is probably due to catalytic effects on ozone loss, not accounted for by our model. Despite catalysis, the long life for ozone at pH 2-2.7 shows that ozone is stable in the presence of molecular peroxide because the chain reactions initiated by peroxide anion are negligible. However, the half-life of ozone at pH 7 of less than 50 seconds is caused by chain reactions with HO_2^- , which is in the range of $\sim 10^{-10} \text{ M}$.

Figures 17 and 18 show the measured and calculated losses of B and ozone in a O_3/Dark system in the presence of 6 μM B and P at pH 7.0. The experimental half-lives of B and ozone are 2400 and 5450 seconds, respectively compared with calculated half lives of 2400 and 5600 seconds. Based on the calculated losses of B, ozone, and the measured relative reactivity of B and P, we conclude that HO^\bullet is also the principal oxidant in the O_3/Dark system and that $[\text{HO}^\bullet]_{\text{ss}}$ can be simulated properly in the model.

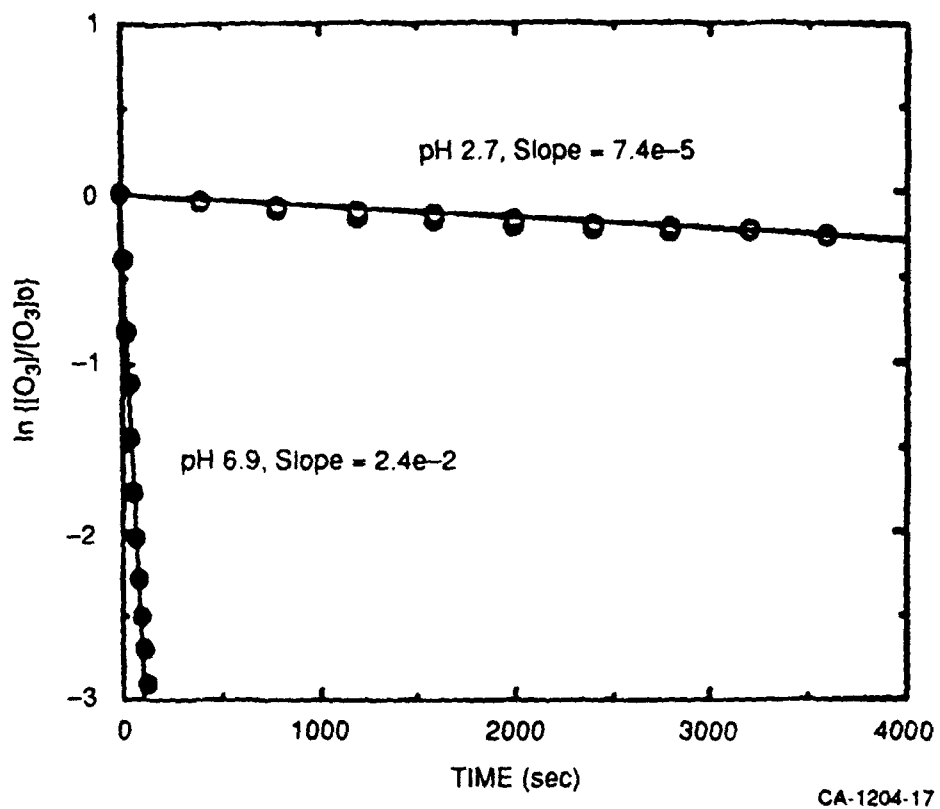


Figure 15. Measured Ozone Loss in the Presence of 10 μM Peroxide in a $\text{O}_3/\text{H}_2\text{O}_2/\text{Dark}$ System at Different pHs.

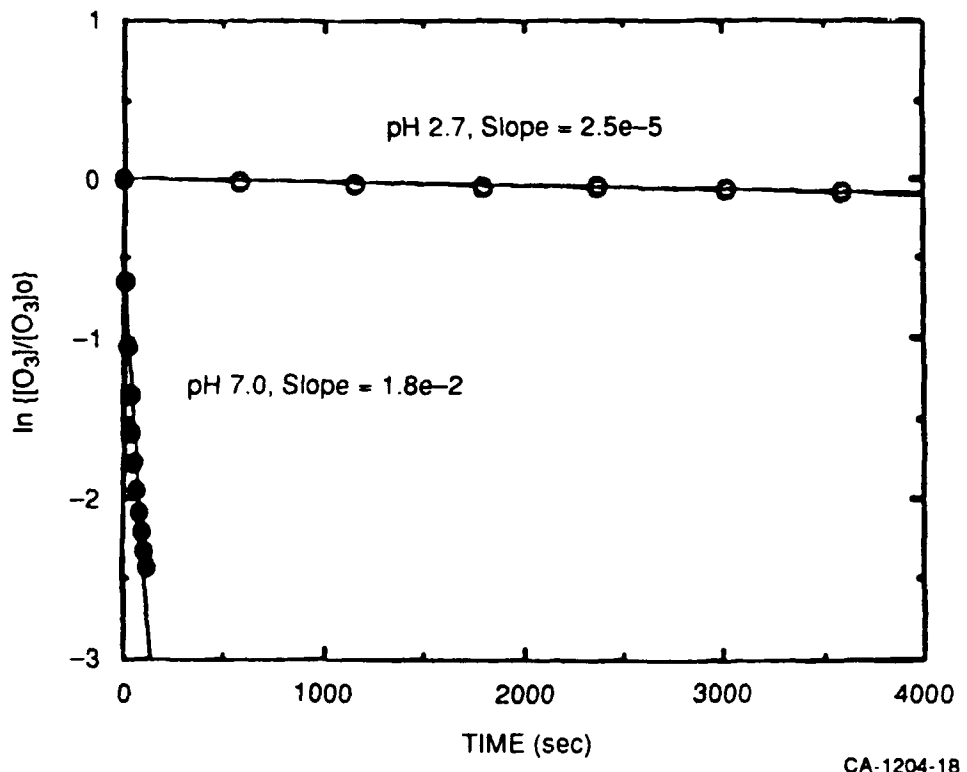


Figure 16. Calculated Ozone Loss in the Presence of 10 μM Peroxide in a $\text{O}_3/\text{H}_2\text{O}_2/\text{Dark}$ Model at Different pHs.

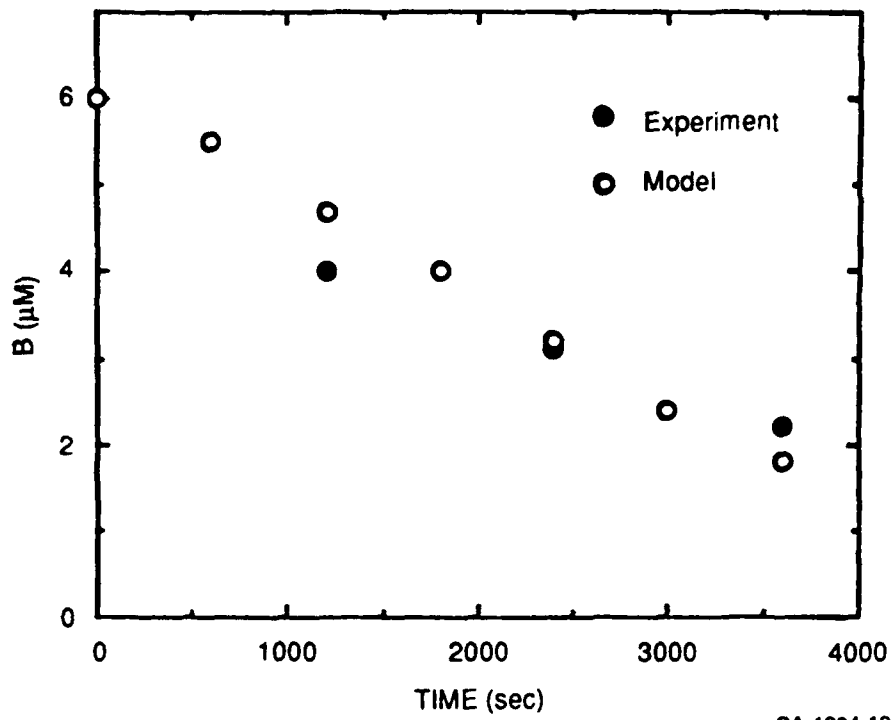


Figure 17. Measured and Calculated Losses of B in a O_3 /Dark System in the Presence of 6 μM B and P and in the Absence of Peroxide at pH 7.0.

CA-1204-19

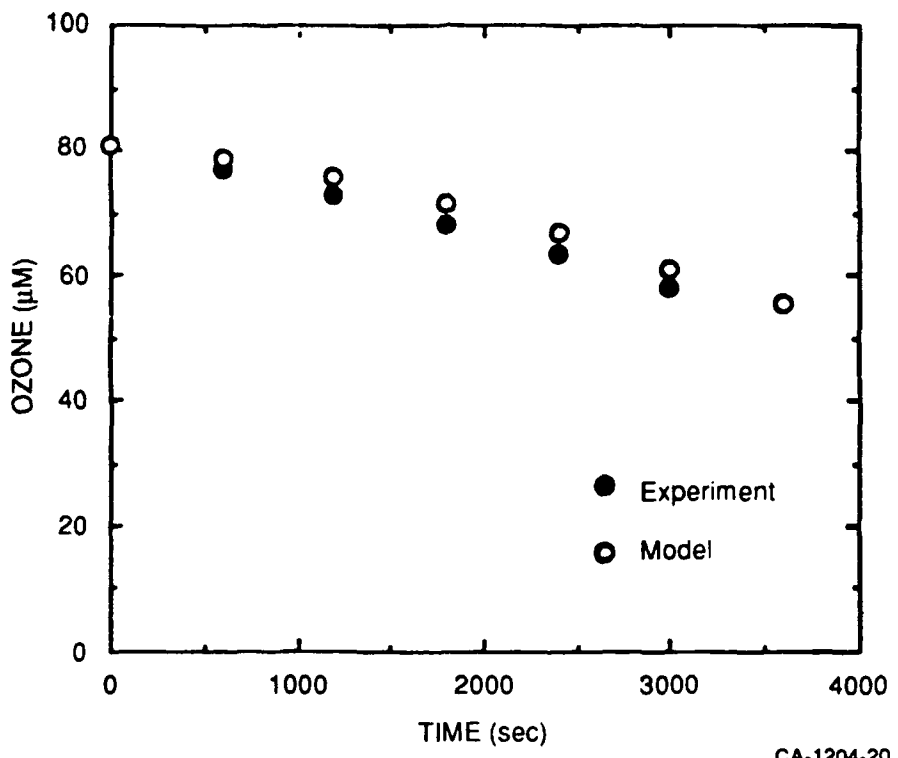


Figure 18. Measured and Calculated Losses of Ozone in a O_3 /Dark System in the Presence of 6 μM B and P and in the Absence of Peroxide at pH 7.0.

3. **TiO₂/UV Systems and TiO₂/UV/Sonication**

Experiments with TiO₂ were conducted with mixtures of 500 μM phosphate, 6 μM propionate and butyrate(P and B), and 0.1 percent anatase TiO₂ powder sieved to remove fine particles (< 60 μM). A BLAK-RAY longwave ultraviolet lamp was used to photolyze TiO₂.

Some experiments with TiO₂ were also conducted with an ultrasonic generator focused on the reactor. Experiments at SRI by Alan Johnston had previously shown that sonicated TiO₂ mixtures photooxidized organics 2 to 5 times faster than unsonicated systems (46).

Figure 19 compares loss rates for B in the TiO₂ systems in the absence of HA and HCO₃⁻ at pH 7.2. The TiO₂/Dark , UV (longwave length) without TiO₂, and TiO₂ sonication without UV experiments serve as three controls that show no oxidation. With UV but without sonication, the average loss rate for B is $2.8 \times 10^{-3} \mu\text{M/s}$; with sonication the rate increases almost three times to $7.2 \times 10^{-3} \mu\text{M s}^{-1}$.

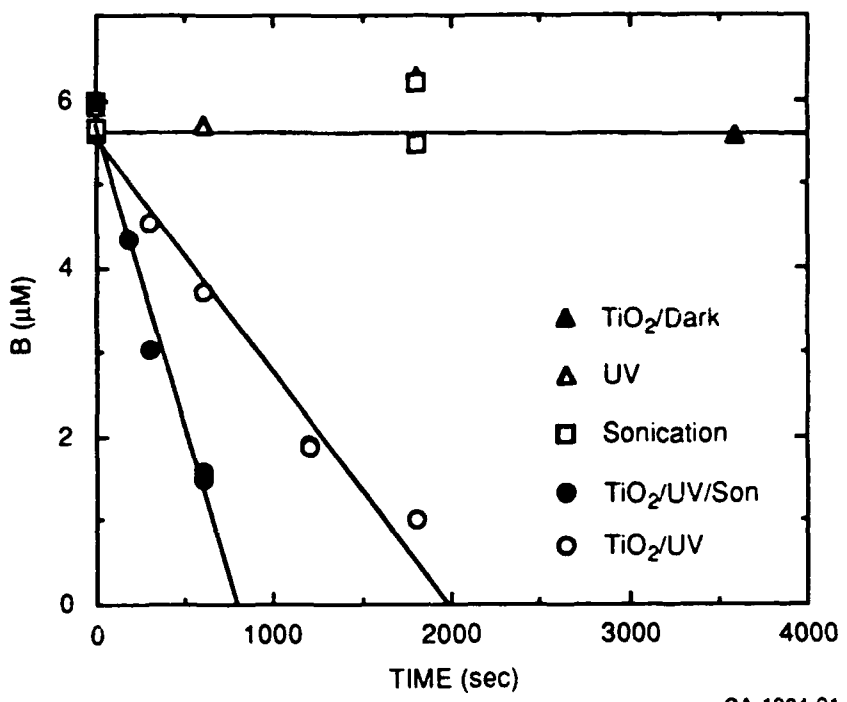
4. **Humic Acid (HA) Effects Among AOPs**

HA may simultaneously scavenge and generate HO[•] in each system. We performed several experiments to characterize the role of HA.

a. **Hydroxyl Radical Consumption Rate For HA**

To verify that Aldrich HA scavenges HO[•] as efficiently as natural HA, we measured the consumption rate of HO[•] by Aldrich HA using the method developed by Hoigné and Bader (11) and p-chlorobenzoic acid (PCBA) as a substrate. We chose PCBA as the substrate because it is nonvolatile and it reacts negligibly slowly with ozone directly ($k \leq 0.15 \text{ M}^{-1} \text{ s}^{-1}$; (21)). In this method, ozone is added to a water sample containing dissolved organic matter (DOM) and a substrate (PCBA) that does not react significantly with ozone directly. The ozone is then allowed to decompose to HO[•], which in turn oxidizes the substrate in competition with the DOM. The rate of substrate oxidation is then equal to the rate of HO[•] generation times the fraction of HO[•] trapped by the substrate:

$$\frac{d[\text{PCBA}]}{dt} = \eta \frac{d(\text{O}_3)}{dt} \times \frac{k_{\text{PCBA}}[\text{PCBA}]}{k_d^{\text{HO}}} \quad (24)$$



CA-1204-21

Figure 19. Measured Losses of Butyrate Ion in a TiO_2 System at pH 7.2.

where η is the stoichiometric yield of HO^\bullet from decomposed ozone, k_{PCBA} is the rate constant for reaction of PCBA with HO^\bullet , and k_d^{HO} is the consumption rate constant of hydroxyl radicals in the water, resulting predominantly from reaction with HA. If Equation (24) is integrated:

$$\ln \frac{[\text{PCBA}]_0}{[\text{PCBA}]} = \eta \frac{k_{\text{PCBA}}}{k_d^{\text{HO}}} \Delta[\text{O}_3]_{\text{added}} \quad (25)$$

A plot of $\ln\{[\text{PCBA}]_0/[\text{PCBA}]\}$ versus added ozone concentration thus has a slope of $\eta k_{\text{PCBA}}/k_d^{\text{HO}}$.

$$\Delta(\text{O}_3)_{37}^{\text{PCBA}} = \frac{k_d^{\text{HO}}}{\eta k_{\text{PCBA}}} = 1/\text{slope} \quad (26)$$

The ΔO_3 value for HA was estimated from the remaining PCBA in solutions with various amounts of ozone in tubes containing 10 ppm HA and 2 μM PCBA at pH 7.2.

The results are shown in Figure 20, which gives a $\Delta(\text{O}_3)_{37}^{\text{PCBA}}$ value of 57 μM . If $\eta = 0.5$ and k_{PCBA} is $5 \times 10^9 \text{ M}^{-1} \text{ s}^{-1}$ (21), $k_d^{\text{HO}} = 1.4 \times 10^5 \text{ s}^{-1}$ (3). Since HO^\bullet scavenging rates are proportional to DOC we need to normalize the value of Aldrich HA to DOC which is 48 percent carbon. Therefore 10 mg L^{-1} HA equals 4.8 mg L^{-1} DOC and dividing $1.4 \times 10^5 \text{ s}^{-1}$ by 4.8 mg L^{-1} DOC gives $k_{\text{HO}}(\text{DOC}) = 3.0 \times 10^4 \text{ L mg}^{-1} \text{ s}^{-1}$. Using the same method Haag and Yao (21) found values for U.S. surface waters in the range of $(1.6 - 8.6) \times 10^4 \text{ L mg}^{-1} \text{ s}^{-1}$ with an average value of $2.3 \times 10^4 \text{ L mg}^{-1} \text{ s}^{-1}$. Thus, Aldrich HA appears to scavenge HO^\bullet as efficiently as natural HA.

b. Effect of Humic Acid in $\text{H}_2\text{O}_2/\text{UV}$ System

Addition of 5 mg L^{-1} of HA to a $\text{H}_2\text{O}_2/\text{UV}$ system slows the rate of oxidation of B and P as well as H_2O_2 in nearly the amounts predicted by models (see Tables 2 and 3). This result is qualitatively consistent with predictions of scavenging of about 90 percent of HO^\bullet by HA without producing HO^\bullet .

c. The Effect of Humic Acid in Ozone Systems

Figure 21 presents the measured B/BH losses in the presence and absence of HA in a O_3/UV system at pH 2.2 and 7.0. The effect of added HA on rates of loss of B is less than expected, based on the apparent rate constant for HO^\bullet scavenging by HA. At pH 7 we observed only a two fold decrease in rate on adding 5 ppm HA whereas we calculate that the fraction of HO^\bullet

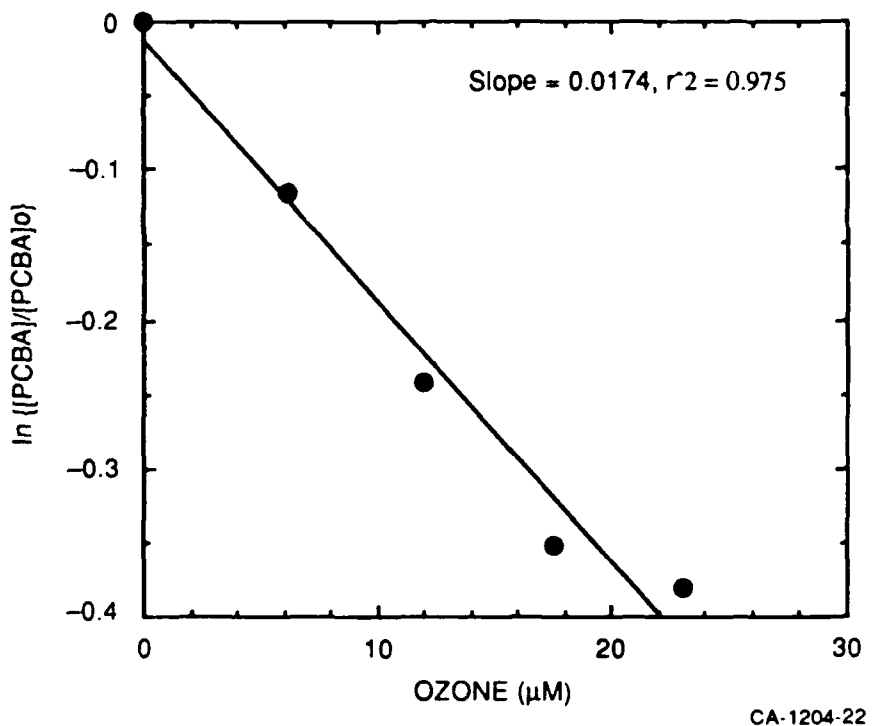
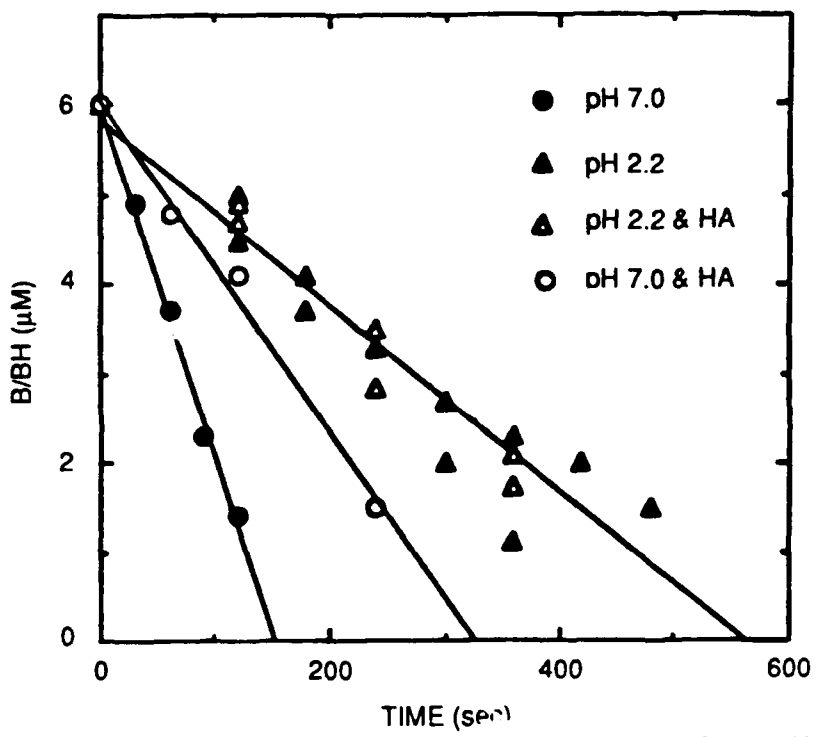


Figure 20. PCBA Loss as a Function of Ozone Addition.



CA-1204-23

Figure 21. Measured B/BH Losses in the Presence and Absence of 5 ppm HA in a O_3/UV System at pH 2.2 and 7.0.

oxidizing B is reduced from 0.4 to 0.1. Figure 22 shows the measured ozone losses in the presence and absence of HA in a O₃/UV system at pH 2.2 and 7.0. The ozone loss rate at pH 2.2 is unaffected by HA. In the absence of HA, the ozone loss rate at pH 7.0 is about 1.8 times faster than at pH 2.2.

Figure 23 presents the losses of butyrate versus the loss of ozone for the above experiments. The efficiency factor $\Delta B / \Delta O_3$ (with and without HA) are the same at pH 2.2 (0.045) and about four-fold larger without HA at pH 7 (0.10 versus 0.02). Since the fraction of HO[•] available to oxidize B/BH will be reduced from 0.40 to 0.12 with HA, the average efficiency with HA should be smaller than in its absence by about a factor three. These unexpected results suggest that HA not only scavenges HO[•] but also produces HO[•] at the lower pH. The ability of HA to inhibit oxidation seems to vary with AOP systems and further characterization of the reactions of HA is needed to predict the behavior of the AOPs.

C. OXIDATION RATES AND RELATIVE CHEMICAL EFFICIENCIES

Our experimental system used a low-pressure mercury lamp with >85 percent of its emission at 254 nm and then filtered to remove light below 250 nm. All experiments were conducted with 100 μ M peroxide or ozone in a batch reactor. The UV absorbances of ozone and hydrogen peroxide influence the relative consumption rates of these oxidants in the light. Figure 24 presents the UV spectra for ozone and hydrogen peroxide. The UV spectrum of H₂O₂ is weak with $\epsilon_{254} = 19 \text{ M}^{-1} \text{ cm}^{-1}$, while the UV spectrum of O₃ is strong with $\epsilon_{254} = 2850 \text{ M}^{-1} \text{ s}^{-1}$. Figure 25 indicates the relative measured loss rates of oxidants in various systems in the absence of BH and PH. The H₂O₂/UV system is much less reactive in UV light than the O₃/UV system, simply because the UV spectrum of H₂O₂ is about 150 times weaker than that of ozone. The rate of loss of ozone at high pH (pH 9.0) in the dark is only two times slower than in the light at pH 2.2. Thus, ozone loss rates in the dark at pH 9 are nearly as fast as in light at low pH. The O₃/H₂O₂ system with 10 μ M peroxide at pH 7 has a loss rate only about four times slower than the dark ozone alone system at pH 9, while dark ozone alone at pH 7 has a rate about 50 times slower than at pH 9. These results show that a small amount of added peroxide at pH 7 can be used to increase the loss rate of ozone and offset the need for higher pH. The conclusion is confirmed by the experiment at pH 7 in a ozone/UV system.

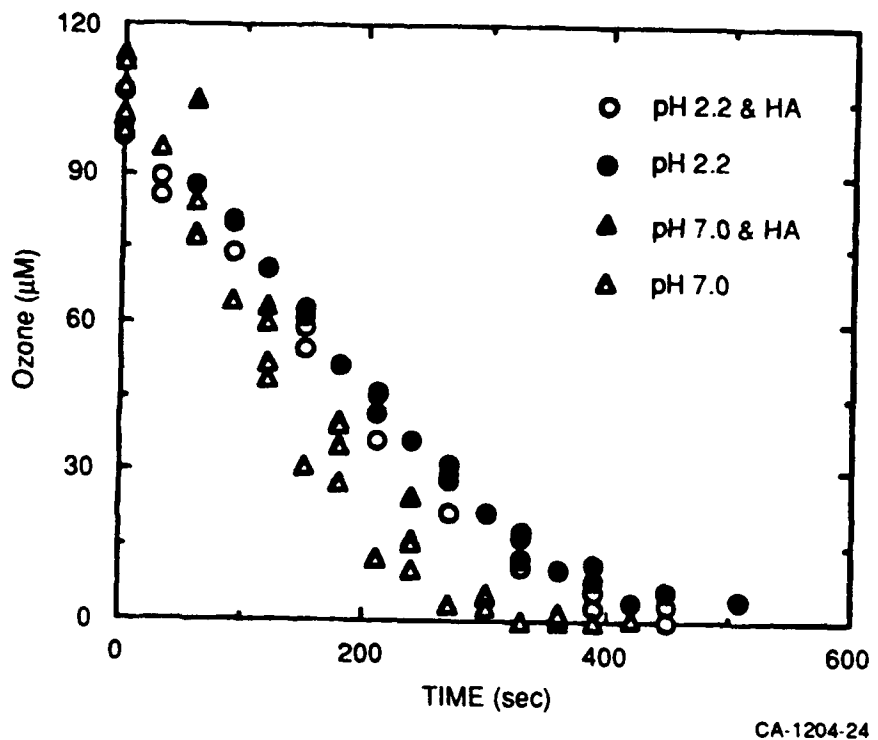
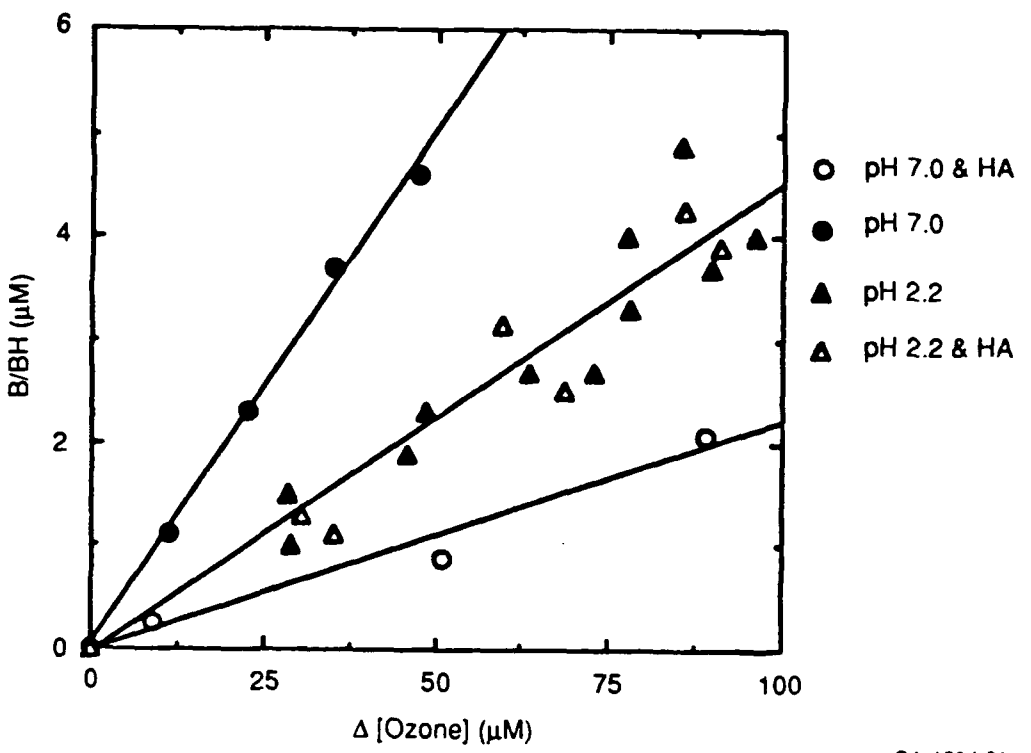


Figure 22. Measured Ozone Losses in the Presence and Absence of HA in a O₃/UV System in the Presence of B/BH and P/PH at pH 2.2 and 7.0.



CA-1204-25

Figure 23. Loss of Butyrate versus the Loss of Oxidants under Different Conditions in a O_3 /UV System.

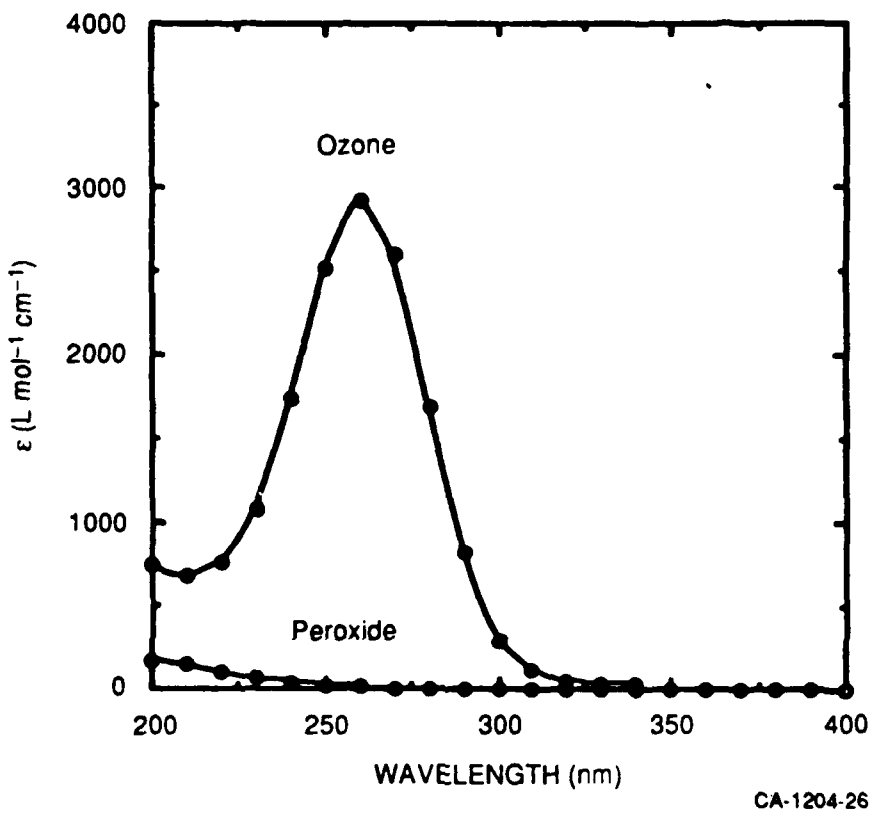
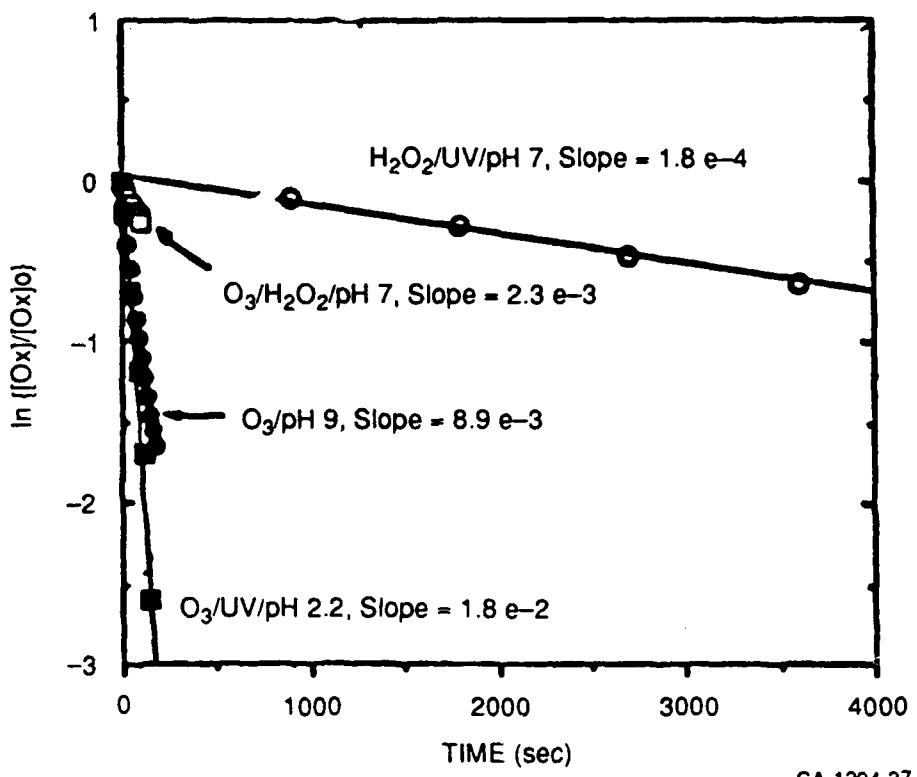


Figure 24. UV Spectra for Ozone and Peroxide



CA-1204-27

Figure 25. Comparison of Measured Loss Rates of Oxidants in Different AOPs in the Absence of BH and PH.

Table 5 summarizes the measured and calculated zero order rates of oxidation of B in five different AOPs. The calculated rates among the AOPs are in good agreement with the experiments within a factor two. The O₃/H₂O₂ system in the light at pH 7.0 has the highest

TABLE 5. ZERO ORDER RATES OF OXIDATION OF BUTYRATE IN AOPs.

AOP	pH	k[Bo] × 10 ⁹ (Ms ⁻¹)	
		Measured Rate (μM ⁻¹ × 10 ²)	Calculated Rate (μM s ⁻¹ × 10 ²)
O ₃ /UV	2.2	19.2	16.2
H ₂ O ₂ /UV	2.2	12.0	12.0
O ₃ /DARK	7.0	1.5	2.0
O ₃ /H ₂ O ₂	7.0	43.2	75.0
O ₃ /H ₂ O ₂ /UV	7.0	73.2	96.2

oxidation rate, but this is only 20 to 40 percent higher than the O₃/H₂O₂ system in the dark. This difference is due to photolysis of ozone and peroxide. No simple ozone/UV system can be observed at pH >4 without a contribution from the O₃/H₂O₂ system because the O₃/UV system produces mostly H₂O₂ in the initial reaction in water. Among all AOPs tested, O₃/Dark at pH 7.0 has the lowest oxidation rate.

The O₃/H₂O₂/UV system includes contributions from the O₃/HO[•], O₃/H₂O₂, O₃/UV and the H₂O₂/UV systems. The rates of photolytic generation of HO[•] by ozone and peroxide are independent of pH, but do depend on the concentration of oxidant. Scavenging of HO[•] by organics may be pH dependent (e.g., butyrate ion is more reactive than butyric acid) and is certainly concentration dependent.

Thus, the oxidation rate of the O₃/H₂O₂/UV system at pH 7 is nearly the sum of oxidation rates of the O₃/UV system at pH 2 (purely photolysis of ozone), the O₃/Dark system at pH 7 (contribution of HO[•]), the O₃/H₂O₂ system at pH 7 (contribution of HO[•]) and about 10 percent of the rate of the H₂O₂/UV system at pH 2.

Table 5 shows that the rates of loss of ozone in the O₃/H₂O₂ system in light and dark are similar and Table 6 shows that the efficiencies of these two systems are very similar. The H₂O₂/UV system is the most efficient of the AOPs, but with a relatively slow oxidation rate.

The other five AOPs have smaller and similar efficiencies. We could compare electrochemical oxidation with the AOPs, but rates of oxidation of B were so much slower that the comparison is not very meaningful.

TABLE 6. EFFICIENCIES OF AOPs^a.

AOP	pH	Measured ^b E, %	Ratio of Measured Rates ^c
O ₃ /UV	2.2	5.0	1.0
H ₂ O ₂ /UV	2.2	50	0.63
O ₃ /Dk	7.0	13.8	0.078
O ₃ /H ₂ O ₂	7.0	8.3	2.25
O ₃ /H ₂ O ₂ /UV	7.0	8.6	3.8
TiO ₂ /UV	7.0	10 ^d	0.4

^aDuring oxidation of 5 μ m butyrate.

^bE = Δ Butyrate/ $(\Delta$ added oxidant).

^cNormalized to O₃/UV.

^dBased on quantum yield = 0.1 (Reference 38).

SECTION III

SELECTION AND OPTIMIZATION OF AOPS

A. FACTORS IN SELECTION OF ADVANCED OXIDATION PROCESSES

The choice of an oxidation system for a specific treatment depends on the costs of equipment, operation, and maintenance. In this project we evaluated the operating expenses for each AOP in terms of a unit \$/kgal for the same treated water. The variables affecting the operating costs include the water characteristics, treatment process design, and operation. The variables related to waters characteristics include the type and concentration of inorganic and organic contaminants, light transmittance of the water, and type and concentration of suspended solids (if any). The variables directly related to treatment process design and operation are the UV dosage, the oxidant dosage, pH, temperature, the volume of water treatment per unit time, and the residence time of the water in the reactor. Although lamp maintenance and operating costs are fixed, the type and the number of lamps used for the oxidation processes can be varied. The oxidant dosage, pH, and temperature also will vary according to the needs of the particular system.

B. UV LAMPS

The UV lamps are essential for forming HO[•] from H₂O₂ and TiO₂ and are often used with O₃. In some cases, direct photolysis of organics also occurs. If the organic contaminants absorb UV light directly and decompose, their products may become more susceptible to reaction with HO[•]. The amount of energy absorbed by the contaminants and oxidants is related to the intensity of the UV light, the absorbance coefficients, contaminant and oxidant concentrations, and path length (10). Therefore, oxidation times can be greatly reduced by increasing the intensity of UV light, using short wavelengths (> 300 nm), high concentration of oxidants, and long path lengths. Very fast rates of photolysis to form HO[•] are somewhat offset by increased rates of termination so that in general the rate increases only by a fractional order in light intensity ($I^{0.5-0.7}$). Besides, the efficiency in generating photons is also very important in controlling cost efficiency.

C. DEFINITION OF CHEMICAL EFFICIENCY AND OPERATION COST EFFICIENCY

AOPs generate and consume HO[•] by different paths. The chemical efficiency of oxidants may be defined as in Equation (27).

$$E(\%) = \Delta[\text{Probe chemical}] / (\Delta[\text{ozone}] + \Delta[\text{H}_2\text{O}_2]) \quad (27)$$

If consumption of ozone and peroxide are changed into dollars (chemical cost efficiency), Equation (27) now is redefined as Equation (28).

$$Ec(\$) = \Delta[\text{Probe chemical}] / (\$ \text{ of oxidants consumed}) \quad (28)$$

Three parameters need to be considered to compare the efficiencies among AOP systems: loss of the added oxidant, formation of oxidant (if any), and loss of substrate. In ozone systems (dark and light), peroxide, either added to the system or generated from ozone, plays an important role in controlling the efficiencies of the system under different conditions.

Operational costs include oxidants, electricity for lamps, and acid or base for pH changes. The operation efficiency can be defined as

$$E_o(\$) = \Delta[\text{Probe chemical}] / (\$ \text{ for the operation}) \quad (29)$$

D. AN EXAMPLE IN SELECTION AND OPTIMIZATION OF AOPS

A typical question to be raised before using any aqueous treatment is: What is the cheapest way to reduce the concentration level of the contaminant to the acceptable level within the required time period? Here we present a procedure to select conditions for reducing a 10 ppm of an aliphatic compound (AC) (~100 μM), 6-ppm HCO_3^- (100 μM) solution at pH 9 to 100 ppb AC within two minutes in each batch. For simplification, we omitted HA, but, we believe that the conclusions on relative rankings of AOPs will be unchanged by addition of 2-5 ppm HA.

Our approach to selecting and optimizing AOPs for a specific treatment was to compare the information for AOPs that is available in the literature and combine that information with the model results. The literature information indicates which system is not competitive and the price range

available on the market. The model indicates the nearly optimum conditions and possible costs for each AOP to meet the required parameters, such as volume per day, residence time, and the concentration level after the treatment.

1. Literature Review

Tables 7 and 8 summarize the cost data gleaned from manufacturers literature, from a review paper by Peyton (7), and from other sources. Treatment costs vary with the type and concentration of the contaminants to be removed and to some extent on the chemical characteristics of the natural water matrix. Therefore, treatment costs have been divided into two groups: low concentrations of contaminants in groundwater and high concentrations such as in an industrial wastewater. Actually, treatment costs are roughly proportional to the concentration of compounds to be oxidized (7) and treatment costs per unit volume decrease significantly with increasing plant size and increase with increasing organic load. Therefore, the boundary between these two groups is somewhat arbitrary.

We have attempted to present total treatment costs, including both operation and maintenance (O & M) and amortization of capital costs in Tables 7 and 8. However, the results should be used with caution because it is sometimes difficult to ascertain whether or not the reported "operating" costs include capital amortization, which is often a major portion of the total. Manufacturers' literature often contains only O&M; note, for example, that Topudurti's (28) estimate of total costs for the Ultrox system, from Ultrox Inc is about an order of magnitude higher than Zeff's (27) claims.

a. TiO_2 -Catalyzed Solar Photooxidation

To a first approximation, the costs for all the methods are competitive in their applicable concentration ranges, except an estimate of the UV/ TiO_2 process by the Solar Energy Research Institute (SERI) (33). We therefore compare how the cost was estimated for TiO_2 /UV systems by Ollis (29) and Link (33).

Ollis' estimate for UV/ TiO_2 is based on the use of conventional (254 nm?) UV lamp; he assumed (for lack of data) that the oxidation efficiency and rate at a given dose are the same as for the UV/ O_3 method, which is probably not true because the quantum yield of ozone photolysis is 0.62 at 254 nm (1) while that for generation of HO^- by TiO_2 is on the order of 0.1, even when H_2O_2 is added to increase efficiency (38). Ollis's estimate also assumes that the catalyst is free, i.e., has an infinite lifetime, which is contrary to more recent experience at the

TABLE 7. ESTIMATED COST FOR TREATING CONTAMINANTS IN GROUNDWATER TO REDUCE THEM BELOW DRINKING WATER LIMITS^{a,b}

System	Capacity (gallons per day)	Cost (\$/kgal)	Reference
O ₃ /H ₂ O ₂ 200 ppb TCE, 20 ppb PCE	2,900,000	0.094	25
O ₃ /H ₂ O ₂ 500-5000 ppb chloronitrobenzene	8,000,000	0.06 - 0.31 (O&M)	26
O ₃ /H ₂ O ₂ /UV (Ultrox) 600 ppb DCE, TCE, DCA, TCA, CH ₂ Cl ₂ , vinyl chloride	72,000	0.33 (O&M)	27
1000 ppb THF	216,000	0.39 (O&M)	
O ₃ /H ₂ O ₂ /UV (Ultrox) 100 ppb TCE, 40 ppb vinyl chloride at RCRA Superfund sites	360,000 140,000 30,000	2.20 3.10 7.50	28
UV/O ₃ 50 ppb PCB	2,440,000 230,000 29,000	1.78 2.78 7.34	29
UV/O ₃ (WEDECO) 500 ppb chlorinated hydrocarbons	63,500	0.67	30
UV or UV/H ₂ O ₂ (Purus)	?	0.10 - 0.75 (O&M?)	31
UV/H ₂ O ₂ (Perox. Systems) 10 ppm TCE, 50 ppm H ₂ O ₂ , 30 KW UV	86,000	1.00 - 1.35 (O&M?)	32
UV/H ₂ O ₂ 400 ppb TCE	100,000	4.00	33
UV/TiO ₂ 50 ppb PCB, 254 nm lamps, optimistic	2,440,000 230,000 29,000	1.13 1.81 5.56	29
UV/TiO ₂ (SERI Solar Trough) 400 ppb TCE optimistic	100,000	14.00 → 2.00 (current) (est. 1995)	33
γ-Radiation, 50-1000 ppb TCE or PCE, optimistic	?	0.25-0.78 (O only)	34
GAC 50 ppb PCB	2,440,000 230,000 29,000	1.10 1.80 4.40	29
GAC 200 ppb TCE, 20 ppb PCE	2,900,000	0.40	25

^a Drinking water limits are 200 ppb for TCA, 5 ppb for TCE, 4 ppb for PCE, and 2 ppb for vinyl chloride.

^b Cost estimates include capital amortization unless only operation and maintenance (O&M) is indicated.

TABLE 8. TREATMENT COSTS FOR TOC INDUSTRIAL/MUNICIPAL WASTEWATER

System	Capacity (gallons per day)	Cost (\$/kgal)	Reference
O ₃ /H ₂ O ₂ , electroprocess waste 70 → 10 ppm TOC		1.06	35
UV/H ₂ O ₂ (peox, systems) 4000 ppm total of THF, MEK, MIK, toluene, cyclohexane in groundwater		2.40 (O&M)	36
120 ppm phenolic water		15.00 (O&M)	
GAC, 4000 ppm total of THF, MEK, MIK toluene, cyclohexane in groundwater; with regeneration		5.00	36
O ₃ /H ₂ O ₂ /UV (Ultrox) 5,000 ppm hydrazine, methyl hydrazine, UDMH; discharge to bioreactor	600-1,500	86.00 (O&M)	27
Supercritical water ox. (Modar) 100,000 ppm TOC	2,500-25,000	800.00-150.00	37
Wet air ox. (Zimpro) 27,000 ppm total of MEK, i-PrOH, phenol, o-diClbenzene, o-xylene, PCE, Freon-11	20,000	280.00	37

SERI (38,33). We decided that the estimated cost for TiO_2/UV system from SERI is more trustworthy.

SERI, in conjunction with Sandia National Laboratory, was conducting pilot tests of the oxidation of TCE in groundwater using a 300-m tube containing a slurried TiO_2 catalyst mounted at the focal point of a 2-meter wide parabolic solar trough. The system removes 99 percent of the TCE in a residence time of ~3 minutes in sunlight when 100 ppm of H_2O_2 is added. Because recycling the powdered TiO_2 requires separation and is expensive, SERI is currently testing the use of TiO_2 immobilized on glass. The immobilized catalyst, supplied by NuLite Corporation, has a slightly lower efficiency than the powdered form (DeGussa P25), and the efficiency drops further (factor of 2 to 4) following the first use.

SERI's cost estimate for the TiO_2 -catalyzed process assumes that catalyst efficiency is constant and equal to that of the powdered form and that natural solutes have no effect on oxidation effectiveness. Current costs were estimated at \$14.00/K gal to remove 0.4 ppm of TCE in a groundwater, compared to their estimate of \$4.00/K gal for the $\text{UV}/\text{H}_2\text{O}_2$ method at the same site. SERI hopes to reduce the cost to \$2.00/K gal by 1995 by using three times more efficient catalysts and two times less expensive light collection systems (possibly nonconcentrating) and by extending the wavelength range to convert more solar photons to useful oxidants. Solar concentrators currently have high capital costs and the need to clean and repair solar collector surfaces causes operating costs to be as high or higher than competitive methods such as UV/O_3 or $\text{UV}/\text{H}_2\text{O}_2$.

One interesting concept was that groundwater cleanup can be cost-effective when performed in an intermittent manner, because of the slow desorption of contaminants from the aquifer material. Therefore, the intermittent nature of solar radiation is not a drawback for this purpose, in contrast to most other applications.

b. Short-Wavelength Photolysis and $\text{UV}/\text{H}_2\text{O}_2$.

Advanced Photolysis Technologies (APT) sells water clean-up systems that use nonmercury lamps, which convert about 30 percent of electrical energy into photons at $\lambda < 300$ nm and have considerable output between 200 and 250 nm. Details of the lamp discharge gases and reactor design are proprietary, but the lamp spectrum appears to be similar to the antimony halide lamps mentioned by Peyton (7), and the design probably uses lamps placed concentrically in a cylindrical reactor. The inside of the reactor is coated with reflective material to allow the light to pass repeatedly through the solution until it is absorbed. The system can operate with or without

the addition of H_2O_2 depending on waste type; often H_2O_2 is generated *in situ* from oxidation. For trichloroethene (TCE), 99 percent destruction is reported to occur in ≤ 30 seconds in various groundwaters; for chloroform, the reaction is complete in ≤ 2 min. ATP projects operating costs of \$0.10 – \$0.75/1000 gal, depending on contaminant type and concentration.

c. Ozone-Based Methods.

Gary Peyton has a UV/ O_3 reactor in his laboratory and mobile UV/ O_3 + H_2O_2/O_3 pilot plant. The laboratory reactor has an ozone diffuser at the bottom and contains four low-pressure mercury lamps (254 nm) with a pathlength of ~ 10 cm between the lamps and between each lamp and the glass reactor walls. The mobile unit is constructed in a tractor-trailer and has a pre-aerator to oxidize and precipitate iron as well as three reactors that can be used for UV/ O_3 and/or H_2O_2/O_3 in various combinations. Peyton's group has found that a sequential combination of H_2O_2/O_3 followed by UV/ O_3 is more effective than either process alone. They suggest that the H_2O_2/O_3 method is more effective in the beginning at high initial organic concentrations because competitive light absorption inhibits the UV method, whereas the UV method is more effective in the later stages of oxidation where light transparency has increased and pH has decreased (acid formation), resulting in slower initiation of ozone decomposition by H_2O_2 . Ultrox International has also found that for some waters UV/ H_2O_2/O_3 (all three in combination) is more effective than any pair alone (27).

Thus far, most UV/ O_3 work has been conducted with mercury lamps that have jackets which filter out the 185-nm line to simplify data interpretation. Peyton's pilot unit continues to use these lamps in actual groundwater remediation tests. Significant improvements may be obtained by directly photolyzing HO $^{\cdot}$ -reactive compounds such as CCl_4 with shorter wavelength light such as 185 nm. For H_2O_2/O_3 , there is a general consensus in the literature that optimum efficiency is obtained with ratios of 0.5 to 1.0 mole H_2O_2 : mole O_3 (7).

Peyton (7) has also reported that ozone alone is often nearly as effective as H_2O_2/O_3 or UV/ O_3 in oxidizing HO $^{\cdot}$ -reactive compounds when direct photolysis is not important and the water contains at least a few ppm of natural dissolved organic carbon (DOC). This occurs because DOC contains initiators and promoters that convert ozone to hydroxyl radicals. This conclusion is consistent with observations in this laboratory that p-chlorobenzoic acid, a compound that is essentially inert to ozone in pure water, is >80 percent oxidized in 10 minutes in reservoir water containing 0.23 ppm ozone and 5.6 ppm DOC.

Peyton (7) estimates that costs for UV/O₃ system are similar to those of the O₃/H₂O₂ method. The estimate of Aieta et al. (25) for O₃/H₂O₂ suggests that this method is the most cost-effective, even for a much smaller plant, a conclusion we have reached from modeling the systems. However, because it does not use UV light, the system is more costly to operate when the water contains compounds like CCl₄ or 1,1,1-trichloroethane which react slowly with HO[•].

d. Efficiency and Cost for Generating Photons.

Table 9 lists the efficiency in generating photons with different sources for ozone or peroxide systems. The cheapest source of photons is a low-pressure mercury lamp. The efficiency of using photons depends on how well the solution absorbs photons, reactor design (shape, diameter, number of lamps, and reflection ability of the reactor wall) and residence time. No discussion of reactor design or photon absorption is included in this report. We simply assume that all the photons will be absorbed by oxidants in different reactors.

TABLE 9. EFFICIENCY AND COST FOR GENERATING PHOTONS^a

Photons	Source and Efficiency	Cost (\$/Mole)
172 nm	Xe Excimer, ABB, 20%	0.077
230 nm, broad	Pulsed Xe, Purus, 17%	0.068
240-303 nm	Med Press use. Hg, PSI, 11%	0.094
185, 254 nm	Low Press use Hg, PSI, 40%	0.025

^aFrom W. R. Haag, Purus, Inc.

2. Model Results

Ozone AOPs use 250-nm UV light very efficiently, but no more than 5% of the photolyzed ozone forms HO[•]. Thus only above pH 7, where HO₂[•] is available, is the ozone AOP an efficient source of HO[•]. This result suggests that, below pH 7, the ozone/UV AOPs have no advantage over the H₂O₂/UV AOPs because more than 95% of ozone is photolyzed to H₂O₂. This also suggests that, above pH 7, the ozone/UV AOP has no advantage over the O₃/H₂O₂/Dark AOP for generating HO[•] and oxidizing organics simply because ozone reacts more rapidly with peroxide anions instead of photons to generate HO[•] even when only a small amount of peroxide is used (see Table 5).

At low pHs, the $\text{H}_2\text{O}_2/\text{UV}$ system is the better choices among AOPs because it is the most efficient although it is the slowest system. The number of lamps needed to meet the residence time requirement can be calculated from the oxidation rate with a single lamp. The TiO_2/UV system may compete with the $\text{H}_2\text{O}_2/\text{UV}$ system (33) in the future, but only after better catalysts are developed and the cost is reduced.

Above pH 7, the reaction time in the $\text{O}_3/\text{H}_2\text{O}_2$ system is controlled by the amount of peroxide present. Adding more peroxide to the ozone system shortens the residence time, but with a lower cost efficiency.

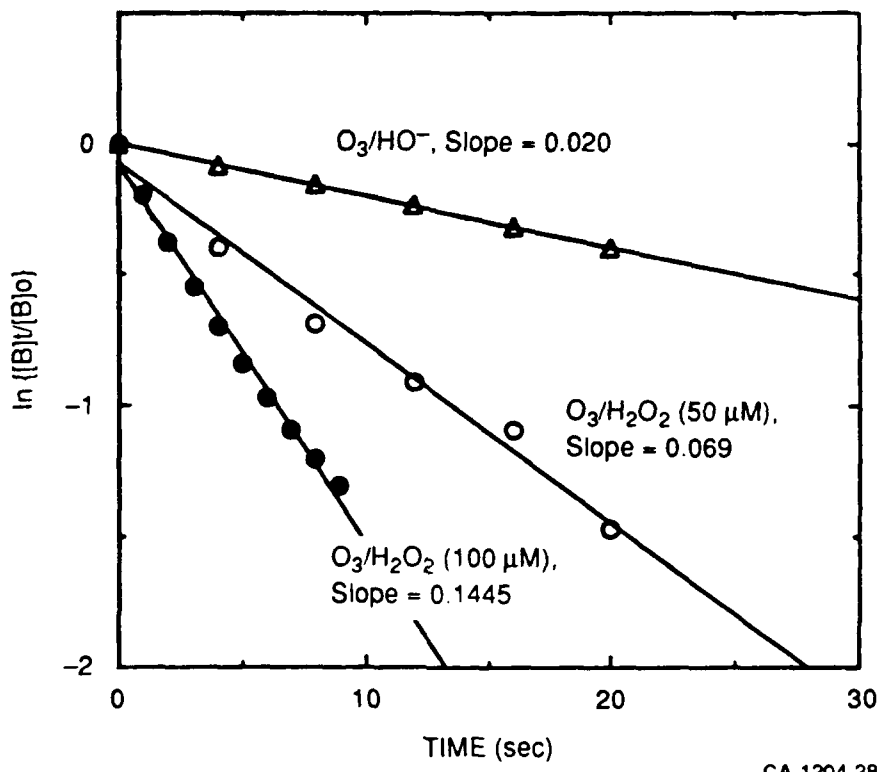
a. Chemical Efficiency and Residence Time

Table 10 lists the reaction rates of ozone with important species in AOPs. At pH 9 with 10 μM peroxide, 98 percent of consumed ozone reacts with peroxide anions ($1 \times 10^{-1} \text{ s}^{-1}$) instead of with photons ($2.2 \times 10^{-3} \text{ s}^{-1}$) to generate HO^\bullet . This result implies that the UV lamp is unnecessary in this ozone system. Figure 26 compares the calculated butyrate loss rates in the $\text{O}_3/\text{H}_2\text{O}_2$ systems with 1mM O_3 and 0.1 mM butyrate (to scavenge all HO^\bullet) at pH 9. It is not a surprise that the oxidation rate of butyrate is doubled when the initial peroxide concentration is changed from 50 to 100 μM . The unexpected result is that in this system, the efficiency is not sacrificed when the oxidation rate is increased (Figure 27) because only ~2 percent of HO^\bullet is scavenged by peroxide in the system.

TABLE 10. REACTIONS OF OZONE WITH IMPORTANT SPECIES IN AOPs

Species	Conc (M)	$k (\text{s}^{-1})$
HO_2^-	2×10^{-8}	1×10^{-1} (10 μM , pH 9)
$\text{h}\nu(\text{UV lamp})$		2.2×10^{-3}
HO^-	1×10^{-5}	7×10^{-4}
HO^\bullet	$10^{-11}-10^{-14}$	$1.1 \times 10^{-3}-1.1 \times 10^{-6}$
HCO_3^-	1×10^{-4}	$<1 \times 10^{-6}$
B	100×10^{-6}	6×10^{-7}

Among the AOPs, the $\text{H}_2\text{O}_2/\text{UV}$ system is the slowest (Figure 25) but with highest efficiency (Table 6), and the HO^\bullet generation rate will not vary much with pH changes.



CA-1204-28

Figure 26. Comparison of Calculated Butyrate Loss Rates in the O_3/H_2O_2 Systems with 1 μ M O_3 and 0.1 μ M Butyrate at pH 9.0.

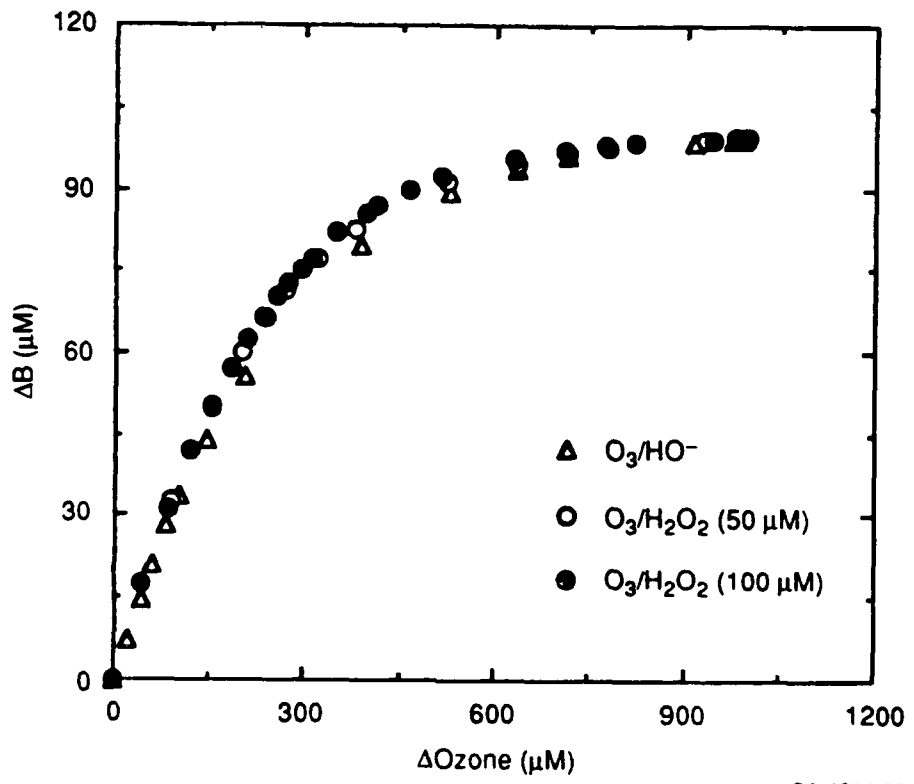


Figure 27. Efficiency Comparisons of the O_3/H_2O_2 /Dark System with Different Concentrations of H_2O_2 .

The number of lamps needed to meet the requirement can be calculated from the oxidation rate with a single lamp. However, the number needed to oxidize B in two minutes (30) is so large as to make the system uncompetitive.

b. Selection and Optimization

Table 11 lists the estimated costs for AOPs based on a system containing 10 ppm of aliphatic organic compounds in a pH 9 solution. We selected a 2-minute residence time in a 100-L reactor during which time the concentration of organics is reduced to 0.1 ppm. We include the cost of using UV lamps and replacing 5% of TiO₂ in each cycle, and the cost of raising the pH of the solution from 9 to 10, but not the cost of drying the air or oxygen used to make ozone. AOPs are optimized to meet the requirements for residence times of 2 minutes, and estimated costs are based on that specific condition and prices of \$0.10/mole ozone, \$0.05/mole H₂O₂, and \$0.14/kwh electricity.

TABLE 11. ESTIMATED OPERATING COST FOR AOP TREATMENTS OF ALIPHATIC ORGANIC COMPOUNDS^{a,b}

AOP	No. of Lamps	O ₃ (mM)	H ₂ O ₂ (mM)	Cost Estimate (\$/Kgal)
H ₂ O ₂ /UV	30	0	1	2.50
O ₃ /Dark (pH 9)	0	5	0	1.90
O ₃ /Dark (pH 10)	0	2	0	1.25
O ₃ /H ₂ O ₂ (pH >7)	0	1	0.2	0.42
O ₃ /UV	8	1	0	1.05
O ₃ /H ₂ O ₂ /UV	1	1	0.2	0.50
TiO ₂ /UV	100 ^c	-	-	2.00

^apH 9 solution.

^bInitial concentration of 10 ppm is reduced to 0.1 ppm in 2 min.

^cEach lamp is 1 Kw with 75000 μ W/cm² intensity at 350 nm.

Table 11 indicates that the O₃/H₂O₂ system is the most cost efficient system and that O₃/H₂O₂/UV is only slightly higher. Again, light systems have demonstrated no advantage over the ozone/dark systems at high pHs. For generating enough photons to photolyze ozone to peroxide, the O₃/UV system spends 60 percent of the operating cost in electricity and is about 2.5 times more expensive than the O₃/H₂O₂ system. The oxidation rate in the O₃/Dark (pH 9) system needs 5 mM ozone to meet the time requirements. The O₃/Dark (pH 10) system oxidizes

contaminants fast enough, but needs only 2 mM ozone because some of HO[•] is scavenged by HO₂⁻ (R16 in Table 4). The H₂O₂/UV system, the least cost efficient system, puts 90% of the cost in electricity. A better designed reactor which required only three lamps to meet our goal, would make the H₂O₂/UV system competitive with the O₃/H₂O₂ system. The cost estimate for the TiO₂/UV system is based on the data in Table 6 and Figure 19.

SECTION IV

ELECTROCHEMICAL OXIDATION

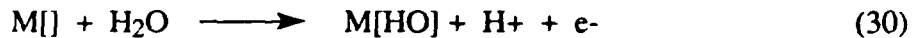
Electrooxidation of organics in water is generally slow at metal electrodes. Oxidations are much faster on illuminated semiconductor electrodes, but with serious electrode corrosion and fouling. We examined direct and indirect electrochemical oxidation of B and P in AOP studies under the same conditions to learn if oxidant properties are similar to those of the chemical systems and to evaluate their efficiency.

A. BACKGROUND

Unlike AOPs which are well developed systems, electrochemical oxidation (ECO) is not well studied nor well understood. Therefore, we have grouped the ECO experiments separately.

For electrochemical oxidation, each electrochemical cell was constructed with three electrodes: reference, counter, and working electrodes. The reference electrode was of calomel, the counter electrode was of platinum or graphite rod, and the working electrode was PbO_2/Pt electrode.

The general reaction mechanism was described as follows. On the surface of the cathode electrode, surface active sites, $\text{M}[\cdot]$, can bind oxygen from water to form surface-bound sites $\text{M}[\text{HO}\cdot]$, existing as adsorbed hydroxyl radical and an intermediate product of the oxygen evolution reaction, Equation (30). The $\text{M}[\text{HO}]$ can oxidize organic pollutants (Equation 31) or evolve oxygen (Equation 32) which is not desired.



B. THE CONSTRUCTION OF THE REACTION CELLS

Two types of electrodes were constructed for this project: fluidized bed and fixed bed. For fluidized bed reaction, the volume of the particles and active surface area of PbO_2 both influence the oxidation efficiency. To receive good electrical contact and mixing, the lead dioxide particle size should be around $500 \mu\text{m}$. No commercial product is available at this size. All manufactured lead dioxide particles are very fine sized ($< 100 \mu\text{m}$) and form a suspension that settles too slowly to give good electrical contact. We found the easiest and most efficient way to achieve this particle size was to thermally oxidize lead particles ($500 \mu\text{m}$) at 400°C to form lead dioxide in an oxygen-rich environment. Brown and reddish lead oxides were formed, which we believe to be a mixture of PbO_2 and PbO , with predominantly the former. The reaction cell was constructed as shown in Figure 28.

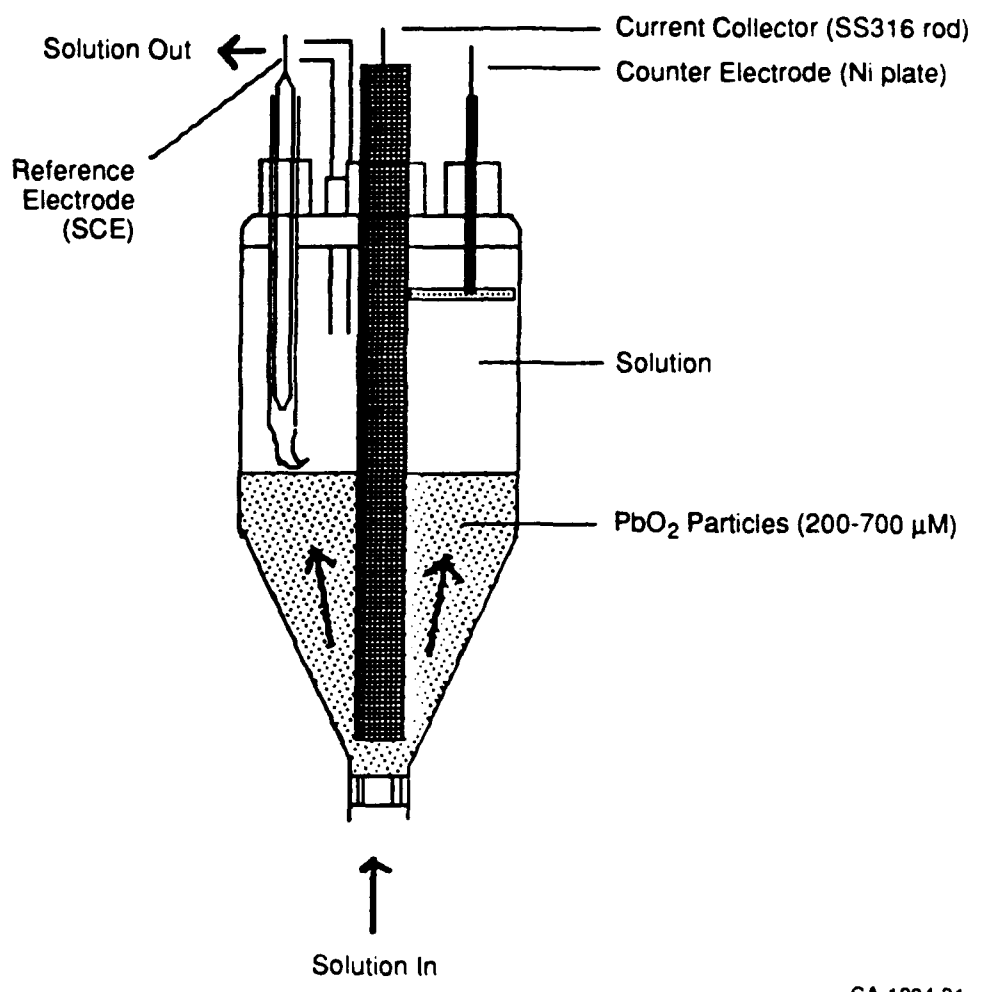
For fixed-bed reaction, PbO_2 film was electrochemically deposited on Ni or Pt mesh in $1.4 \text{ mM Pb}(\text{NO}_3)_2$ in 1.0 M HClO_4 solution with $1.6 \text{ V}(\text{vs. SCE})$. For improving oxidation ability, a Cl doped- PbO_2 electrode was also studied. Chloride was doped on PbO_2 particles electrochemically at a controlled concentration ratio 0.7 of chloride ion to lead ion (39). The reaction cell was constructed as Figure 29.

C. RESULTS AND DISCUSSIONS

Table 12 summarizes the results for the electrochemical oxidation experiments. For the PbO_2 surface, fluidized bed reaction has an oxidation rate an order higher than that of fixed bed reaction simply because the former has higher active surface area.

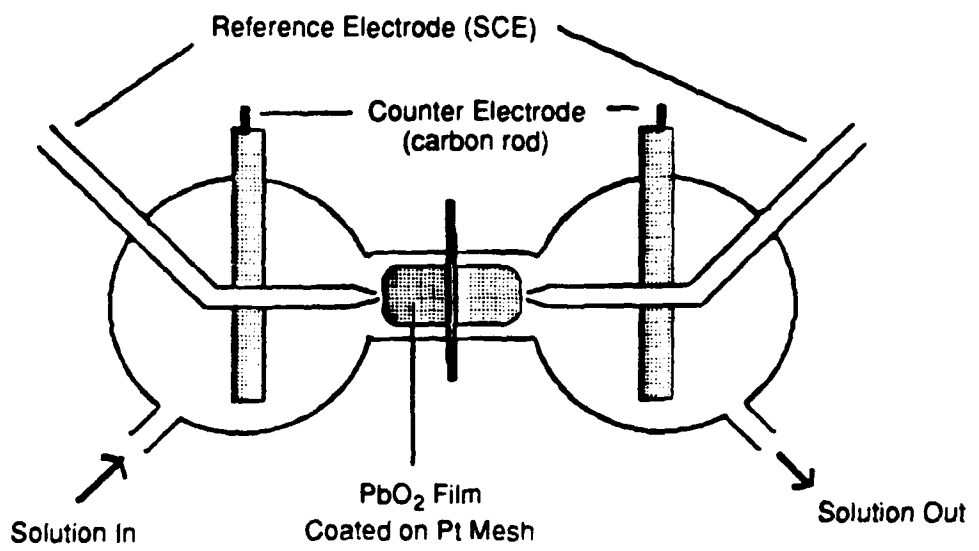
Cl-doped- PbO_2 surface was studied in fixed bed reaction cell. The oxidation rate of this doped surface has about an order higher than that of undoped surface. To confirm this result we performed an experiment for oxidizing potassium indigotrisulfate (PITS). A control experiment without current showed 49 percent decomposition of PITS by possible catalytic reaction on platinum. The total disappearance rate, which includes the catalytic reaction and electrochemical oxidation, was 0.036 min^{-1} . The doped surface enhanced the oxidation rate because the surface active sites were increased, and chloride provided charge compensation within the surface matrix.

The overall observed low oxidation rates were caused by the corrosion of the PbO_2 particles. The corrosion continually reduced the active site and efficient contact. The electrochemical deposition of PbO_2 on the current collector also biased the real measurements.



CA-1204-31

Figure 28. Fluidized-Bed Cell for Electrochemical Oxidation.



CA-1204-32

Figure 29. Fixed-Bed Cell for Electrochemical Oxidation.

Table 12. SUMMARY OF ELECTROCHEMICAL OXIDATION

System	Electrode	Compounds	Rates (min ⁻¹)
Fluidized bed	PbO ₂ particles	Propionate	0.0053
		Butyrate	0.0033
Fixed bed	PbO ₂ on Pt mesh	Propionate	0.00050 ^a
		Butyrate	0.00051 ^a
Fixed bed	Cl-PbO ₂ on Pt mesh	Propionate	b
		Butyrate	b
Fixed bed	Cl-PbO ₂ on Pt mesh	HBA	0.01

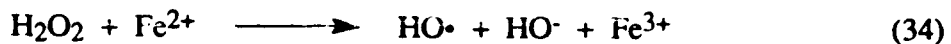
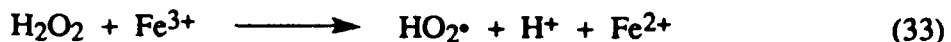
^aFirst order reaction; ~50 percent organics remain after 1400 minutes.

^bNot first order reactions; ~55 percent propionate and butyrate left after 200 minutes.

SECTION V

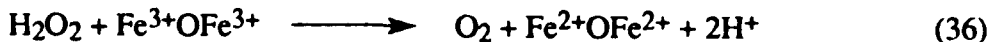
FeO_x or Fe³⁺ CATALYSTS

Peroxide decomposes to form HO• radical with ferric/ferrous ion in the familiar Fenton's reagent system, usually in acid solution, but also at higher pH with chelated iron or with insoluble ferric/ferrous oxo hydroxides (designated at FeO_x) (40, 41).



Early experiments at SRI with colloidal FeO_x showed it to be highly effective in decomposing H₂O₂. However organics were not oxidized unless they were preabsorbed on the FeO_x surface. For example, phthalate ion was readily oxidized whereas a nonionic methylphosphonate ester was not.

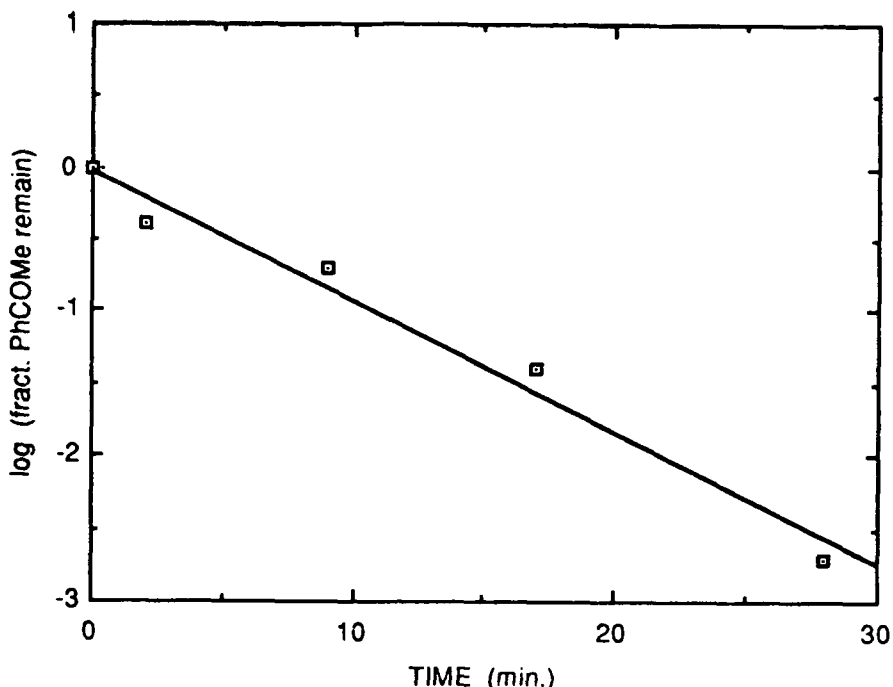
One explanation for this effect is that most H₂O₂ was oxidized directly to O₂ by FeOFe dimers on the catalyst surface with no significant formation of HO•.



To test the idea, we dispersed Fe³⁺ by cation exchange onto perfluorinated sulfonate polymer (Nafion), zeolite-NaY and montmorillonite clay surfaces and tested the catalyst' abilities to oxidize acetophenone (C₆H₅COCH₃), a neutral, unreactive aromatic compound in solution.

Figure 30 shows that the Nafion-Fe catalyst system will completely oxidize 1 mM (120 ppm) acetophenone in about 30 minutes with 100 mM H₂O₂. Similar results were obtained with Fe³⁺-exchanged zeolite-y. These preliminary results suggest that dispersed Fe³⁺ can convert

H_2O_2 to HO^\bullet radicals and act as an effective catalyst for oxidizing dilute solutions of organics in water.



CM-340581-40

Figure 30. Oxidation of acetophenone with Fe^{3+} /Nafion membrane.

We also examined the utility of a combined photocatalytic system employing UV light and FeOx. This system gave a rate approximately ten times more rapid than with acetophenone and the Fe-Nafion in the dark. The increased rate is due to the rapid photoreduction of Fe^{3+} with H_2O_2 , an otherwise slow reaction in the dark (see Reaction 33), plus the additional HO^\bullet formed.



SECTION VI

CONCLUSIONS

This study has shown that HO• is the major oxidant in all the AOPs we examined. Therefore, choice of an AOP for a specific treatment is based on the most cost efficiency in generating HO•. The most efficient system for generating HO• is the H₂O₂/UV system. However, this AOP is too slow to use with high flow systems where short residence times require high rates of HO• generation. Faster rates could be obtained, but only at much higher cost.

Ozone AOPs use 250 nm UV light very efficiently, but no more than 5 percent of the photolyzed ozone forms HO•. Thus only above pH 7 where HO₂⁻ is available is the ozone AOP an efficient source of HO•. This also means that above pH 7, the ozone/UV system has no advantage over the O₃/H₂O₂/Dark system for generating HO• and oxidizing organics. The efficiency for generating HO• in the O₃/H₂O₂/Dark system is unaffected by adding more H₂O₂ to speed up the reaction, thus this AOP can both rapidly and efficiently make and use HO• for oxidations. Physical mixing of H₂O₂ with ozone is the chief limitation on the amount of H₂O₂ that can be added to speed up this reaction.

Kinetic models to describe the time dependence of the AOP reactions were developed for peroxide and ozone AOPs and shown to be reliable predictors of the rates and concentrations of the oxidants and organics in the systems. The models provide a valuable tool for optimizing conditions and for selecting and efficiently using a specific AOP with a specific hazardous waste stream. Although the models did not include any direct reaction of ozone with organics, these reactions can be included where they are important. Current limitations on use of these kinetic models include effects of humic acids on rates of oxidation of organics and possible complications associated with oxidations of halogenated compounds.

SECTION VII

EXPERIMENTAL METHODS AND CALCULATIONS

A. STOCK SOLUTIONS

The water used to prepare all solutions was from a Milli-Q purification system (Millipore Corporation) featuring reverse osmosis, activated carbon, ion exchange, and 0.2- μm membrane filters. Buffer solutions of the stock 0.5 M phosphate for pH 8.0 and 2.2 were prepared by mixing 0.5 M phosphate solution at different pHs.

The humic acid solution was prepared by dissolving 10 g of Aldrich humic acid in 1 L of 0.1 M NaOH, neutralizing with H₃PO₄, filter-sterilizing through 0.2- μm membranes, and preaging in sunlight for 3 days in summer and 4 days in other seasons. The humic acid solution had an absorbance of about 0.20 cm⁻¹ at 260 nm at about 5 mg/L.

Ozone solutions were prepared using a 0.5 L·min⁻¹ oxygen feed into a Welsbach Model T-408 ozone generator. The gas stream first passed through pH 6 phosphate buffer (to remove nitrogen oxides) and then into distilled water cooled in ice. Continuous gas flow maintained an ozone concentration of about 100 μM .

Solutions of organic compounds were prepared by weight by rapidly stirring with Milli-Q water an amount calculated to give at most half their water solubility. The organic compounds were propionic, butyric, and hexanoic acids (Aldrich) and were reagent grade. Stock solutions were used within 7 days.

Titanium dioxide P25 (Degussa Corporation, Teterboro, NJ) was screened by 270-mesh screen scales. A 0.1 percent per cent titanium dioxide suspension was made with particles larger than 270 mesh and buffered with 500 μM phosphate to pH 7.0.

Titanium sulfate solution was prepared by diluting the reagent grade solution of 15 percent w/v Ti(SO₄)₂ with 23 percent sulfuric acid (BDH Chemicals, Ltd.) and adding concentrated H₂SO₄ to make a solution 12.5 mM Ti(SO₄)₂ with ~ 3 N sulfuric acid. Albone 35 was a 35 percent w/w H₂O₂ solution was from Du Pont. Perchloric acid (70 percent-72 percent J.T. Baker Chemical Co.) was used for preparing pH 2.2 solution.

B. UV LIGHT SOURCE

UV light for the H_2O_2 and ozone systems was supplied by a 25×0.5 cm low-pressure Hg penlight (Model 3 SC-9, UV Products, San Gabriel, CA), with >85 percent output at 254 nm. The lamp was immersed in a filter solution of 0.4 M nickel sulfate and 0.6 M cobalt sulfate, placed between the lamp and the reaction solutions to remove light below 220 nm and above 380 nm (Figure 31). A fresh solution was used for each photolysis, and the penlight was heated more than 10 minutes before exposing the solution.

UV light for TiO_2 systems was provided by a longwave ultraviolet Hg lamp (model B-100A, UV Products, San Gabriel, CA), with >85 percent output at 365 nm. The distance between lamp and reactor was 20 cm.

C. REACTION SYSTEMS

Figure 32 shows the reaction system for $\text{H}_2\text{O}_2/\text{UV}$ system. The ozone/UV reaction system is presented in Figure 33 and the TiO_2/UV system in Figure 34. The sonicator and tip (Model XL 2020) were supplied by Heat Systems, Inc. (Farmingdale, NY) and the UV lamp was 20 cm from the reactor.

D. OZONE MONITORING METHODS - UV AND INDIGO

Ozone was monitored in a 1- or 10-cm cuvette at 260 nm. At $\text{pH} \geq 9$, ozone is not stable in solution and reactions were initiated by injecting buffer into a 1-cm cuvette containing ozone solution, followed by rapid mixing. Below $\text{pH} 7$ in solution, reactions were initiated by injecting buffer solution into 1 L of 100- μM ozone water. After mixing, samples were withdrawn at regular intervals and transferred into a 1-cm cuvette for UV analysis.

When the solution had too great an absorbance to allow direct measurement of ozone by UV as in the presence of humic acid, the ozone loss was monitored by the indigo method (22). In such cases, large (1000-mL) reaction vessels were used to limit volatilization of ozone into the headspace created by sample removal. After mixing of the reactants, samples were withdrawn at regular time intervals and transferred to vials containing indigo solution and 30 μL of 85 percent w/w phosphoric acid. The vials were immediately mixed, and ozone was monitored by bleaching of indigo absorbance at 596 nm.

Experimental rate constants (k_{exp}) for ozone consumption were evaluated from the absorbance data (A_t) assuming pseudo-first order kinetics:

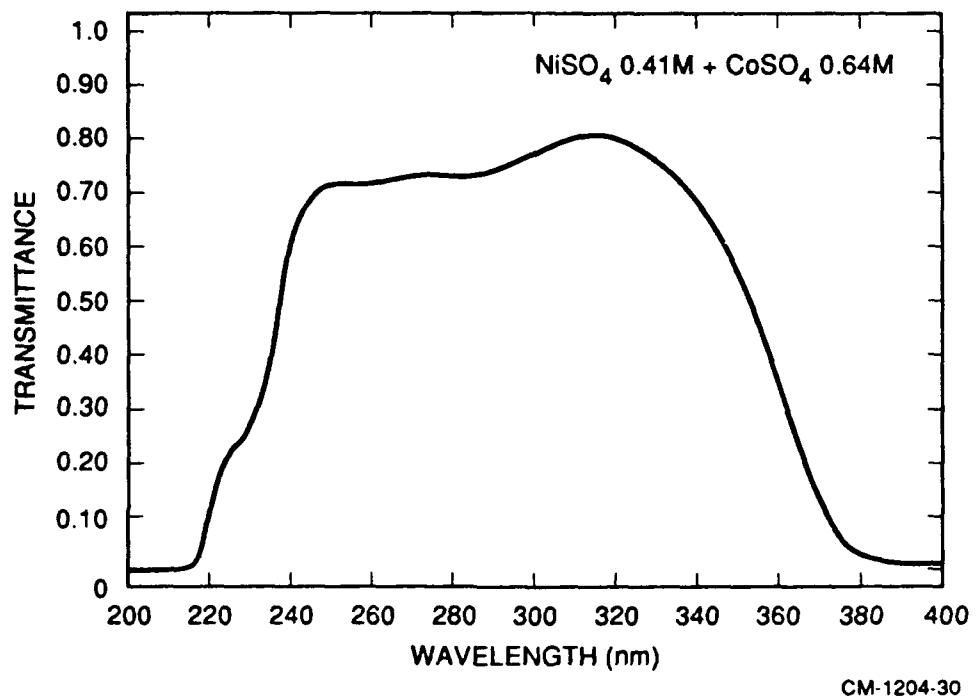
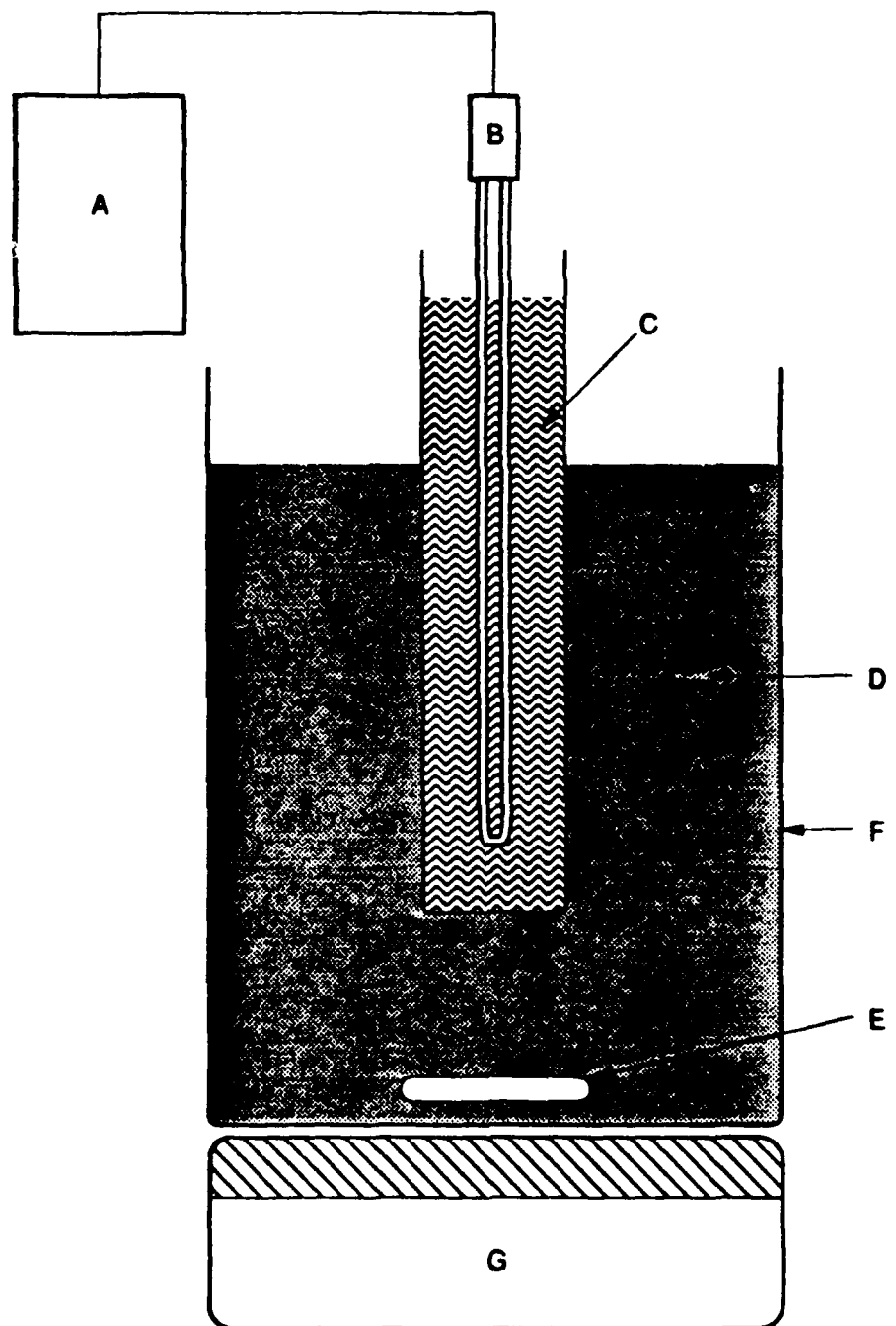


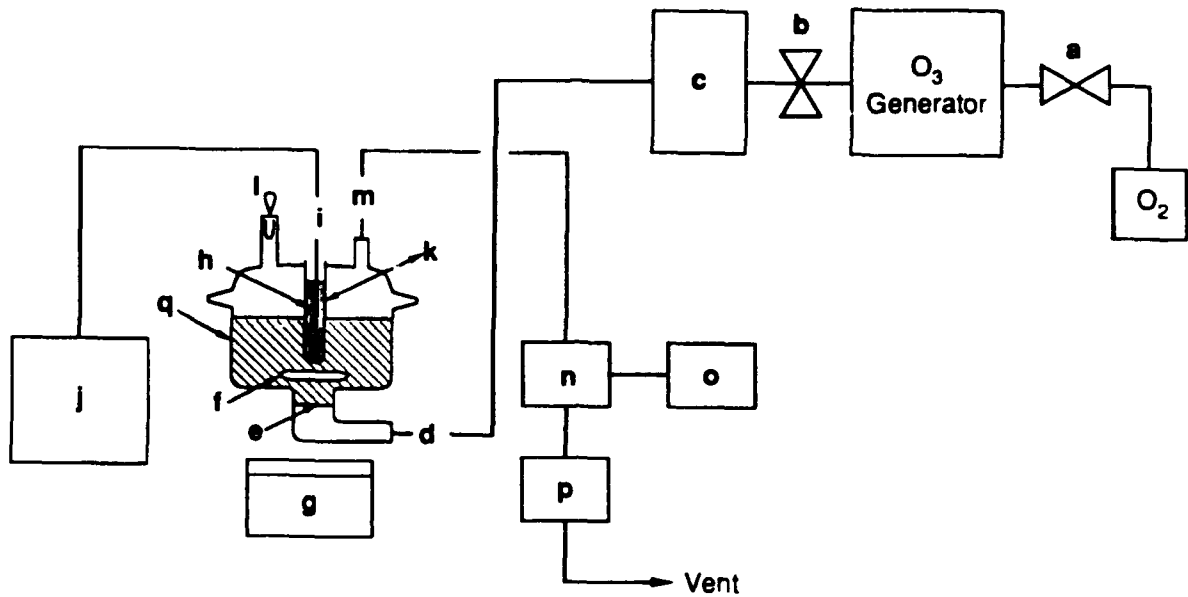
Figure 31. Spectrum of Filter Solution for UV Light Source.



A - Power Supplies	E - Magnetic Bar
B - UV Lamp	F - Reactor
C - Filter Solution	G - Stirrer
D - Reaction Solution	

RM-1204-2

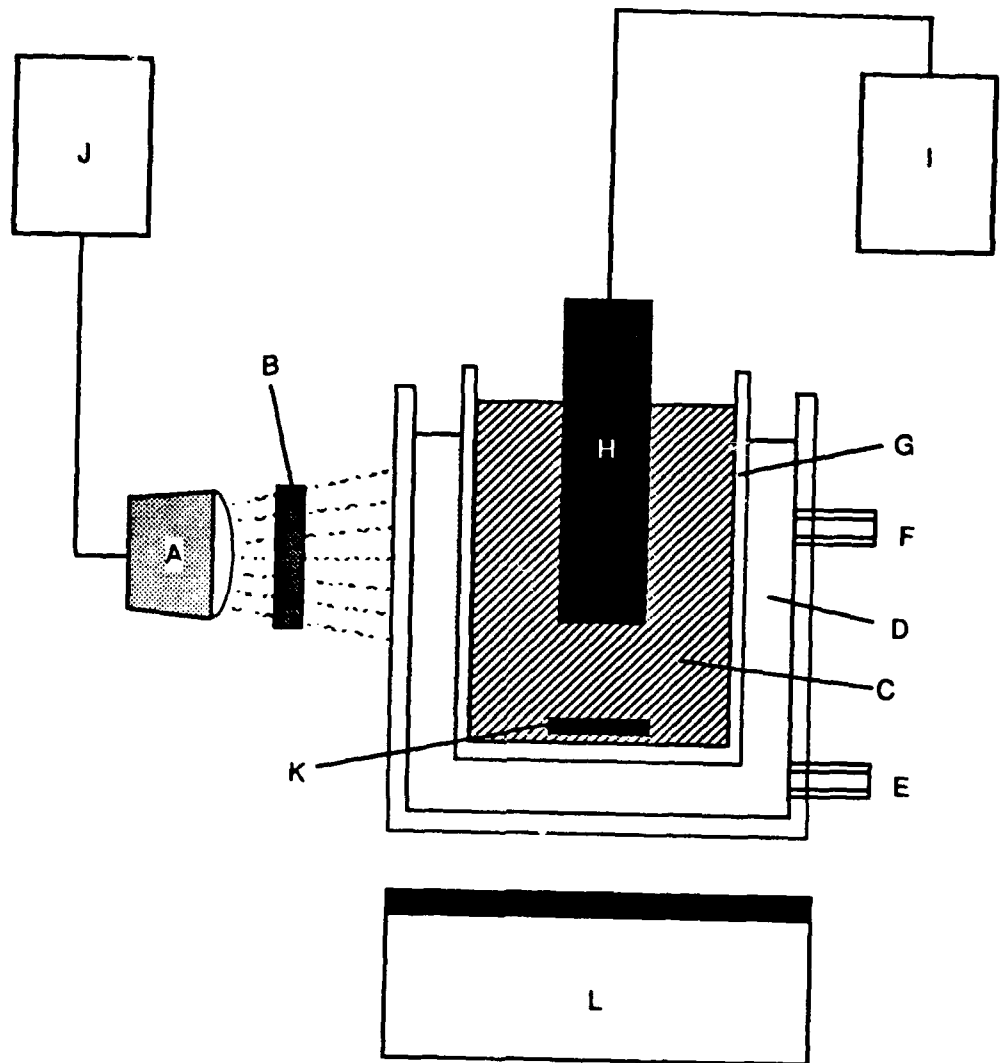
Figure 32. Peroxide/UV Reaction System.



a. Valve	j. Power Supplies
b. Flow Control Valve	k. Quartz Tube
c. NO _x Destruction Unit	l. Sampling Port
d. Ozone Gas Entrance to Reactor	m. Ozone Gas Outlet
e. Quartz Frit	n. UV/VIS Spectrometer
f. Magnetic Bar	o. Recorder
g. Stirrer	p. Ozone Chemical Destruction Unit
h. Filter Solution	q. Reaction Mixture
i. UV Penlight	

C-1204-001

Figure 33. Ozone/UV Reaction System.



A -	UV Lamp	E -	Water Inlet	I -	Controller
B -	Filter Solution	F -	Water Outlet	J -	Power Supplies
C -	Reaction Solution	G -	Reactor	K -	Magnetic Bar
D -	Water	H -	Sonication Probe	L -	Stirrer

CM-320581-92A

Figure 34. TiO_2/UV and $\text{TiO}_2/\text{UV/Sonication}$ Systems.

$$\ln \frac{A_0 - A_\infty}{A_t - A_\infty} = k_{\text{expt}} \quad (37)$$

In the direct UV method, k_{expt} was evaluated automatically by the HP8950 computer system controlling the spectrometer. However, for slow reactions that were stopped well before the consumption of ozone went to completion, the computer failed to give accurate results because of larger errors in estimating the final absorbance of the solutions. In these cases, we used sufficient nitrogen gas to purge the remaining ozone and then measured the background absorbance corresponding to infinite reaction time.

E. MEASUREMENT OF H₂O₂

Hydrogen peroxide was monitored in a 1-cm cuvette at 420 nm, using the titanium complex method (39). Even though ozone had no significant effect on the measurement, ozone-free samples were preferred. Samples were withdrawn at regular intervals and divided equally into two vials. Stock Ti(SO₄)₂ solution was added to one sample and MQ water was added to the other, both in the ratio of 1/10(v/v). After mixing, the samples were transferred to 1-cm cuvettes and measured. The concentration was calculated using a calibration curve determined from known concentrations of hydrogen peroxide.

F. MEASUREMENT OF ORGANIC SUBSTRATES

Probe chemicals B and P were measured by gas chromatography (GC) using a flame ionization detector. At regular intervals, fixed amounts (10 mL) of ozone/organic reaction mixture were pipetted into vials and purged with nitrogen to remove the remaining ozone. Each sample was purged about 30 seconds with no significant loss of probe chemicals. Mixtures were adjusted to pH > 11 by adding 1 N NaOH solution and evaporated to dryness. Residues were dissolved in 0.5 mL solution containing 120 μ M internal standard of hexanoate ion acidified to pH < 2 with 4 M HCl solution and chromatographed.

G. INSTRUMENTS

Acids were measured with a Varian 3700 GC equipped with a AT-1000 10-m x 0.54-mm-i.d. Megabore column with 1.2- μ m film thickness, and an flame ionization detector. An HP8452A diode array spectrophotometer with an HP89500A UV/Vis ChemStation was used for absorption measurements of ozone and hydrogen peroxide.

H. COMPUTER SYSTEM AND PROGRAMS

Acuchem (18) is a computer program for solving the system of differential equations describing the temporal behavior of homogeneous multicomponent chemical reactions. Acuplot is a program for the output file and the graphics. Both programs were supplied by National Institute of Standards and Technology (Gaithersburg, MD) and run on an IBM personal computer with a math coprocessor, display, EPSON MX-100III printer, and a 200-MB hard disk (Procom Technology).

REFERENCES

1. Taube, H. (1957). "Photochemical Reactions of Ozone in Solution." Trans. Farad. Soc. 53: 656-667.
2. Prengle, H. W. Jr. (1983). "Experimental Rate Constants and Reactor Considerations for the Destruction of Micropollutants and Trihalomethane Precursors by Ozone with UV Radiation." Environ. Sci. Technol. 17: 743-747.
3. Staehelin, J. and J. Hoigné. (1985). "Decomposition of Ozone in Water in the Presence of Organic Solutes Acting as Promoters and Inhibitors of Radical Chain Reactions." Environ. Sci. Technol., 19: 1206-1213.
4. Peyton, G. R., Smith, M. A., and Peyton, B. M. (1987). "Photolytic Ozonation for Protection and Rehabilitation of Groundwater Resources: A Mechanistic Study." University of Illinois, Water Resource Center, Research Report No. 206.
5. Peyton, G. R., and Glaze, W. H. (1987). "Mechanism of Photolytic Ozonation, in Photochemistry of Environmental Aquatic System." R. G. Zika and W. J. Cooper, Eds., ACS Symposium Series, No. 327. (Washington, DC in American Chemical Society) 76-88.
6. Peyton, G. R., and Glaze, W. H. (1988). "Destruction of Pollutants in Water with Ozone in Combination with Ultraviolet Radiation. 3. Photolysis of Aqueous Ozone." Environ. Sci. Technol. 22: 761-767.
7. Peyton, G. R. (1990). "Oxidative Treatment Methods for Removal of Organic 313-362 Compounds from Drinking Water Supplies in Significance and Treatment of Volatile Organic Compounds in Water Supplies." N. M. Rem et al. Eds. Chapt. 14. (Lewis Publishers Inc.).
8. Namba, K, and Nakayama, S. (1982). "Hydrogen Peroxide-Catalyzed Ozonation of Refractory Organic. 1. Hydroxyl Radical Formation." Bull. Chem. Soc. Jpn. 55:3 38-3340.
9. Glaze, W. H., King, J-W., and Chapin, D. H. (1987). "The Chemistry of Water Treatment Processes Involving Ozone, Hydrogen Peroxide and Ultraviolet Radiation." Ozone Sci. Eng. 9: 335-352.
10. Zepp, R. G. and Cline, D. M. (1977). "Rates of Direct Photolysis in Aquatic Environment." Environ. Sci. Technol. 11: 357-366.
11. Hoigné, J. and Bader, H. (1979). "Ozonation of Water: Oxidation-Competition Values of Different Types of Waters Used in Switzerland." Ozone Sci. Eng. 1: 357-372.
12. Buxton, G. V., Greenstock, C. L., Helman, Ross W. P. (1988). "Critical Review of Rate Constants for Reactions of Hydrated Electrons, Hydrogen Atoms, and Hydroxyl Radicals ($\cdot\text{OH}/\cdot\text{O}^-$) in Aqueous Solution." J. Phys. Chem. Ref. Data 17: 513-886.

13. Neta, P., Huie, R. E., and Ross, A. B. (1988) "Rate Constants for Reactions of Inorganic Radicals in Aqueous Solution." J. Phys. Chem. Ref. Data. 17: 1027-1284.
14. Bieski, B.H.J., Cabeilli, D. E, R. L. Arudi, and Ross, A. B. (1985). "Reactivity of HO₂/O₂[·] Radicals in Aqueous Solution." J. Phys. Chem. Ref. Data. 14: 1041-1100.
15. Peterson, M. W., Turner, J. A., and Nozik, A. J. (1991). "Mechanistic Studies of the Photocatalytic Behavior of TiO₂ Particles in a Photoelectrochemical Slurry and the Relevance to Photodetoxification reactions." J. Phys. Chem. 95: 221.
16. Turchi, C. S., and D. F. Ollis. (1990). "Photocatalytic Degradation of Organic Water Contaminants: Mechanisms Involving Hydroxyl radical Attack." J. Catal. 122, 178.
17. Mill T., Haag, W. R., and Yao, C. C. D. (1992). "Kinetic Features of Advanced Oxidation Processes for Treating Aqueous Chemical Mixtures, in Chemical Oxidation Technology For The Nineties," 2nd International Symposium, Nashville, Tennessee.
18. Braun W., Herron, J. T., and Kahaner, D. K. (1988). "Auchem: A Computer Program for Modeling Complex Chemical Reaction Systems." International Journal of Chemical Kinetics. 20: 51-62.
19. Hoigné, J. and Bader, H. (1979). "Ozonation of Water; Selectivity and Rate of Oxidation of Solutes." Ozone Sci. Eng., 1: 73-85.
20. Stumm, W. and J. J. Morgan, 1981. "Dissolved Carbon Dioxide in Aquatic Chemistry," New York: John Wiley and Sons Inc., Chapter 4.
21. Yao, C.C.D. and W.R. Haag (1991). "Rate Constants for Direct Reactions of Ozone with Several Drinking Water Contaminants." Water Res., 25: 761-773.
22. Bader, H., and Hoigné, J. (1981). "Determination of Ozone in Water by the Indigo Method." Water Res. 15: 449-456.
23. Bader, H. and Hoigné, J. (1982). "Determination of Ozone in Water by The Indigo Method; A submitted Standard Method." Ozone: Science and Engineering, 4: 169-176.
24. Haag, W.R. and Hoigné, J. (1985). "Photo-Sensitized Oxidation in Natural Water via OH Radicals." Chemosphere 14: 1659-1671.
25. Aiera, E.M., Reagan, K.M., Lang, J.S., McReynolds, L., Kang, J-W. and Glaze, W.H. (1988). "Advanced Oxidation Processes for Treating Groundwater Contaminated with TCE and PCE: Pilot Scale Evaluations." J. Am. Water Works Assoc. 80: 65-72.
26. Duguet, J.P, Anselme, C., Mazounie, P. and Mallevaille, J. (1987). "Application of ozone - Hydrogen Peroxide combination for the Removal of Toxic Compounds from Groundwater." Presented at the Water Quality Technology Conference, Baltimore, MD.
27. Zeff, J.D. (1990). "Ultriox Operating Experiences with UV/Oxidation; Economics." Presented at the NAS/NRC Workshop of the Committee on Potential Applications of Concentrated Solar Photons, 7-8 Nov., SERI, Golden, CO.

28. Topudurti, K.V. 1990. PRC Environmental Management, Inc., personal communication.
29. Ollis, D.F. (1988). Process economics for water purification: A Comparative Assessment. In Photocatalysis and Environment: Trends and Applications, M. Schiavello (Ed.), NATO ASI Series C, Vol. 237, Kluwer Academic Publishers, Boston, MA. pp. 663-677.
30. Lietzke O. and Whitby, G.E. "The Combined Application of Ozone and UV Irradiation for the Treatment of Water." WEDECO company literature.
31. Advanced Photolysis Technologies, Inc. (APT) (1990). "In-situ Organic Contaminant Destruction with Advanced Ultraviolet Flashlamps." Company Literature.
32. Hager, D.G., Loven, C.G. and Giggy, C.L. (1988). "Chemical Oxidation Destruction of Organic Contaminants in Groundwater." Presented at the AWWA Annual Conference and Exposition, Orlando, FL. Available as sales literature from Peroxidation Systems, Inc., Tucson, AZ.
33. Link, H. (1990). "Economics of Solar Photocatalyzed Water Detoxification." Presented at the NAS/NRC Workshop of the Committee on Potential Applications of Concentrated Solar Photons, 7-8 Nov., SERI, Golden, CO.
34. Gehringer, P., Proksch, E., Szinovatz, W., and Escweiler, H. (1986). "Der strahlenchemische Abbau von Trichloräthylen- und Perchloräthylenlenspuren in Trinkwasser." Zeit. Wass.-Abwass.-Forsch. 19: 196-203.
35. Nakatama, S., Esaki, K., Namba, K., Taniguchi, Y. and Tabata, N. (1979). Improved Ozonation in Aqueous Systems. Ozone Sci. Eng. 1: 119-131.
36. Hager, D.G. and Loven, C.G. (1987). "On-site Destruction of Organic Contaminants in Water." In Proceedings of the National Conference on Hazardous Wastes and Hazardous Materials, 16-18 Mar., Washington, DC. pp. 129-133.
37. Ma, J.J.L., Bolan, R. and Leu, M-H. (1986). "Advances in Hazardous Waste Treatment." SRI International Process Economics Program Report No. 187.
38. Blake, D. (1990). SERI Personal communication.
39. Hsiao Y. and Johnson D. (1989) "Electrolysis of Anodic Oxygen-Transfer Reactions: Chloride-Doped Lead Dioxide Electrodes." C. J. Electrochem. Soc., 136: 3704.
40. Walling, C. (1975). "Fenton's reagent revisited." Accs. Chem. Res. 1-12.
41. Mill , T., T. Pettit, and W.R. Haag. (1989) "Oxidation Processes for Transforming Organic Compounds in Hazardous Waste Systems." Proceedings of the ACS Symposium on Chemical and Biochemical Detoxification of Hazardous Waste. J. Glaser (Ed.), Lewis Publishers, Ann Arbor, MI.
42. Staehelin, J.; Buhler, R. E.; Hoigné, J. J. (1984) "Ozone Decomposition in Water Studies by Pulse Radiolysis 2. OH and HO₄ as Chain Intermediates." Phys. Chem. 88: 5999.

43. Tomiyasu, H., Fukutomi, H. and Gordon, G. (1985). Kinetics and Mechanism of Ozone Decomposition in Basic Aqueous Solution. Inorg. Chem., 224: 2962.
44. Hoigné, J., Staehelin, J., and Buhle. (1984). J. Phys. Chem. 88: "Ozone Decomposition in Water Studied by Pulse Radiolysis 1. HO₂/O₂⁻ and HO₃/O₃⁻ as Intermediate" (a) 2560 (b) Additions and Corrections 5450.
45. Satterfield C. N. and Bonnell, A. H. (1955). "Interferences in the Titanium Sulfate Method for Hydrogen Peroxide." Anal. Chem., 27: 1174-1176.
46. Johnson, A. J. and Hocking, P. "Ultrasonically Accelerated Photocatalytic Waste Treatment," in press.